Appendix E.

Underwater noise monitoring survey (JASCO 2016a)

Passive Acoustic Monitoring of Ambient Noise and Marine Mammals—Barossa Field

July 2014 to July 2015

Submitted to:
Christopher Teasdale
Senior Consultant–Marine Science
ANZ Infrastructure & Environment
Jacobs

Authors:
Craig McPherson
Katie Kowarski
Julien Delarue
Christopher Whitt
Jeff MacDonnell
Bruce Martin

10 August 2016

P001241-001
Document 00997
Version 1.0

JASCO Applied Sciences (Australia) Pty Ltd.
Unit 4, 61-63 Steel Street
Capalaba, Queensland, 4157
Tel: +61 7 3823 2620
Mob: +61 4 3812 8179
www.jasco.com

Suggested citation:

McPherson, C., K. Kowarski, J. Delarue, C. Whitt, J. MacDonnell and B. Martin. 2016. *Passive Acoustic Monitoring of Ambient Noise and Marine Mammals—Barossa Field:* . JASCO Document 00997, Version 1.0. Technical report by JASCO Applied Sciences for Jacobs.

Contents

Figures

Tables

Executive Summary

JASCO Applied Sciences (JASCO) conducted a twelve month—July 2014 to July 2015—baseline acoustic environment characterisation program at and surrounding the Barossa field for Jacobs on behalf of ConocoPhillips. Three JASCO Autonomous Multichannel Acoustic Recorders (AMARs) were deployed close to the seabed at three stations. The AMARs captured data that were analysed to quantify ambient sound levels, the presence of sounds related to anthropogenic activity, and the acoustic presence of marine mammals and fish.

Ambient Sound Levels

The minimum levels of ambient sound (in root-mean-squared sound pressure level) were consistent across all stations. The maximum levels were consistent at the two stations (Station J1 and J3) farthest from the Barossa field where the Mobile Offshore Drilling Unit (MODU) *Nan Hai VI* was operating between October 2014 and March 2015. The closest station (Station J2) showed higher levels, but only during Deployment 1 when the MODU was 8 km away. During Deployment 1 the southernmost station, near the Caldita field (Station J3), had the lowest levels across all exceedance percentiles time periods. However, during Deployment 2 this occurred at the Barossa field (Station J2). The distances from the MODU to the three stations, J1–J3 respectively, was 48 and 71 km, 8 and 15.5 km (Deployment 1), and 36 and 49 km (Deployment 2), for the two drilling locations.

The ambient data showed low levels of diel variations in sound levels attributable to biological events such as fish chorusing, but were otherwise primarily affected by weather events such as wind, at times producing a noticeable diel variation in sound levels, with levels increasing during the day and decreasing at night. During the period April–September when the highest call rates from Omura's a whales were detected, they were the dominant contributor to the soundscape at 26-28 Hz.

Anthropogenic Activity

The amount of shipping was quantified with automated detectors. Shipping was a minor contributor to the soundscape. The MODU *Nan Hai VI* and its support vessels did not change the soundscape considerably from its natural state at a regional level, although at closer ranges (8 and 15.5 km) operations contributed sound levels exceeding natural levels moderately.

Biological Sounds

Automated analysis techniques, including manually validated automated detectors, were used to determine the presence of vocalising marine life. A more detailed analysis based on the automated detection results was conducted to extract more information about the usage of and movements through the region by pygmy blue, Omura's and Bryde's whales. Based on the analysis:

- Omura's whales were detected consistently from April to September inclusive, with a peak in June and July. Based on the year of recordings, the whales seemed to enter the region in a south-west to north-east direction, then maintain a higher presence within the Barossa field area (than compared to the Evans Shoal or Caldita field areas) for the autumn and winter months. They appeared to leave the region in a north-east to south-west direction, reversing their entry path, leaving the area by the start of November. When present they created a pronounced peak at 26-28 Hz that is visible in the spectrograms and power spectral density plots.
- Pygmy blue whales were detected during their northward migration once in August 2014, over a few consecutive days in late May-early June 2015, on the 16 and 30 June, and 1 July 2015. The detections are over 400 km further east than the north-bound migration corridor of pygmy blue whales described in Double et al. (2014). No detections were logged from the south-bound migration, suggesting a different migration path. The highest calling rates of the three monitoring station occurred at the Barossa field, which may reflect its greater depth and proximity to the trench.
- Bryde's whales, distinguished from the Omura's whales through variations in the spatial and temporal occurrence of vocalisations, were present in the region from January to October. They appear to move into the area in a south to north direction during summer and autumn, then utilise the region with a preference for the shallower sections (Evans shoal and Caldita field areas) over the Barossa field region. They then leave the area in a north – south direction, with the last detections in early October.
- Odontocetes were extremely common. Many species were detected on a daily basis, with a primarily nocturnal diel cycle.

- Unknown beaked whale species were detected on four days over the entire program at Stations J2 (Barossa field) and J3 (Caldita field).
- Fish chorused at dawn and dusk over the entire deployment period at all three stations. Their chorusing varied in intensity over the deployment period, but was consistent in diel pattern.

1. Introduction

ConocoPhillips Australia Exploration Pty Ltd (ConocoPhillips), as proponent on behalf of the current and future joint venturers, are proposing to develop the gas and condensate reserves in the Barossa gas field and surrounds, located approximately 300 kilometres (km) north of Darwin, Northern Territory.

To characterise the existing marine environment within and surrounding the Barossa area, ConocoPhillips has undertaken an environmental baseline studies program. Baseline studies were undertaken with reference to petroleum retention lease permit NT/RL5 (referred to as the 'permit area' in this report), as shown in Figure 1. While this represents the area of primary interest as part of ConocoPhillips' staged field development, the broader surrounds were also characterised.

As part of this program, Jacobs contracted JASCO to deliver a long-term acoustic monitoring program, which in part coincided with the 2014–2015 exploration drilling campaign in the Barossa field. This report details the methods (Section 2) and results (Section 3) of this acoustic monitoring program, characterising the baseline acoustic environment within and surrounding the Barossa field whilst also providing data on sound generation from Mobile Offshore Drilling Unit (MODU) and support vessel activities.

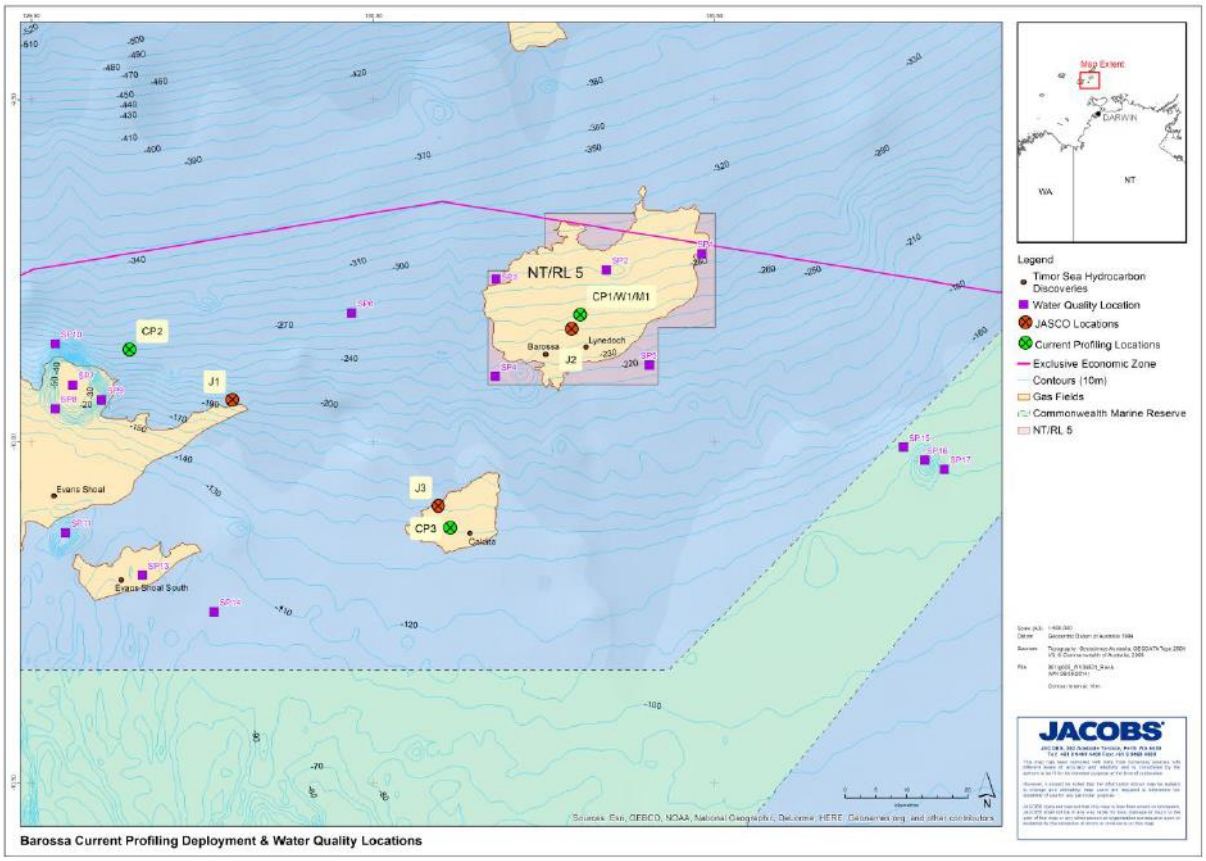

Figure 1. Barossa field and locations of JASCO recorders J1, J2, and J3.

1.1. Acoustic Monitoring Study

This report provides the results from a twelve-month autonomous acoustic monitoring program. The acquired acoustic data were analysed to quantify the acoustic presence of marine mammals (Section 3.2), ambient sound levels (Section 3.3) and the presence of anthropogenic activity such as vessels (Section 3.4), and the. The total sound level data provide a statistical noise floor for current conditions, which is a required input for modelling the area over which noise associated with construction and operation of facilities could be heard by marine life. The recorded total sound levels

and current vessel activity levels are inputs for cumulative effects modelling. Finally, the marine mammal presence data documents the seasonal use of sound by marine mammals for foraging, navigation, and socialising.

Current knowledge on marine mammal presence near the Barossa field location is limited and primarily derived from information available from the Australian Government's Department of the Environment (DoE) Protected Matters Search Tool (2015). JASCO's acoustic monitoring study will contribute additional knowledge regarding the spatial and temporal distributions of several marine mammal species in this area, including potential migration pathways.

Data were acquired using three Autonomous Multichannel Acoustic Recorders (AMARs) deployed on the seabed for two six-month periods at three stations (Figure 1).

1.2. Anthropogenic Activity near the Barossa Field

1.2.1. Drilling Activity

A drilling program was conducted by ConocoPhillips at the Barossa field during the monitoring program, with two wells being drilled during this phase of the project. The dates and location of the drilling program were provided by ConocoPhillips (Table 1). The distances from the well to the three acoustic monitoring stations are provided to contextualize the potential for the activities associated with the drilling operation to influence the sound levels at each station.

In association with the drilling activity, there is typically at least one support vessel at the MODU location (e.g., a rig tender), with support vessels periodically supplying the rig with equipment and stores. When a rig or MODU is moved, it is towed using two rig tenders.

Table 1. ConocoPhillips Barossa field MODU drilling locations during monitoring study.

Well	Latitude	Longitude	Mooring Date	Drilling start date	Release date	Distance to stations (km)		
						J1	J2	J3
3	9° 47.736' S	130° 13.678' E	12 Oct 2014	14 Oct 2014	15 Jan 2015	48	8	36
4	9° 47.953' S,	130° 25.678' E	15 Jan 2015	18 Jan 2015	26 Mar 2015	71	15.5	49

1.2.2. Seismic Survey

A seismic survey was detected in the last two weeks of the monitoring program, with pulses detected between 04-15 July 2015. It is most likely that the operator responsible for the survey was CGG, conducting the 2D BandaSeisV in Indonesian waters between Babar Island (part of the Babar Islands group) and Selaru Island (in the Tanimbar Islands group), over 160 km from the closest recording station.

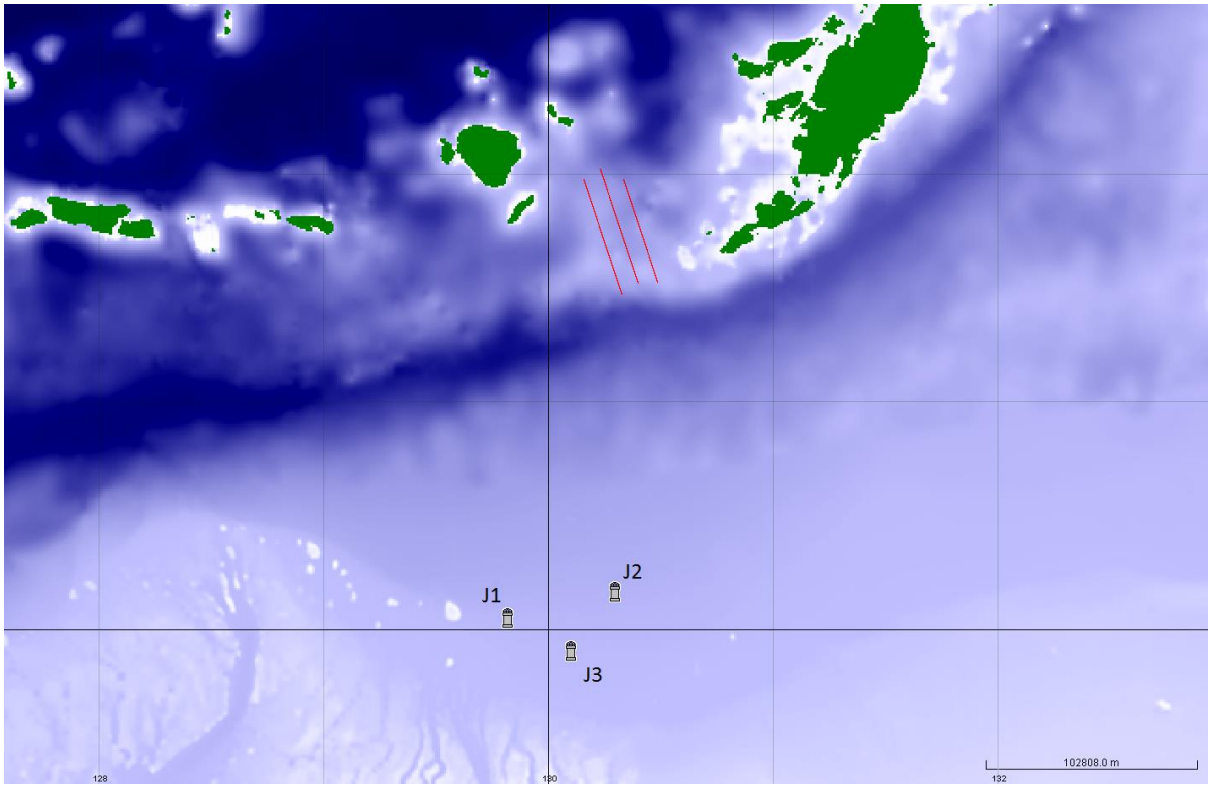

Figure 2. CGG 2D BandaSeisV Seismic survey lines (red lines) and recorder locations.

1.3. Biological Sounds

A search was conducted of the *Environment Protection and Biodiversity Conservation Act 1999* (EPBC Act) Protected Matters Database (DoE 2015) determine the species identified by the DoE that may occur in, or may relate to, the Barossa area and surrounds (Table 2). It is believed that blue whales identified as potentially occurring in the Barossa area are in fact pygmy blue whales (*Balaenoptera musculus brevicauda;* Ichihara (1966); Rice (1998)), a sub species of the true blue whale (B*. m. musculus*). In addition to the Protected Matters search results, the Omura's whale (*Balaenoptera omurai;* Wada et al. (2003)), a recently described species basal to the Bryde's/sei whale clade, is also known to be present off northwest Australia (Cerchio et al. 2015) and suspected to be present in the area. This species is not currently listed as a threatened species under the EPBC Act and is therefore not included in the EPBC search tool, and hence not listed in Table 2.

Table 2. EPBC Act Protected Matters Database listing of marine mammals present in the Barossa area and surrounds (DoE 2015).

Species	Common name
Mysticetes	
Balaenoptera bonaerensis	Antarctic minke whale, dark shoulder minke whale
Balaenoptera edeni	Bryde's whale
Balaenoptera musculus	Blue whale
Megaptera novaeangliae	Humpback whale
Large odontocetes	
Orcinus orca	Orca, killer whale
Globicephala macrorhynchus	Short-finned pilot whale
Pseudorca crassidens	False killer whale
Kogia breviceps	Pygmy sperm whale
Kogia simus	Dwarf sperm whale
Physeter macrocephalus	Sperm whale
Ziphius cavirostris	Cuvier's beaked whale, goose-beaked whale
Small odontocetes	
Feresa attenuata	Pygmy killer whale
Peponocephala electra	Melon-headed whale
Delphinus delphis	Common dolphin, short-beaked common dolphin
Grampus griseus	Risso's dolphin, grampus
Lagenodelphis hosei	Fraser's dolphin, Sarawak dolphin
Stenella attenuata	Spotted dolphin, pantropical spotted dolphin
Stenella coeruleoalba	Striped dolphin, euphrosyne dolphin
Stenella longirostris	Long snouted spinner dolphin
Steno bredanensis	Rough-toothed dolphin
Tursiops aduncus	Indian Ocean bottlenose dolphin, spotted bottlenose dolphin
Tursiops aduncus (Arafura/Timor Sea populations)	Spotted bottlenose dolphin
Tursiops truncatus s. str.	Common bottlenose dolphin

2. Methods

2.1. Data Acquisition

Three Autonomous Multichannel Acoustic Recorders (AMARs) were deployed in the Timor Sea for 188–190 days and 179-181 days respectively (Table 3, Figure 3). Each AMAR was fitted with an M8E-V35 dB omnidirectional hydrophone (GeoSpectrum Technologies Inc.; −164 dB re 1 V/µPa sensitivity). For Deployment 1, the AMARs at Station J1 and J3 were each deployed in a mooring configuration that consisted primarily of a bottom-sitting plate fitted with two identical remotely activated pop-up retrieval line canisters (Figure 4). The AMAR at Station J2 was deployed directly on the seabed, tethered to a long ground line along the seabed to a float, anchor and a remotely activated release mechanism to bring the line to the surface for retrieval (Figure 5). A different design was used for Station J2 due to depth limitations on the acoustic release pop-up floatation. For Deployment 2, all three stations used the bottom plate mooring design (Figure 4) due to access to 400 m rated floatation for Station J2.

The bottom plate moorings were deployed by allowing them to sink to the seabed, using additional temporary buoyancy to slow their descent. The AMAR at Station J2 for Deployment 1 was lowered directly to the seabed using the long ground line, after which the vessel moved away to a safe distance to drop the acoustic release, anchor and float. To retrieve the bottom plate moorings, one of the pop-up retrieval line canisters was activated, allowing an integrated float to bring a retrieval line to the surface. At Station J2 (Deployment 1), the acoustic release was triggered to free the float from the anchor and bring the ground line to the surface. After the retrieval line surfaced, the equipment was brought on board using the vessel's winch.

The AMARs sampled on a 30-minute duty cycle: 840 s at 48 ksps, then 65 s at 250 ksps, and then 895s of sleep. The 48 ksps recording channel had a 24-bit resolution with 6 dB of gain resulting in a spectral noise floor of 23 dB re 1 µPa^2/Hz and could resolve a maximum sound pressure level (SPL) of 165 dB re 1 µPa. The 250 ksps data were recorded at 16-bit resolution, with a spectral noise floor of 35 dB re 1 µPa^2/Hz and could resolve a maximum SPL of 171 dB re 1 µPa (no gain). The spectral noise floor represents the quietest sounds that can be recorded, and is directly comparable to the Wenz ocean noise spectra (Figure 10). Acoustic data were stored on internal solid-state flash memory.

Table 3. AMAR deployment and retrieval dates and locations.

Station	Deployment date	Record end / Retrieval date	Latitude (°S)	Longitude (°E)	Water depth (m)	Range to MODU (km)
Deployment 1						
J1	10 Jul 2014	15 Jan 2015	-09°56.9130'	129°48.8280'	179	48
J2	09 Jul 2014		-09°49.9600	130°17.3340'	243	8
J3	11 Jul 2014		-10°05.7188'	130°05.7632'	153	36
Deployment 2						
J1	16 Jan 2015	16 Jul 2015	9° 56.910'	129° 48.8243'	181	71
J2	17 Jan 2015	15 Jul 2015	9° 50.1282'	130° 17.4774'	240	15.5
J3	17 Jan 2015	15 Jul 2015	10° 5.7072'	130° 5.7196'	143	49

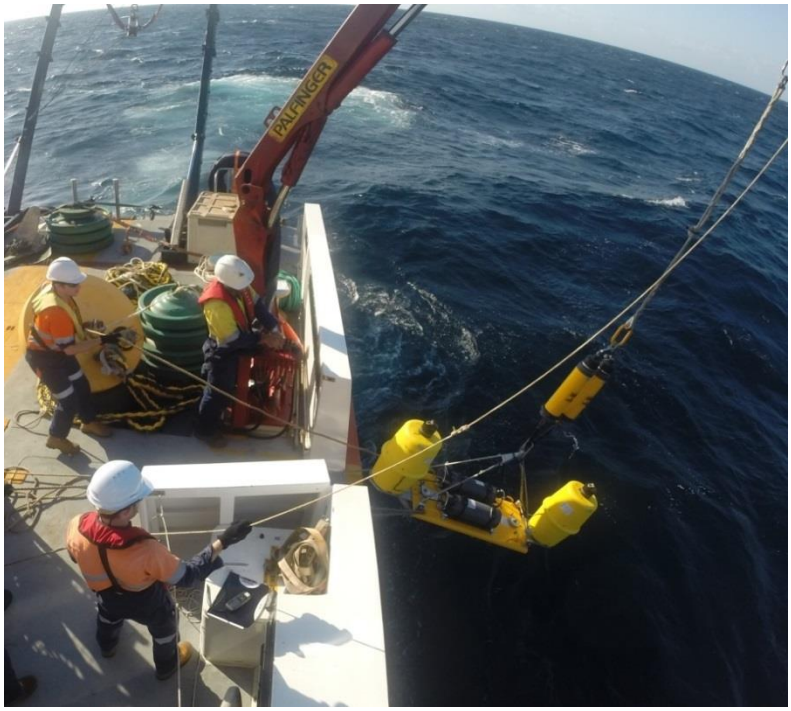

Figure 3. AMAR and mooring float being deployed from the *MV Warrego*.

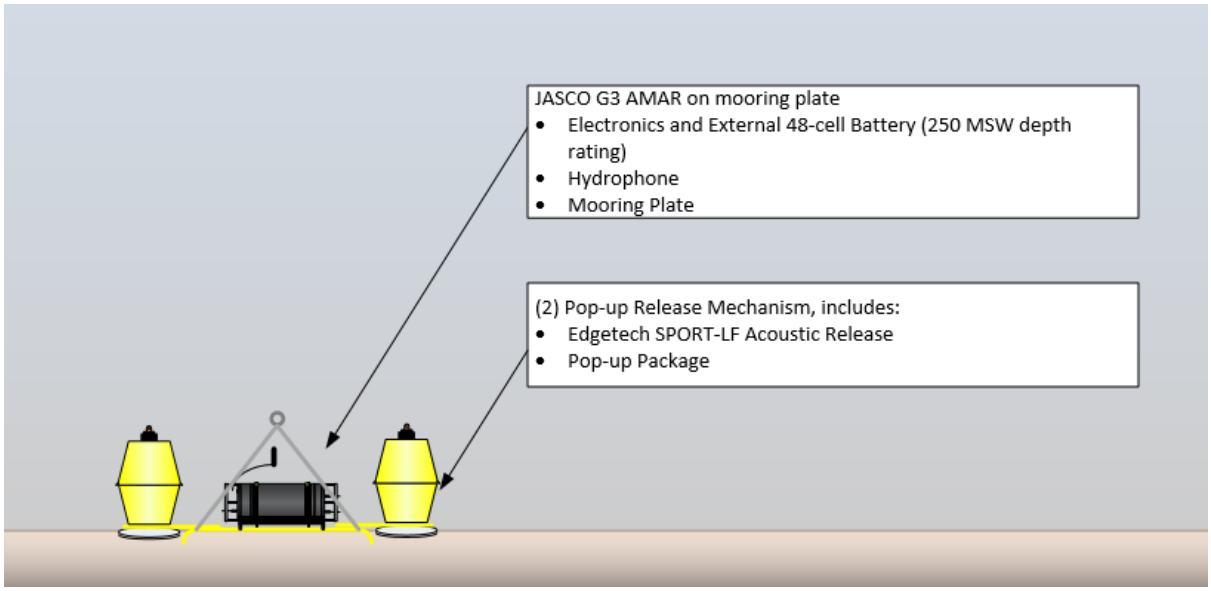

Figure 4. Mooring diagram for AMARs at Stations J1 and J3 Deployment 1, and all stations for Deployment 2.

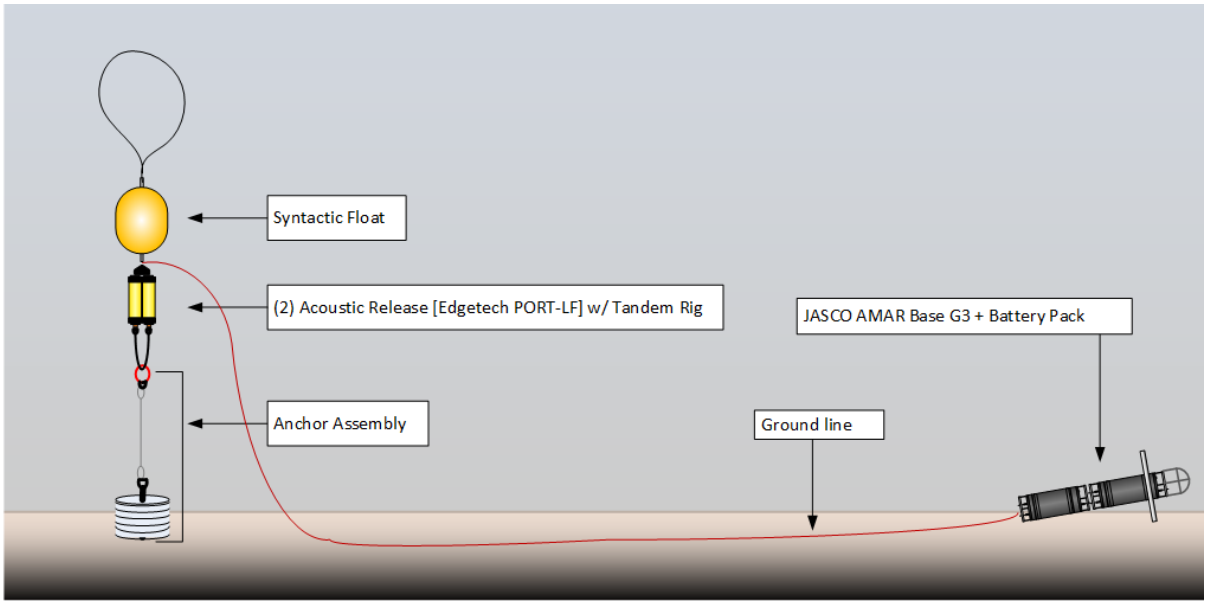

Figure 5. Mooring diagram for AMAR at Station J2, Deployment 1.

2.2. Recorder Calibrations

A GRAS 42AA pistonphone calibrator (Figure 6), which is National Institute of Standards and Technology (NIST) traceable, was used to verify the sensitivity of the recording apparatus as a whole, i.e., the hydrophone, pre-amplifier, and AMARs. Calibration was undertaken in JASCO's warehouse prior to deployment in the field and upon retrieval. The pistonphone and its adapter were placed over the hydrophone and produced a known pressure signal on the hydrophone element (a 250 Hz sinusoid at 133.3 dB re 1 µPa) to verify the pressure response of the recording system. The system sensitivity was measured independently of the software that performed the data analysis, which allowed an independent check on the correct calibration of the analysis software. Both readings were verified for consistency before data analysis was performed.

Figure 6. Split view of (left) a GRAS pistonphone calibrator, (middle) adaptors, and (right) a hydrophone.

2.3. Data Analysis

2.3.1. Marine Mammal Detections

JASCO applied automated analysis techniques to the acoustic data. Automated detectors were employed to detect (if present) calls of pilot whales, killer whales, beaked whales, sperm whales, dolphin clicks, dolphin and other odontocetes' whistles, and moans from various mysticetes including Omura's, Bryde's, blue and humpback whales.

2.3.1.1. Automated Click Detectors

The following list shows the stages of the automated click detector/classifier, based on the zero-crossings in the acoustic time series (refer Figure 7); zero-crossings are the rapid oscillations of the click above and below the signal's normal level.

1. The raw data are high-pass filtered to remove all energy below 8 kHz. 8 kHz removes most energy from other sources like shrimp, vessels, wind and cetacean tonal calls, yet allows the energy from all marine mammal click types to pass.
2. The filtered samples are summed to create a time series with 0.5 ms root-mean-square (rms) time series. Most marine mammal clicks have a duration of 0.05–1 ms (e.g. Au (1993), Baumann-Pickering et al. (2013)).
3. A Teager-Kaiser energy detector identifies possible click events.
4. The high pass filtered data are searched to find the maximum peak signal within 1 ms of the detected peak.
5. The high pass filtered data are then searched backwards and forwards to find the time span where the local data maxima are within 12 dB of the maximum peak. The algorithm allows for two zero-crossings to occur where the local peak is not within 12 dB of the maximum before stopping the search. This defines the time window of the detected click.
6. The classification parameters are extracted. The number of zero crossings within the click, the median time separation between zero crossings, and the slope of the change in time separation between zero crossings are computed. Beaked whales can be identified by the increase in frequency (up sweep) of their clicks. The slope parameter helps to identify beaked whale clicks.
7. The Mahalanobis distance between the extracted classification parameters and the templates of known click types is computed. The covariance matrices for the known click types are stored in an external file and were computed based on 1000 s of manually identified clicks for each species. Each click is classified as a type with the minimum Mahalanobis distance, unless none of them are less than the specified distance threshold.

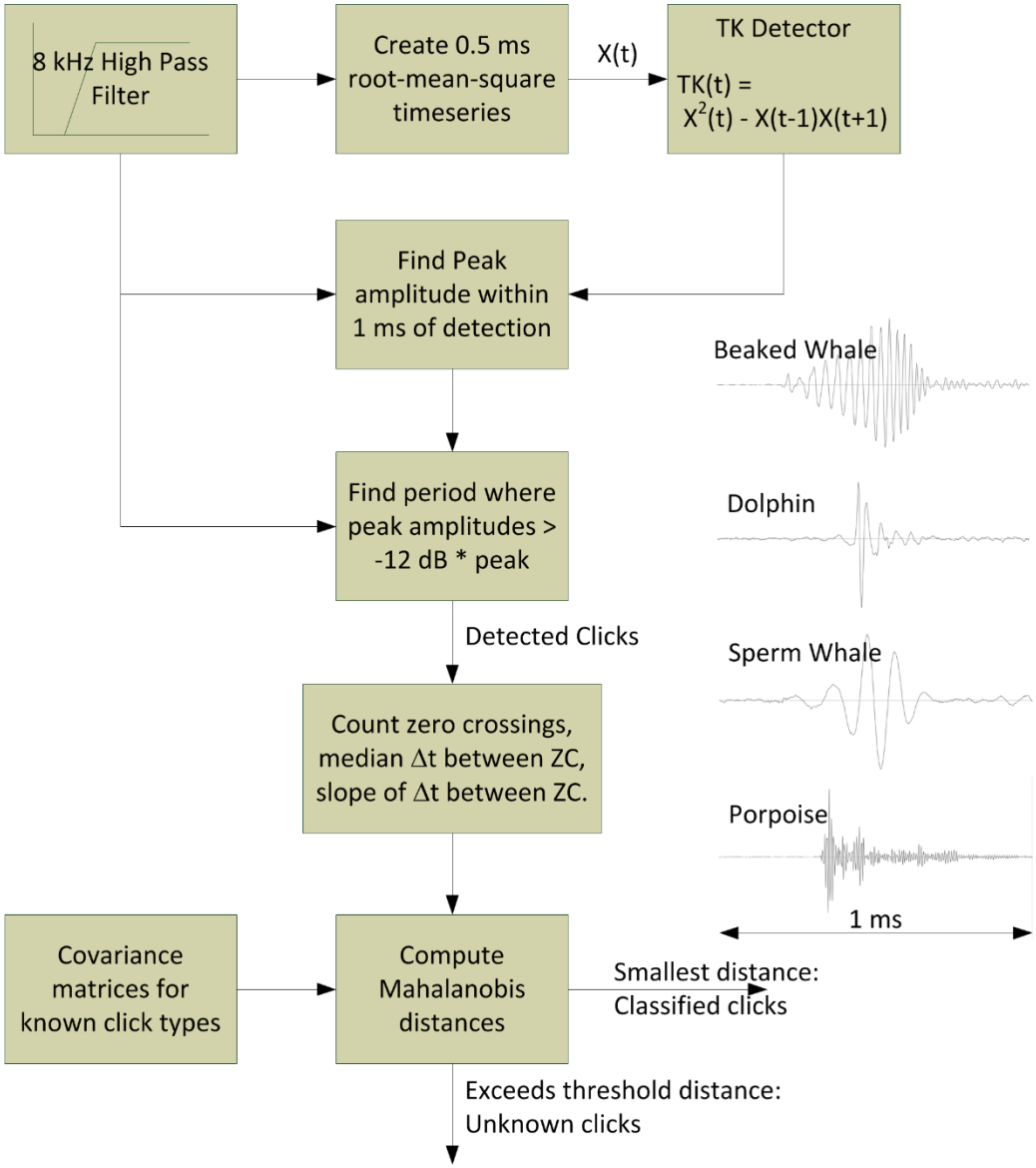

Figure 7. The click detector/classifier and a 1-ms time-series of four click types.

2.3.1.2. Cetacean Tonal Call Detection

The cetacean tonal call detector identifies data likely to contain marine mammal moans, song notes, and whistles. The analysis begins with spectrograms of the appropriate resolution for each mammal call type that are normalised by the median value in each frequency bin for each detection window (Table 4). Contours are formed using the same 3 × 3 kernel used for shipping and seismic airgun analysis. Finally, a call-sorting algorithm determines if the contours match the definition of a mammal call type (Table 5).

Table 4. Fast Fourier Transform (FFT) and detection window settings for marine mammal call detection used in the Barossa analysis. Values are based on JASCO's experience and empirical evaluation of a variety of data sets.

Possible species	Call type	FFT			Detection window (s)	Detection threshold
		Resolution (Hz)	Data duration (s)	Data advance (s)		
Dolphin	Whistle	16	0.032	0.02	30	3
Humpback whale	Moan	2	0.25	0.125	120	3
Bryde's/Omura's whale	Moan	0.5	2	0.25	120	4
Blue whale	Moan	0.5	2	0.125	120	4
Bryde's whale	Downsweep	2	0.25	0.125	120	3

Table 5. Call sorter definitions for the marine mammal calls detected in the Barossa analysis.

Possible species	Call type	Frequency (Hz)	Duration (s)	Bandwidth (Hz)	Other
Pilot whale, killer whale, other dolphin	Whistle	15,000–25,000	0.4–5	>1000	Possibly multiple frequency components, each > 0.4 s long and > 20 Hz bandwidth
Humpback whale	Moan	50–2000	0.5–5	>20	
Omura's/Bryde's whale	Moan	10–70	2–20	>4	
Blue whale	Moan	10–70	10–30	>10	
Bryde's whale	Downsweep	30–200	0.5–3	>10	

2.3.1.3. Validation of Automated Detectors

Automated detectors are often developed and tested with example data files that contain a range of vocalization file types and representative background noise conditions. However, the test files normally cannot cover the full range of possible conditions. Therefore, a selection of files must be manually validated to check on the detector performance and determine the minimum number of detections per sound file required to accept the detector's results. Of the 48 ksps data files, 794 were manually reviewed for the presence/absence of low-frequency baleen whale moans; 387 from deployment 1 and 407 from Deployment 2. Of the 250 ksps data files, 717 were manually reviewed for the presence/absence of high-frequency toothed whale clicks and whistles: 342 from Deployment 1 and 376 from Deployment 2. Files for manual analysis were selected to represent a full range of automated detection results. For each recorder, up to 20 files were selected for each detected species: beaked, sperm, humpback, and baleen whales as well as unidentified small odontocete clicks and whistles. For each species, the following files were randomly selected; 10 files with large numbers of detections, 5 files with a moderate number of detections, and 5 files with a low to moderate number of detections. Files that contained early or late automated detections were primarily selected to help bound the period of occurrence of each species. The automated detector results were checked to note the true presence or absence of every species, as well as vessels and fish. These validated results were fed to a grid search algorithm that maximised the probability of detection and minimised the number of false alarms using the F-score:

$$F = \frac{(1+\beta^2)P*R}{(\beta^2)P+R}; P = \frac{TP}{TP+FP}; R = \frac{TP}{TP+FN}$$

Where P is called the classifier's precision, R is the classifier's recall, TP is the number of correctly detected files (true positives), FP is the number of files that are false detections (false positives), and FN is the number of files that had missed detections (false negatives). P measures exactness; R measures completeness. For instance, a P of 0.9 means that 90% of the detections classified as killer whales for instance were in fact killer whale calls, but says nothing about whether all killer whale vocalisations in the dataset were identified. An R of 0.8 means that 80% of all killer whale calls in the dataset were classified, but says nothing about how many classifications were wrong. Thus, a perfect detector/classifier would have P and R equal to 1. Neither P nor R alone can describe the performance of a detector/classifier on a given dataset; both metrics are required. An F-score of 1 indicates perfect performance–all events are detected with no false alarms. In the equation above β is the relative weight between the recall and precision. A β of 2 means the recall has double the weight of the precision. Conversely, a β of 0.5 means the recall has half the weight of the precision.

The results are the classification threshold, which is defined as the number of detections per file that indicate a valid detection of the species. Table 6 shows the dependence of the classification threshold on the β-parameter and its effect on the precision and recall of the detector and classifier system. To specify that precision (low false alarm rate) was more important than recall, β=0.5 was used.

The classification threshold was used to determine whether mammals were present in each data file. The results were used to generate the presence plots and whisker plots in Section 3.2.The thresholds for other species are contained in Section 3.2.1.

Table 6. Effects of changing the F-score β-parameter on the classification threshold, precision, and recall for the odontocete clicks.

β	Classification threshold	Precision $P = \frac{TP}{TP + FP}$	Recall $R = \frac{TP}{TP + FN}$	F-score
2	25	0.87	0.95	0.93
0.5	50	0.91	0.91	0.91

2.3.1.4. Sound Levels of Mysticete Call Detections

In an effort to observe how the mysticete species moved through the Barossa area, the relative loudness of calls was determined and compared across stations for each call type.

Post-processing in Java extracted the SPL of the detections as well as the SPLs of the time periods immediately before and after each detection. In order to determine the SPL of the actual call, the mean of the SPLs immediately before and after the detection (ambient) was subtracted from the SPL of the detection. Early analysis revealed that the resulting call SPLs could not be reliably compared between stations as they were inherently biased by the threshold setting of the automatic detector that skews them with the ambient. This effect is presented in Figure 8 where the ambient is slightly higher at Station J2 compared to Stations J1 or J3, therefore it appears that the call SPLs are consistently higher at J2 than J1 or J3, when in reality, this is a threshold effect.

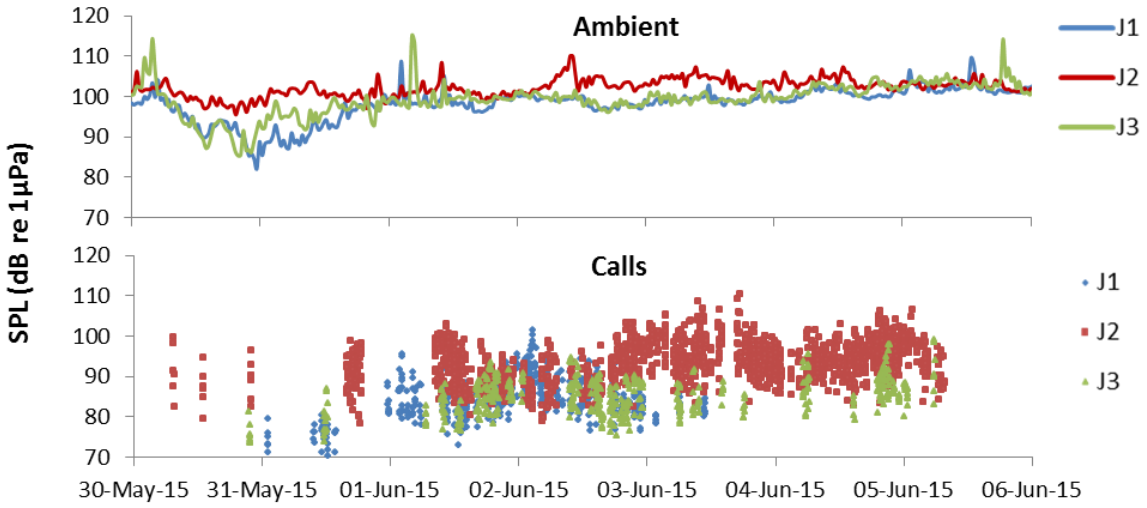

Figure 8. Example line graph of ambient SPL of the 10 to 24,000 Hz band (top) and plot of blue whale call SPL (bottom) at Stations J1, J2, and J3 from 30 May to 6 June 2015 from 30 May to 4 July 2015 at the Barossa area in the Timor Sea.

In order to compare sound levels of calls between stations, the mean station call SPL was subtracted from each call SPL of the associated station. Negative values (those below the mean) were considered to be relatively faint calls and positive values (those above the mean) were considered to be relatively loud calls. In this manner, how call SPLs increased and decreased within and between stations could be reliably observed and presented in a series of plots over time.

2.3.2. Vessel Detections

Vessel detection was performed in two steps. In the first step, narrowband sinusoidal tones (tonals) produced by a ship's propulsion and other rotating machinery (Arveson and Vendittis 2000) are detected in each 840 s file of the 16 ksps data. The tonal detector is based on overlapped FFTs. The number of seconds of data input to the FFT determines its spectral resolution. Arveson and Vendittis (2000) used both 0.5 and 0.125 Hz resolutions. For this study, spectral analysis was performed at 0.125 Hz resolution by using 8 s of real data with a 2 s advance. This frequency resolution separates each tone for easy detection, and the 2 s advance provides suitable temporal resolution. Higher frequency resolutions can reduce detectability of shipping tones, which are often unstable within 1/16 Hz bands for long periods. A 120 s long spectrogram is created with 0.125 Hz frequency resolution and 2 s time resolution (32768-point FFTs, 32000 real data points, 16000-point advance, and Hamming window). A split-window normaliser (Struzinski and Lowe 1984) distinguishes the tonal peaks from the background noise (2 Hz window, 0.75 Hz notch, and detection threshold of 4 times the median). The peaks are joined with a 3 × 3 kernel to create contours. Associations in frequency are made if contours occur at the same time. The event time and number of tones for any event at least 20 s long and 40 Hz in bandwidth are recorded for further analysis.

In the second step, the first step-results of all the 840 s files are combined to detect ship passages. A 'shipping band' is defined at 40–315 Hz and SPL for the band is obtained once per minute. Background estimates of the shipping band SPL and the total SPL are compared to their median values over the 12 hr window, centred on the current time. Shipping is detected when the SPL in the shipping band is at least 3 dB above the median, at least 5 shipping tonals are present, and the SPL in the shipping band is within 8 dB of the total SPL (Figure 9). When these conditions are true, the total per-minute SPL is attributed to shipping.

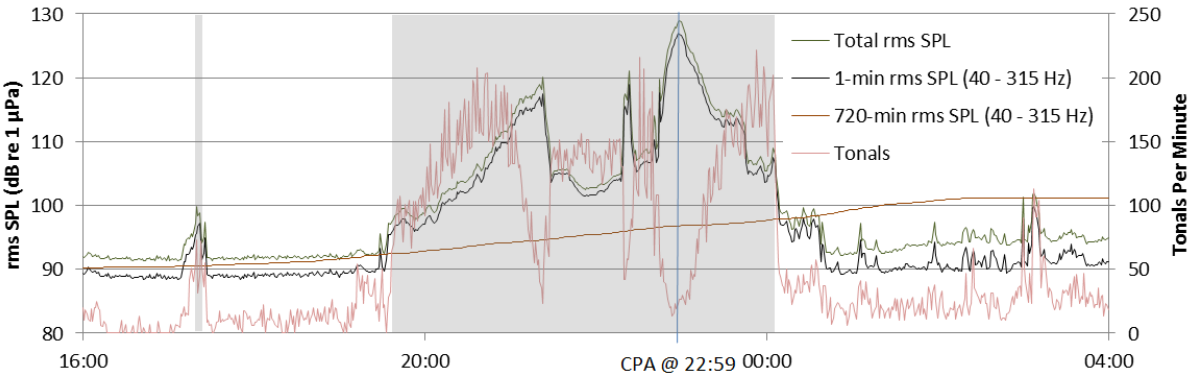

Figure 9. Example of broadband and in-band SPL and the number of 0.125 Hz wide tonals detected per minute as a ship approached a recorder, stopped, and then departed. The shaded area is the time period of shipping detection. All tonals are from the same vessel. Fewer tonals are detected at the ship's closest points of approach (CPA) at 22:59 because of the broadband cavitation noise at CPA and the Doppler shift of the tonals.

2.3.3. Seismic Survey Event Detection

Seismic pulse sequences were detected using correlated detections in spectrogram contours. A 300 s long spectrogram was created using a 4 Hz frequency resolution and a 0.05 s time resolution (Reisz window). Each frequency bin was normalized to the median bin value over the 300 s window. The detection threshold was three times the median value. Contours were created by joining the detected time and frequency bins in the frequency range of 7–1000 Hz using a 5 × 5 kernel. Any contour 0.2–6 s with a bandwidth of at least 60 Hz was kept for further analysis.

An "event" time series is created by summing the normalized value of the frequency bins at each time bin that contains detected contours. The event time series is auto-correlated to look for repeated events. The correlated data space is normalised to its median and a detection threshold of 3 is applied. Peaks larger than their two nearest neighbours are identified and the peaks list is searched for entries with a set repetition interval. The spacing between the minimum and maximum time peaks is appropriately set, typically at 4.8 and 65 s, to allow for the normal range of seismic pulse periods, which are between 5 and 60 s. If at least six regularly spaced peaks occur, the original event time series is searched for all peaks that match the repetition period within a tolerance of 0.25 s. The duration of the 90% SPL window of each peak is determined from the originally sampled time series, and pulses more than 3 s long are rejected.

2.3.4. Total Sound Levels

2.3.4.1. Sound Levels

Underwater sound amplitude is measured in decibels (dB) relative to a fixed reference pressure of p_0 = 1 µPa. Because the perceived loudness of sound, especially impulsive noise such as from seismic airguns, pile driving, and sonar, is not generally proportional to the instantaneous acoustic pressure, several sound level metrics are commonly used to evaluate noise and its effects on marine life.

The zero-to-peak pressure, or PK (dB re 1 µPa), is the maximum instantaneous SPL in a stated frequency band attained by an acoustic pressure signal, $p(t)$:

$$\text{Peak pressure (PK)} = 10\log_{10}\left[\frac{\max\left(\left|p^2(t)\right|\right)}{p_0^2}\right] \quad (1)$$

The peak-to-peak pressure (dB re 1 µPa) is the difference between the maximum and minimum instantaneous SPLs in a stated frequency band attained by an impulse, p(t):

$$\text{Peak-to-peak pressure} = 10\log_{10}\left\{\frac{\left[\max\left(p(t)\right)-\min\left(p(t)\right)\right]^2}{p_0^2}\right\} \quad (2)$$

At high intensities, the PK can be a valid criterion for assessing whether a sound is potentially injurious; however, because the PK does not account for the duration of a noise event, it is a poor indicator of perceived loudness. The root-mean-square (rms) SPL (dB re 1 µPa) is the rms pressure level in a stated frequency band over a time window (T, s) containing the acoustic event:

$$\text{SPL} = 10\log_{10}\left(\frac{1}{T}\int_T p^2(t)dt \Big/ p_0^2\right) \quad (3)$$

The SPL is a measure of the average pressure or of the effective pressure over the duration of an acoustic event, such as the emission of one acoustic pulse, a marine mammal vocalization, the passage a vessel, or a fixed duration in time. Because the window length, *T*, is the divisor, events more spread out in time have a lower SPL for the same total acoustic energy density.

In studies of impulsive noise, *T* is often defined as the "90% energy pulse duration" (T_{90}): the interval over which the pulse energy curve rises from 5% to 95% of the total energy. The SPL computed over this T_{90} interval is commonly called the 90% SPL (dB re 1 µPa):

$$\text{90\% SPL} = 10\log_{10}\left(\frac{1}{T_{90}}\int_{T_{90}} p^2(t)dt \Big/ p_0^2\right) \quad (4)$$

The sound exposure level (SEL, dB re 1 µPa²·s) is a measure of the total acoustic energy contained in one or more acoustic events. The SEL for a single event is computed from the time-integral of the squared pressure over the full event duration (T100):

$$\text{SEL} = 10\log_{10}\left(\int_{T_{100}} (p^2(t)-\overline{n^2})dt \Big/ T_0 p_0^2\right) \quad (5)$$

where T_0 is a reference time interval of 1 s. The SEL represents the total acoustic energy received at some location during an acoustic event; it measures the total sound energy to which an organism at that location would be exposed.

SEL is a cumulative metric if it is calculated over periods with multiple acoustic events or fixed periods. For multiple events the cumulative SEL (dB re 1 µPa²·s) can be computed by summing (in linear units) the SELs of the *N* individual events:

$$\text{Cumulative SEL} = 10\log_{10}\left(\sum_{i=1}^{N} 10^{\frac{\text{SEL}_i}{10}}\right) \quad (6)$$

To compute the SPL and SEL of acoustic events in the presence of high levels of background noise, Equations 4) and 5) are modified to subtract the background noise energy from the event energy:

$$\text{SPL} = 10\log_{10}\left(\frac{1}{T_{90}}\int_{T_{90}} (p^2(t)-\overline{n^2})dt \Big/ p_0^2\right) \quad (7)$$

$$\text{SEL} = 10\log_{10}\left(\int_{T_{100}} (p^2(t)-\overline{n^2})dt \Big/ T_0 p_0^2\right) \quad (8)$$

where $\overline{n^2}$ is the mean square pressure of the background noise generally computed by averaging the squared pressure of a nearby segment of the acoustic recording during which acoustic events are absent (e.g., between pulses).

Because the SPL and SEL are both computed from the integral of square pressure, these metrics are related by a simple expression, which depends only on the duration of the energy time window, *T*:

$$\text{SPL} = \text{SEL} - 10\log_{10}(T) \tag{9}$$

$$\text{SPL} = \text{SEL} - 10\log_{10}(T_{90}) - 0.458 \tag{10}$$

where the 0.458 dB factor accounts for the SPL containing 90% of the total energy from the per-pulse SEL.

2.3.4.2. Spectral and 1/3-octave-band Analysis

The distribution of a sound's power with frequency is described by the sound's spectrum, which shows the fine-scale features of the frequency distribution of a sound. The spectrum of a sound can be split into a series of adjacent frequency bands. Splitting a spectrum into 1 Hz wide bands yields the "power spectral density" of the sound. These values directly compare to the Wenz curves that represent typical deep-ocean sound levels (Figure 10; Wenz 1962). This splitting of the spectrum into passbands of a constant width of 1 Hz, however, does not represent how animals perceive sound.

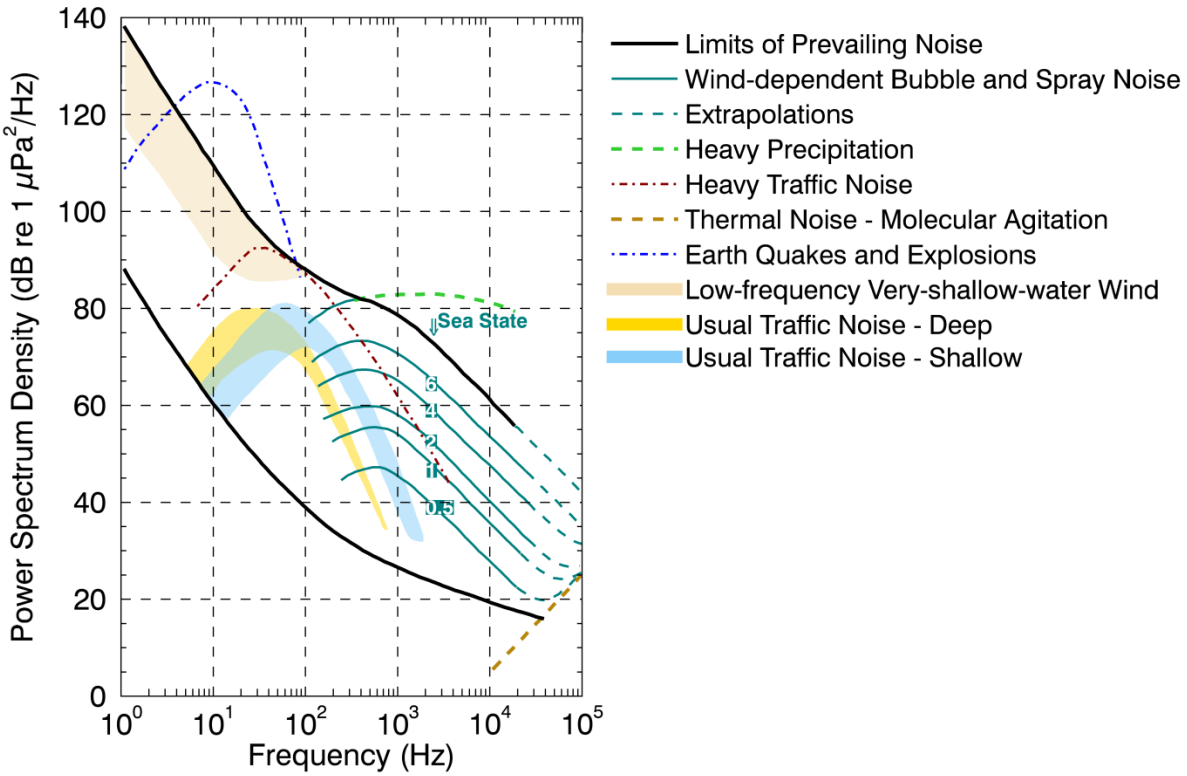

Figure 10. Wenz curves (NRC 2003), adapted from Wenz (1962), describing pressure spectral density levels of marine ambient noise from weather, wind, geologic activity, and commercial shipping.

Because animals perceive exponential increases in frequency rather than linear increases, analysing a sound spectrum with passbands that increase exponentially in size gives more meaningful data. In underwater acoustics, a spectrum is commonly split into 1/3-octave-bands, which are one-third of an octave wide; each octave represents a doubling in sound frequency. The centre frequency of the ith 1/3-octave-band, $f_c(i)$, is defined as:

$$f_c(i) = 10^{i/10} \tag{11}$$

and the low (f_{lo}) and high (f_{hi}) frequency limits of the ith 1/3-octave-band are defined as:

$$f_{lo} = 10^{-1/20} f_c(i) \quad \text{and} \quad f_{hi} = 10^{1/20} f_c(i) \tag{12}$$

The 1/3-octave-bands become wider with increasing frequency, and on a logarithmic scale the bands appear equally spaced (Figure 11).

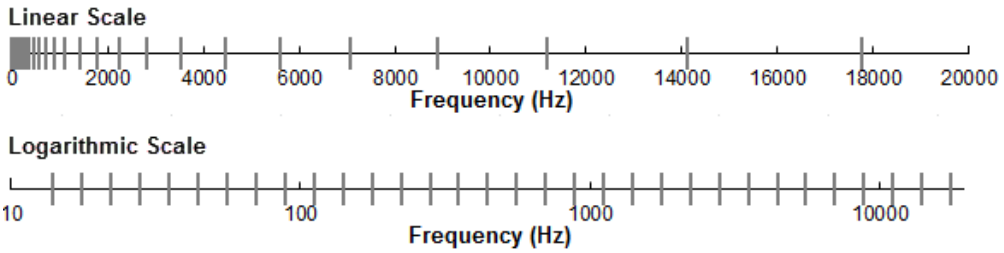

Figure 11. One-third-octave-bands shown on a linear frequency scale and on a logarithmic scale.

The SPL in the *i*th 1/3-octave-band $(L_b^{(i)})$ is computed from the power spectrum $S(f)$ between f_{lo} and f_{hi}:

$$L_{\mathrm{b}}^{(i)} = 10\log_{10}\left(\int_{f_{lo}}^{f_{hi}} S(f)\,df\right) \tag{13}$$

Summing the SPL of all the 1/3-octave-bands yields the broadband SPL:

$$\text{Broadband SPL} = 10\log_{10}\sum_i 10^{L_{\mathrm{b}}^{(i)}/10} \tag{14}$$

Figure 12 shows an example of how the 1/3 octave band SPLs compare to the power spectrum of an ambient noise signal. Because the 1/3 octave bands are wider with increasing frequency, the 1/3 octave band SPL is higher than the power spectrum, especially at higher frequencies. Acoustic modelling of 1/3 octave bands require less computation time than 1 Hz bands and still resolves the frequency-dependence of the sound source and the propagation environment.

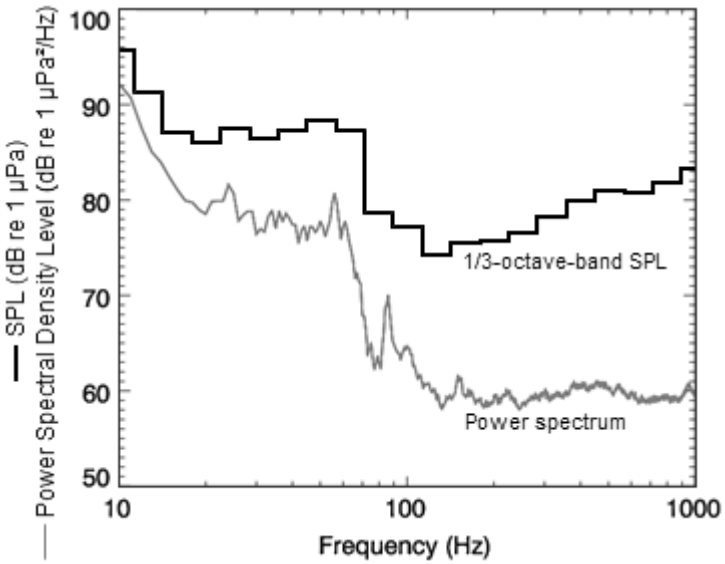

Figure 12. A power spectrum and the corresponding 1/3-octave-band SPLs of ambient noise shown on a logarithmic frequency scale.

2.3.4.3. Sound Level Statistics

Sound level statistics quantify the observed distribution of recorded sound levels. Following standard acoustical practice, the *n*th percentile level (L_n) is the spectral density, SPL or SEL exceeded by *n*% of

the data. L_{max} is the maximum recorded sound level. L_{mean} is the linear arithmetic mean of the sound power, which can be significantly different from the median sound level (L_{50}). In this report, the median level is used to compare the most typical sound level between stations, since the median is not as affected by high outliers as the mean sound level. L_5, the level exceeded by only 5% of the data, generally represents the highest typical sound levels measured. Sound levels between L_5 and L_{max} are due to close passes of vessels, intense weather, or other abnormal conditions. L_{95} represents the quietest typical conditions.

3. Results

3.1. Environmental Data

3.1.1. Tide Height

The tidal station closest to the Barossa area is located at Darwin, approximately 300 km south of the Barossa area. Tidal height data were collected from this station (Figures 13 and 14). During Deployment 1, the mean tidal difference was 4.06 m and the minimum tidal range was 0.58 m. the mean tidal difference was 4.10 m and the minimum tidal range was 0.53 m.

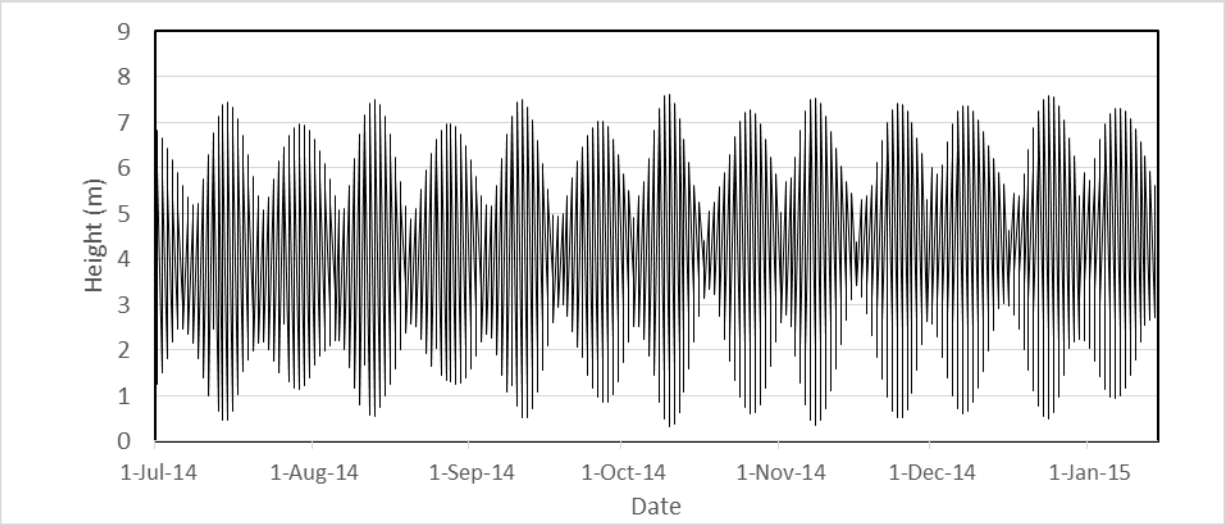

Figure 13. Low and high tide heights (m) at Darwin tidal station 10 July 2014 to 15 January 2015.

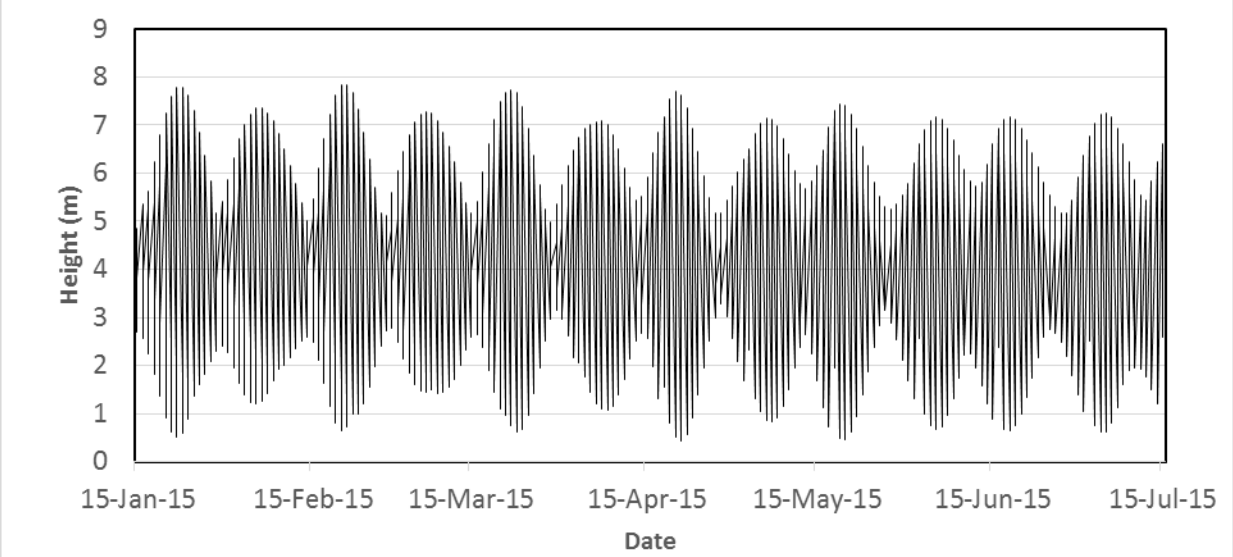

Figure 14. Low and high tide heights (m) at Darwin tidal station 15 January 2015 to 15 July 2015.

3.1.2. Wind Speed

Wind speed data were collected from the Fugro metbouy M1, located at 09° 49.122' S, 130° 18.708' E, close to Station J2, the data is shown in Figure 15. During Deployment 1, the mean wind speed

was 6.7 m/s (24.1 km/h), the maximum wind speed of 20.5 m/s (73.84 km/h) was recorded on 31 December 2014. During Deployment 2, the mean wind speed was 7.3 m/s (26.4 km/h), the maximum wind speed of 21 m/s (75.5 km/h) was recorded on 23 March 2015.

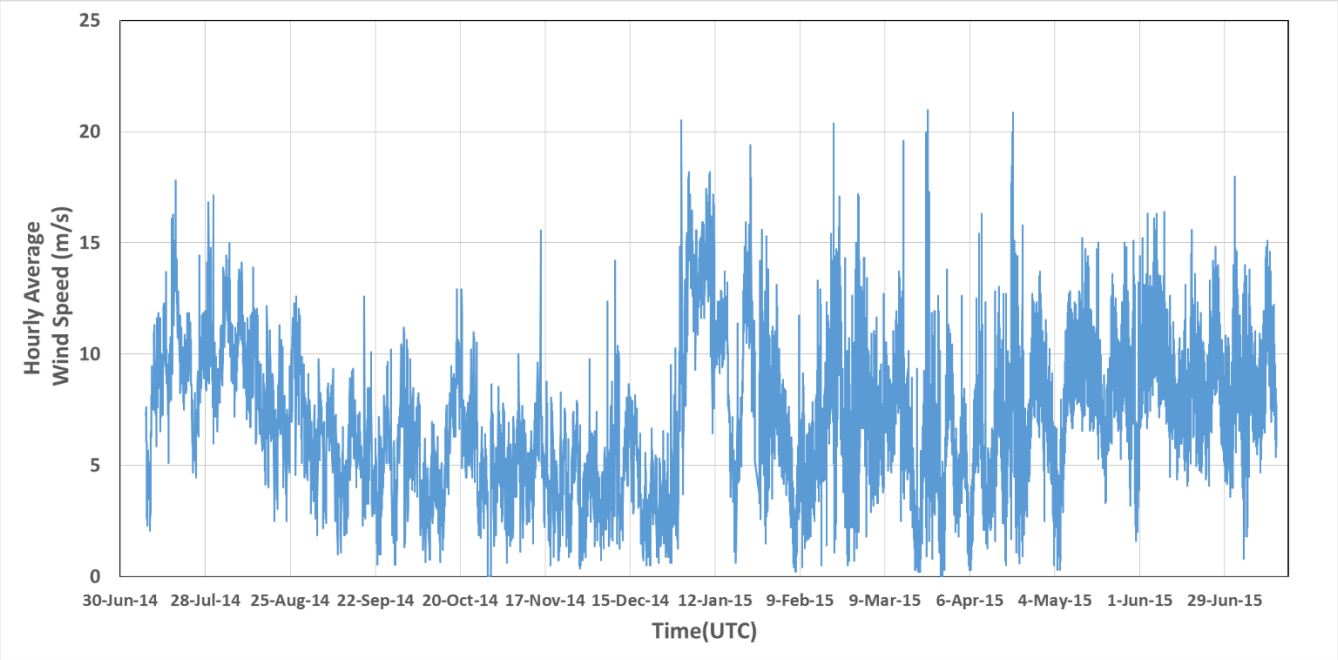

Figure 15. Daily average wind speed recorded at Fugro's M1 metbuoy 8 July 2014 to 15 July 2015.

3.1.3. Wave Height

Wave height data were collected from the Fugro waverider buoy W1, located at 09° 49.115' S, 130° 17.773' E in 260 m of water. During Deployment 1, the mean significant wave height was 1.10 m, while the mean maximum wave height was 1.68 m, the maximum wave height of 5.31 m was recorded on 9 January 2015 (Figure 16). During Deployment 2, the mean significant wave height was 1.28 m, while the overall mean maximum wave height was 2.96 m, the maximum wave height of 5.2 m was recorded on 15 May 2015 (Figure 16).

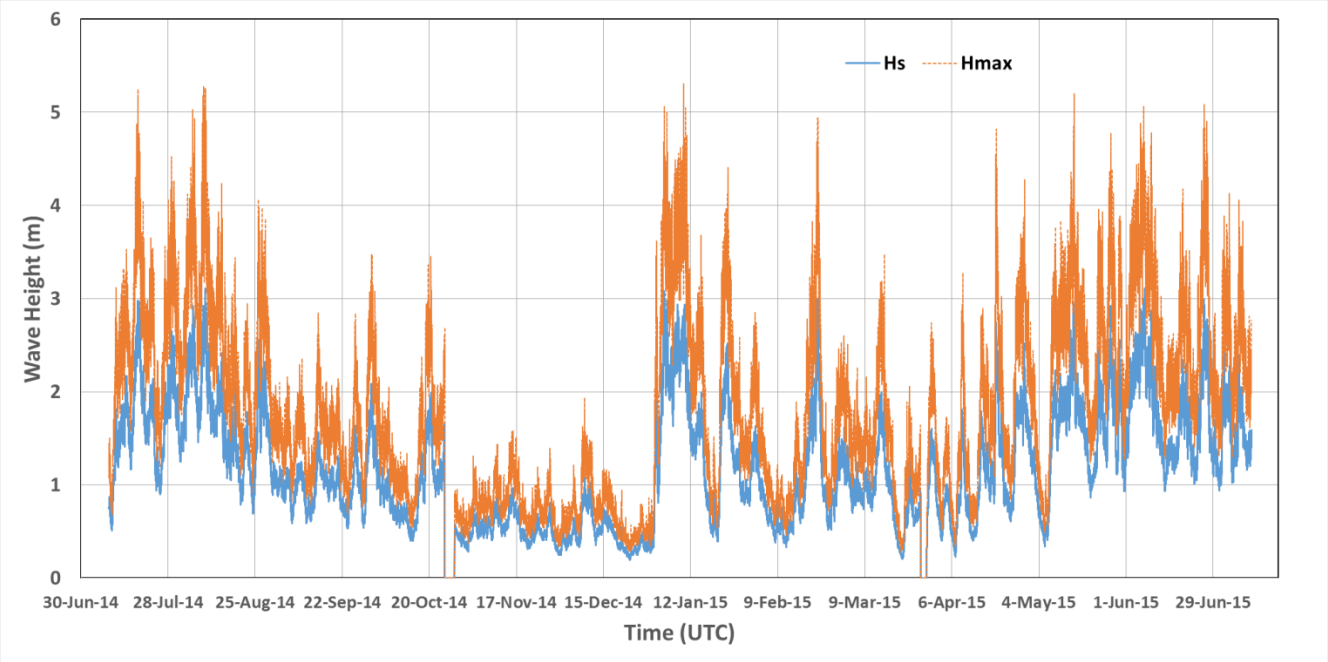

Figure 16. 10-minute wave heights recorded at Fugro's W1 waverider buoy 9 July 2014 to 11 July 2015.

3.2. Marine Fauna

This scope of the acoustic monitoring study did not include detailed manual analysis; instead, JASCO calibrated the automated detection process by manually reviewing 2041 files resulting in over 320 hours of recordings reviewed (Table 7; see Section 2.3.1.3). These files contained pygmy blue whale moans, unidentified baleen whale moans, beaked whale clicks, and unidentified odontocete clicks and whistles. JASCO did not observe humpback whale moans or sperm whale clicks during the manual review.

Table 7. The number of 48 and 250 ksps files manually analysed for deployments 1 and 2 at Stations J1, J2, and J3 recorded in the Timor Sea.

Sampling rate (ksps)	Deployment 1			Deployment 2		
	J1	J2	J3	J1	J2	J3
48 (14min/file)	130	128	129	135	136	136
250 (1min/file)	121	111	110	123	127	125

3.2.1. Detector thresholds

The manual validation results were compared to the automated results for the same files to generate classification thresholds for the manually detected calls (Table 8). The thresholds are the number of automated detections/file (14 min 48 ksps file for mysticete calls and 1 min 250 ksps file for odontocete calls) that provide a high confidence that the species are truly present. The selected thresholds provide a precision of 0.97 for blue whale moans, 0.90 for double-barrel/long calls, 0.55 for downsweeps, 0.75 for beaked whale clicks, 0.92 for odontocete clicks, and 0.88 for whistles (Table 8). These thresholds were applied to the automated detections. Note that the selected thresholds also translate into recall values near 50-60%, which suggest that our method underestimates (conservative) acoustic occurrence and that isolated detections outside of the main period of occurrence could be overlooked.

Table 8. Classification thresholds determined from validating the automated detector outputs. The classification thresholds are the minimum number of detected calls/file required to be confident that detections are not false alarms. The precision (P), recall (R), and F-score (F) before the threshold is applied (original) and after (threshold) is shown.

Vocalisations	$P_{original}$	$R_{original}$	Classification threshold	$P_{threshold}$	$R_{threshold}$	$F_{threshold}$
Pygmy blue whale	0.63	0.82	6	0.97	0.64	0.88
Double-barrel/long monotonic	0.57	0.98	11	0.90	0.60	0.82
Downsweep	0.41	0.61	5	0.55	0.52	0.54
Beaked whale	0.25	0.83	11	0.75	0.50	0.68
Clicks	0.79	0.99	67	0.92	0.89	0.91
Whistles	0.88	0.46	2	0.88	0.46	0.75

3.2.2. Mysticetes

3.2.2.1. Pygmy Blue Whales

3.2.2.1.1. Manual Detections

Pygmy blue whale calls were positively identified during the manual validation of automatic detections based on similarities with previous descriptions (e.g. Gavrilov et al. (2011)). Detections occurred mostly during Deployment 2, when calls were observed over 10 days at Station J1, 7 days at Station J2, and 6 days at Station J3 (Figure 17). One validated detection also occurred at J2 on 2 August 2014. The calls were typically organised into songs, as described by McDonald et al. (2006), Gavrilov et al. (2011). A segment of a pygmy blue whale song composed of two notes is shown in Figure 18. The call has a frequency bandwidth of 77 Hz (15–92 Hz) and a time period of 24 s. Calls had most energy at ~20 Hz and 50–70 Hz and lasted for 15–25 ss. Some calls were detected at all three stations simultaneously (Figure 19). While the time axis is shown as synchronised, the stations have not been synchronised to the point of being able to localise the calling animal.

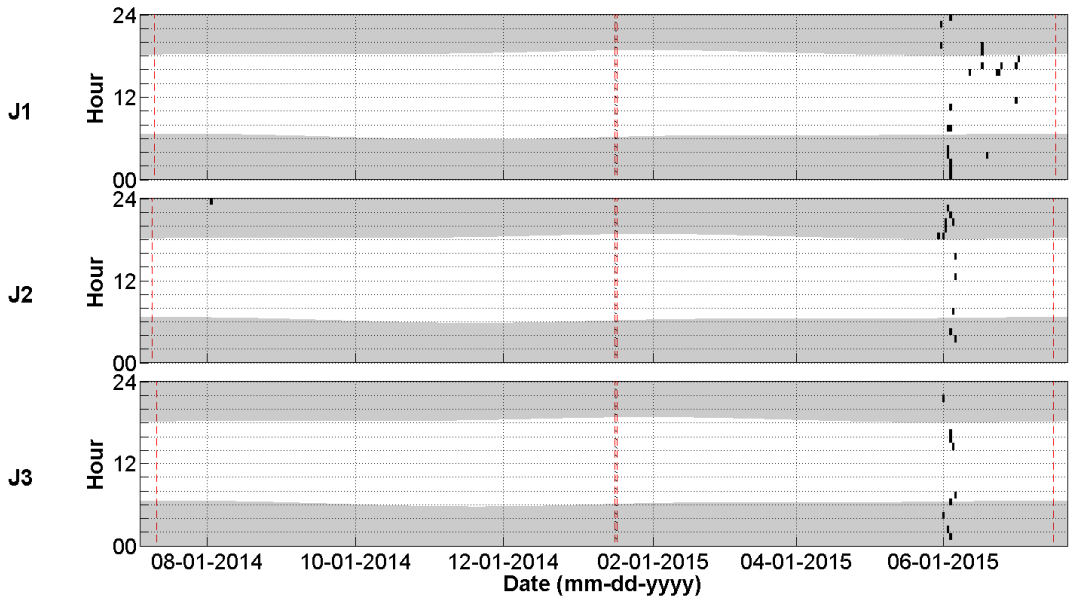

Figure 17. Presence of manually validated pygmy blue whale calls (normalised on a 0.5 h basis) at Stations J1, J2, and J3 from July 2014 to July 2015 in the Timor Sea. The grey areas indicate hours of darkness from sunset to sunrise (Ocean Time Series Group 2009). The red dashed lines indicate the start and end of recording time.

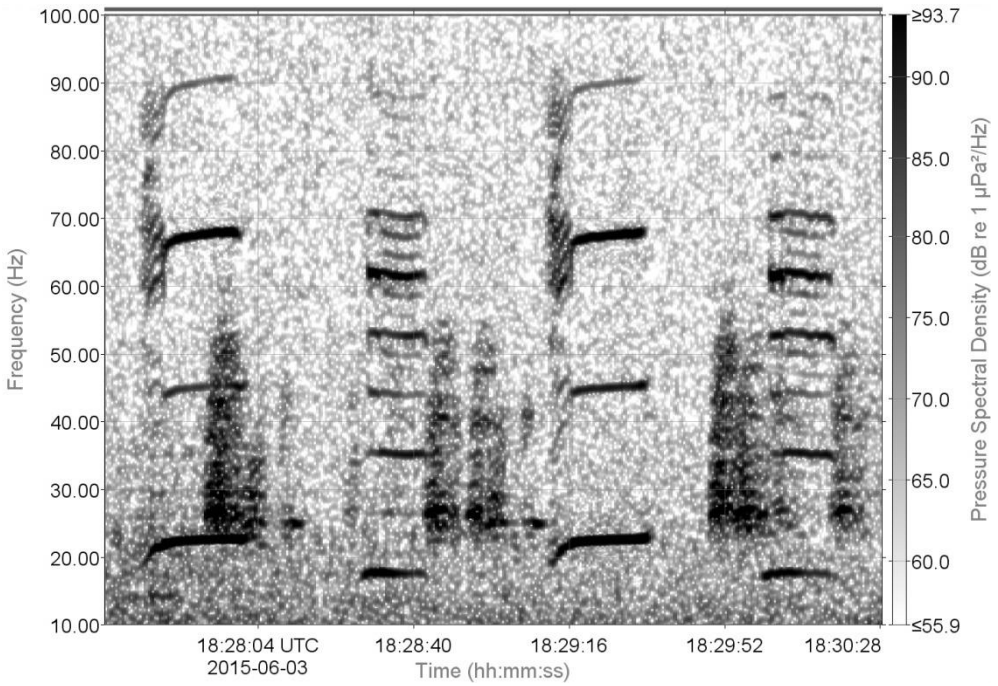

Figure 18. Spectrogram of pygmy blue whale songs showing two repetitions of each call type in sequence and Omura's whale calls in the background, recorded at Station J2 on 3 June 2015 (UTC) (0.0916 Hz frequency resolution, 2 s time window, 0.5 s time step, Hamming window).

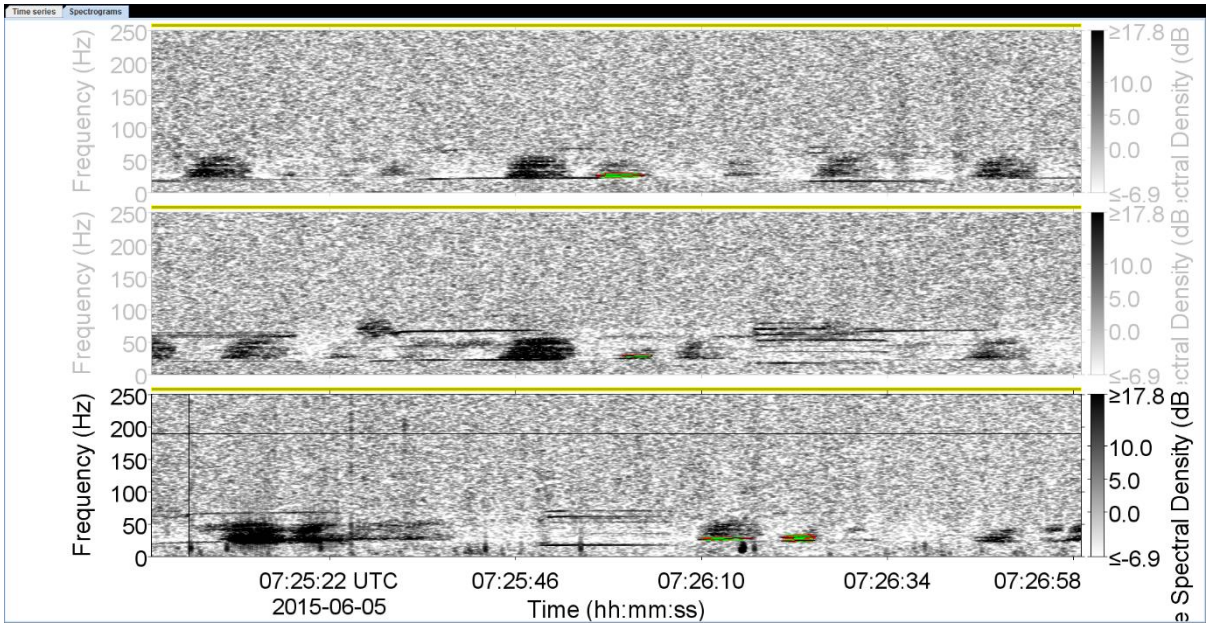

Figure 19. Spectrogram of pygmy blue whale calls recorded at Station (top) J1, (centre) J2 and (bottom) J3 on 5 June 2015 (UTC) (0.5 Hz frequency resolution, 0.5 s time window, 0.05 s time step, and Hamming window).

3.2.2.1.2. Automated Detections

Pygmy blue whales were automatically detected primarily from 29 May to 5 June 2015 (Figures 20 and 21). Detections that occurred outside of this period were verified for pygmy blue whale call absence/presence. A single automated detection at Station J3 on 15 February 2015 was found to be falsely triggered by noise. In contrast, detections on 16 and 30 June 2015 as well as 1 July 2015 were verified as true pygmy blue whale calls. Call detections were greatest at the deepest station, J2, at Barossa field, and lowest at the shallowest station, J3, at Caldita field (Table 9 and Figure 22). No obvious diurnal pattern was observed. It is worth noting that based on manual analysis results and a detector recall of 0.64 (Table 8), the automated detector failed to detect pygmy blue whales on a few days in June when pygmy blue whales were present in the vicinity of Station J1 as determined through manual analysis (Figure 17).

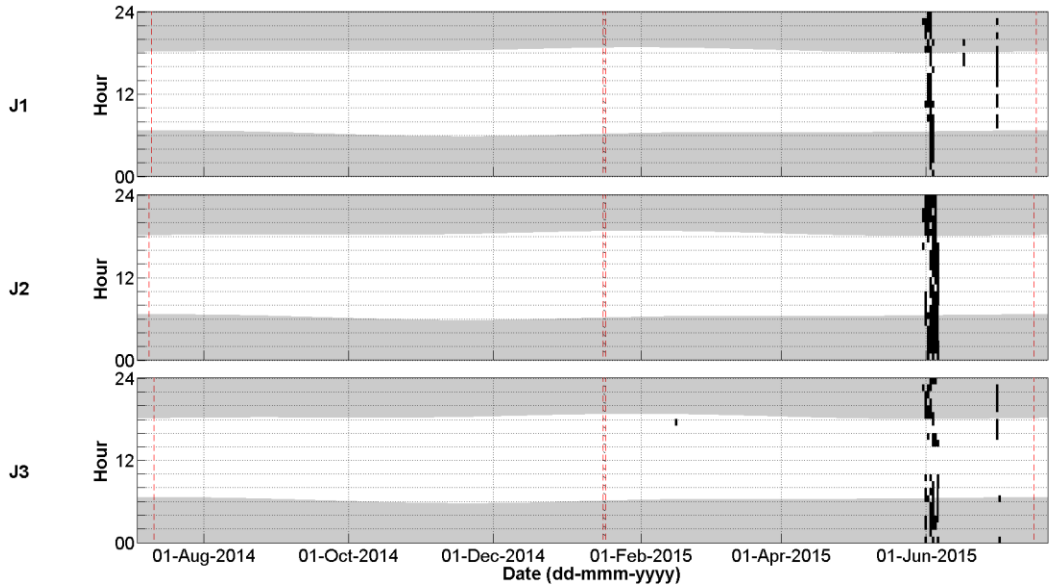

Figure 20. Hourly (expressed as an index) and daily presence of automatically detected pygmy blue whale calls at Stations J1, J2, and J3. Presence of automatically detected pygmy blue whales (normalised on a 1 h basis). The grey areas indicate hours of darkness from sunset to sunrise (Ocean Time Series Group 2009). The red dashed lines indicate the start and end of recording time.

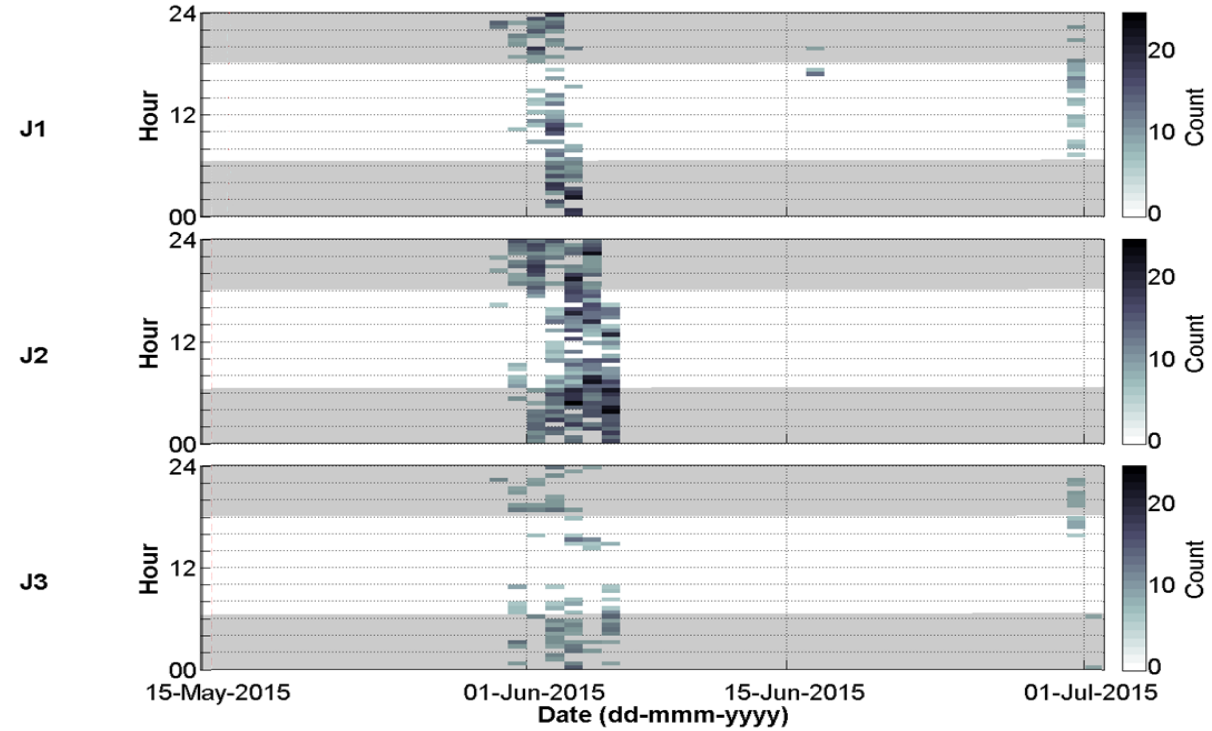

Figure 21. Hourly (expressed as an index) and daily number of automatically detected pygmy blue whale calls at Stations J1, J2, and J3 from 15 May to 1 Jul 2015. Count of automatically detected blue whales (normalised on a 0.5 h basis). The grey areas indicate hours of darkness from sunset to sunrise (Ocean Time Series Group 2009).

Table 9. Pygmy blue whale detection summary

Station	Total detection days	Pygmy blue whale moan detections
Deployment 1, 10–11 Jul 2014 to 15 Jan 2015		
J1	0	0
J2	1	1
J3	0	0
Deployment 2, 16–17 Jan to 15–16 Jul 2015		
J1	7	905
J2	7	2060
J3	9	659

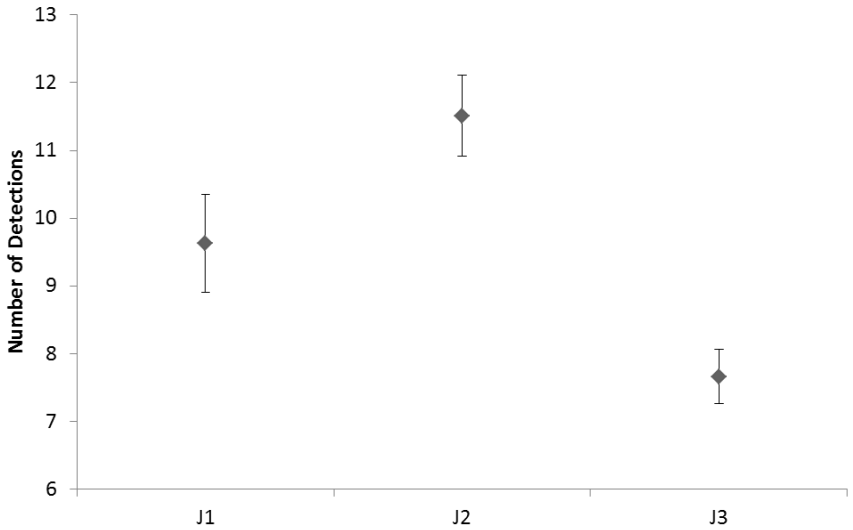

Figure 22. Mean number of pygmy blue whale call detections per 14 min 48 ksps sample for samples with at least 1 detection with 95% confidence intervals for Stations J1, J2, and J3.

A more detailed examination of the June peak in detections revealed that pygmy blue whale call SPLs at all stations had similar variations about the mean station call SPL during the nine days of recordings when calls were detected (Figure 23).

The first main group of calling pygmy blue whales were detected on 31 May initially at Station J1, followed by Station J3, and finally noticeably louder calls were detected at Station J2. Over 5 hours later the second main group was detected, again initially at Station J1, before being detected at Station J3 and finally only Station J2. For the remainder of 1 June and the entirety of 2 June calls were detected almost continuously at all three stations, with detections at Stations J1 and J3 being consistently louder than those of Station J2 for the majority of 2 June. Detections ceased at Station J1 on 3 June. Calls continued to be detected at Station J2, with sporadic detections at Station J3, until the morning of 5 June when the last calling activity was detected at Station J2 (Figure 24).

After the initial detections, pygmy blue whale calls were not detected again until the morning of 16 June at Station J1 (Figure 23). A similar detection event occurred at Station J1 in the night of 29 June (Figures 23 and 25). The final pulse of calls was detected on 30 June at Station J1 followed closely by Station J3. Station J1 calls showed a slight decrease in relative loudness from when they began at 02:23 to when they ceased at 12:01. In contrast, Station J3 calls increased gradually in loudness from when they were first detected at 08:20 to when they were last detected at 15:31 (Figure 25).

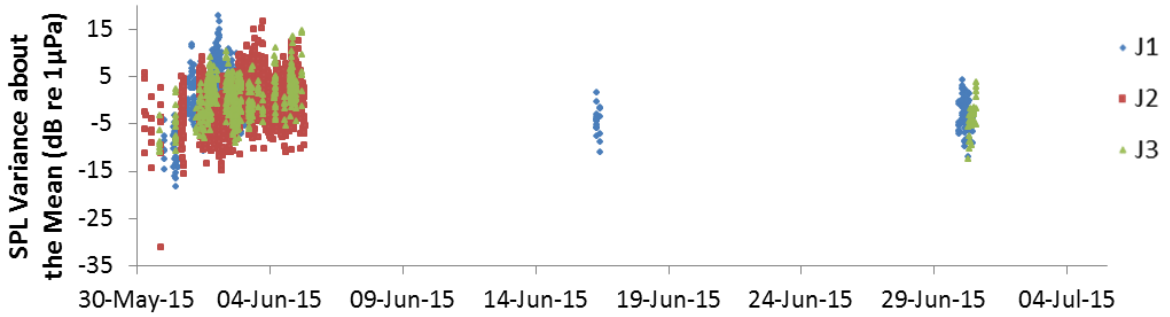

Figure 23. Plot of pygmy blue whale call SPLs above and below the mean call SPL/station for Stations J1, J2, and J3 from 30 May to 4 July 2015.

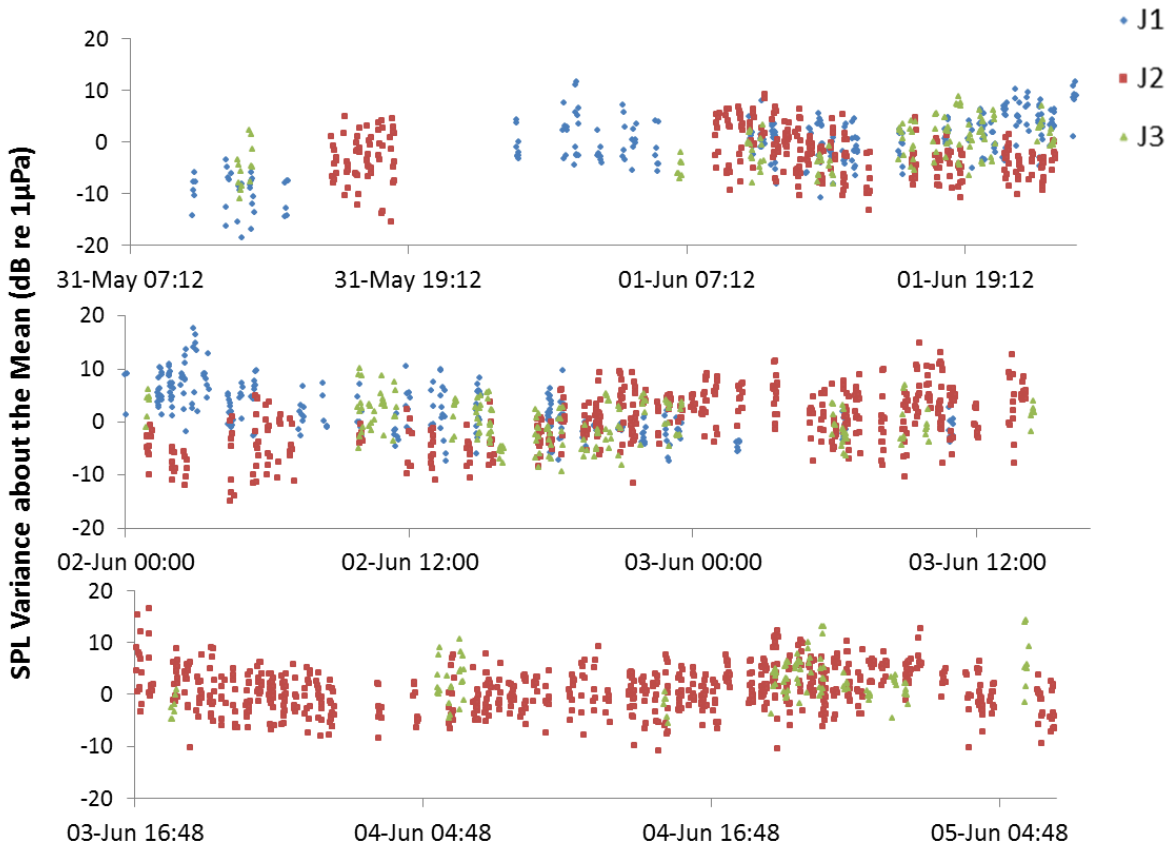

Figure 24. Plot of pygmy blue whale call SPLs above and below the mean call SPL/station for Stations J1, J2, and J3 from 31 May 2015 to 1 June 2015 (top), 2 June to 3 June 2015 (middle), and 3 June to 5 June (bottom).

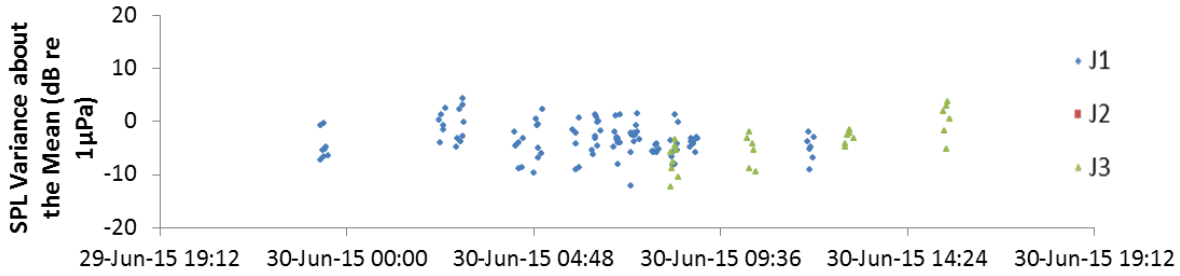

Figure 25. Plot of pygmy blue whale call SPL above and below the mean call SPL/station for stations J1, J2, and J3 from 30 June to 1 July 2015.

3.2.2.1.3. Regional use approximation

To provide some context about the possible migration path of the pygmy blue whales, an estimate of the distance of pygmy blue whales from Station J2 using the minimum, median and maximum received call levels determined through analysis of the automated detections was performed.

Along with the received call levels (Table 10), the source levels from literature of 183 dB re 1 µPa SPL (McCauley et al. 2001) and 179 dB re 1 µPa SPL (Gavrilov et al. 2011) were used. An estimated whale depth of 40 m was selected based on the commonly reported depth of a calling blue whale of 40 m (Thode et al. 2000), and used with a transmission loss curve derived from running JASCO's Marine Operations Noise Model (MONM) over a single transect line at a bearing of 303.96°, taking advantage of the theory of reciprocity. The exact migration path of the whales is unknown, and while a single transect is not accurate, it allows for a comparison of possible distances from Station 2 to the whales. It has been assumed that the whales were migrating offshore from the recorders, in the direction of the trench, the bearing selected is the bearing from Station J2 to the nearest section of the continental slope.

An eigenray is defined as a ray that connects a source position with a receiver position. The principle of reciprocity is applicable for a point-to-point situation, and is where the eigenrays from a source position to the receiver position are the same as when source and receiver change positions. The reflections of the eigenrays at the sea surface and sea floor are symmetric in angles, and therefore the acoustic fields are the same.

The calculated distances of the pygmy blue whales from Station J2 along the selected transect range, are shown in Table 11.

Table 10. Pygmy blue whale call modelling parameters

Call SL (dB)	Received Level (dB)			Call depth (m)	Call Frequency (Hz)	Modelled 1/3 Octave band centre Frequency (Hz)
	Minimum	Median	Maximum			
179	62.8	93.9	110.5	40	20	20
183						

Table 11. Pygmy blue whale distance estimation (km)

Call SL (dB)	Estimated Distance (km)		
	Min. received level	Median received level	Max. received level
179	$8.0x10^4$	$2.3x10^4$	5
183	$>8.0x10^4$	$3.1x10^4$	9

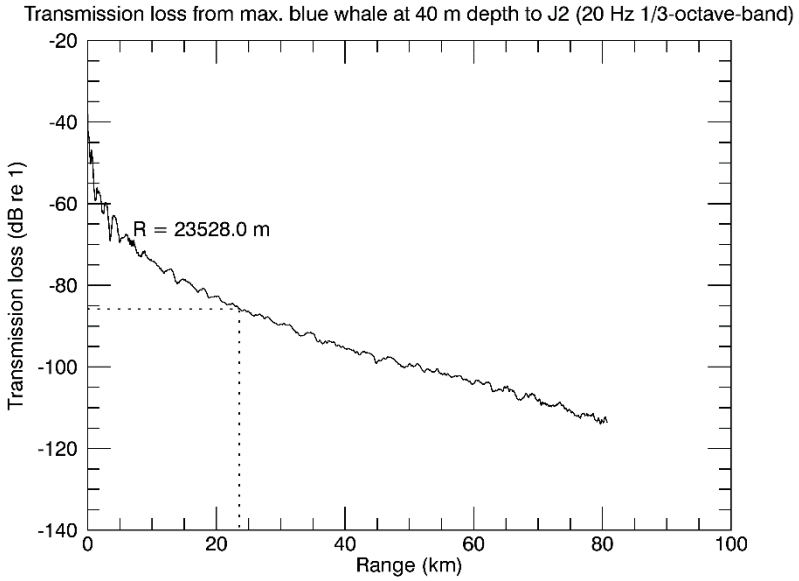

Figure 26. Example transmission loss modelling results for median received pygmy blue whale call using source level 179 dB, using a 1/3 octave band centred at 20 Hz.

3.2.2.2. Omura's and Bryde's Whales

3.2.2.2.1. Manual Detections

Three initially unidentified baleen whale call types were regularly observed: double-barrel moans (Figure 28), long monotonic moans (Figure 30), and downsweeps (Figure 32). The double-barrel calls often occurred in sequence with the monotonic calls suggesting that these two calls were produced by the same species/individuals. Because of their similarities, double-barrel and long calls were both detected by the same automated detector and will therefore be discussed jointly in Section 3.2.2.2.2. Downsweeps almost always occurred within the same file as the other calls, but it was not until a more detailed analysis on the detections occurred that it became apparent they are likely from a different whale to the double-barrel and long monotonic calls. The justification for the attribution of the double-barrel moans and long monotonic calls to Omura's whales and the downsweeps to Bryde's whales is provided in Section 4.1.1.2.

Double-barrel Omura's calls were primarily observed in the months of May-August on 34 days at Station J1, 28 days at J2, and 38 days at J3 (Figure 27). Calls were comprised of three distinct parts: 1) a 6–9 s long 26–28 Hz call, 2) a 2–3 s long 40 Hz call occurring simultaneously above 3) a 2–3 s 26–28 Hz call where calls 1 and 2 were separated by 3–4 s (Figure 28).

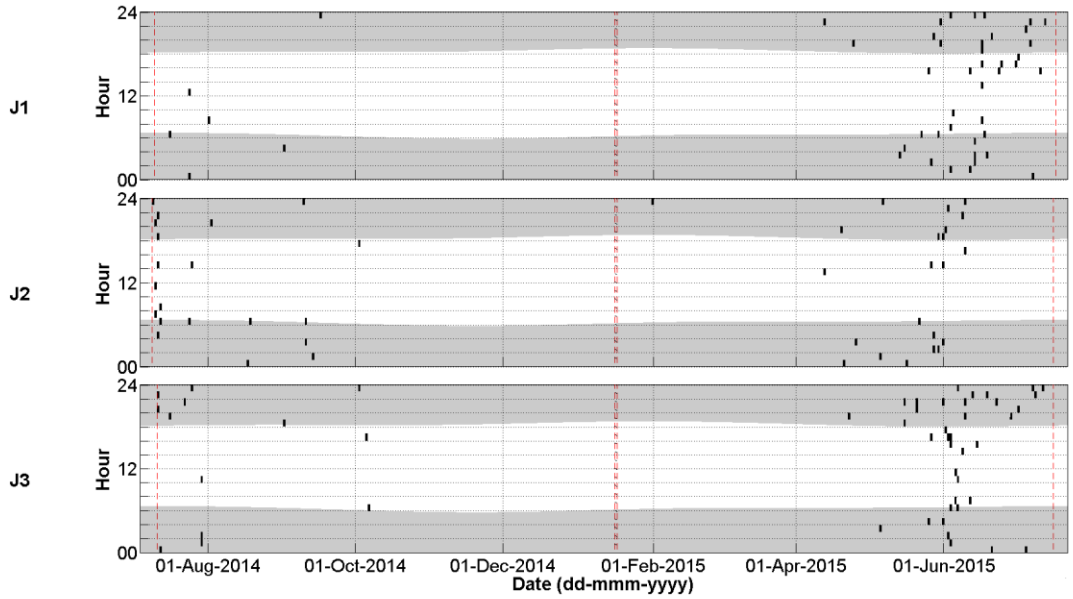

Figure 27. Presence of manually validated double-barrel Omura's whale calls (normalised on a 0.5 h basis) at Stations J1, J2, and J3 from July 2014 to July 2015 in the Timor Sea. The grey areas indicate hours of darkness from sunset to sunrise (Ocean Time Series Group 2009). The red dashed lines indicate the start and end of recording time.

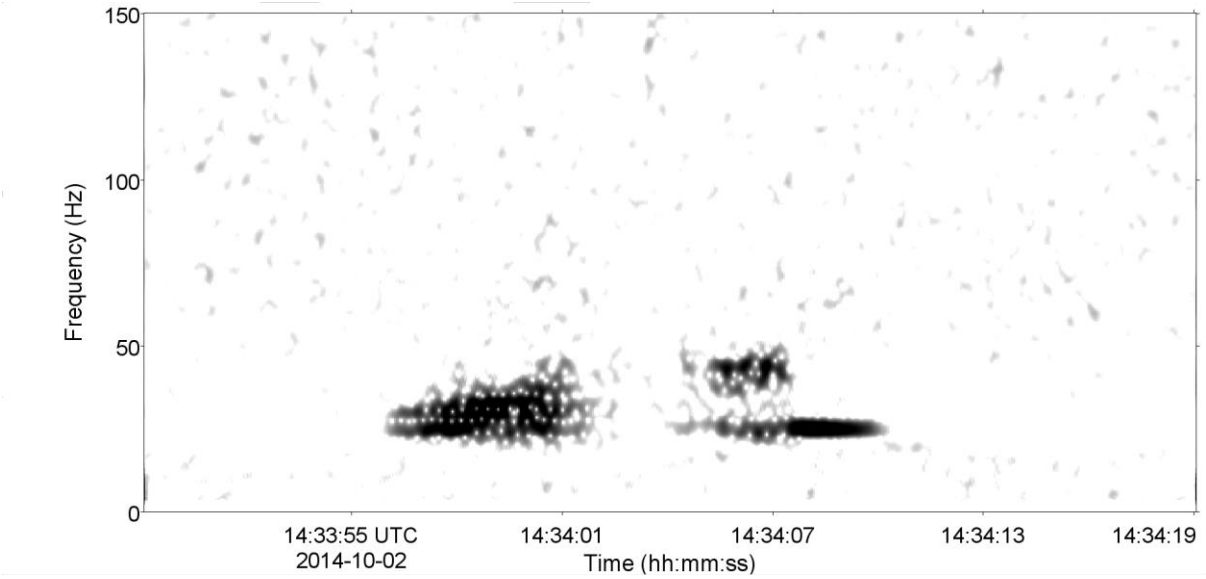

Figure 28 Spectrogram of a double-barrel Omura's whale call recorded at Station J1 on 2 October 2014 (UTC) (0.5 Hz frequency resolution, 0.5 s time window, 0.05 s time step, and Hamming window).

Long monotonic Omura's calls were manually observed on 66 days at Station J1, 73 days at J2, and 58 days at J3. While the call type occurred in all recorded months, it was more abundant in April to August (Figure 29). Long monotonic calls had a centroid frequency of 26–28 Hz and duration of 6–10 s (Figure 30).

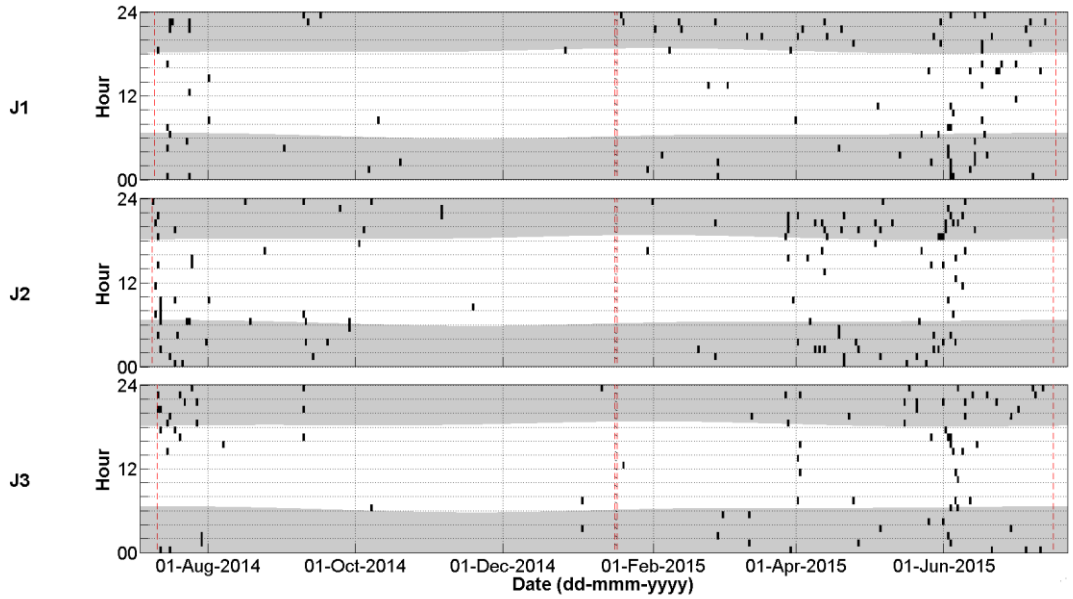

Figure 29. Presence of manually validated long monotonic Omura's whale calls (normalised on a 0.5 h basis) at Stations J1, J2, and J3 from July 2014 to July 2015 in the Timor Sea. The grey areas indicate hours of darkness from sunset to sunrise (Ocean Time Series Group 2009). The red dashed lines indicate the start and end of recording time.

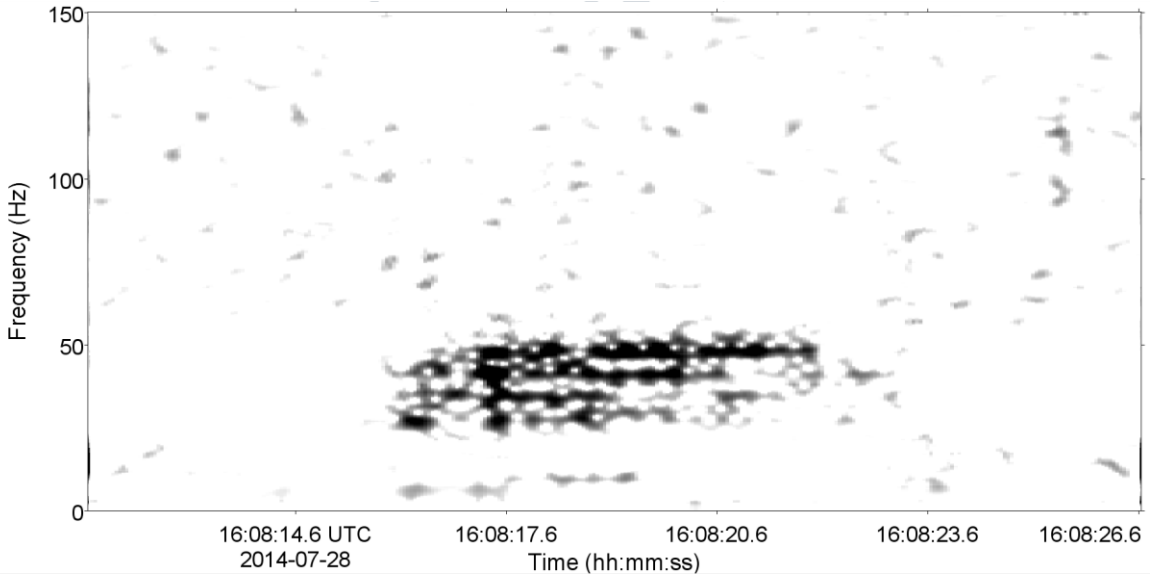

Figure 30. Spectrogram of a long monotonic Omura's whale call recorded at Station J3 on 28 July 2014 (UTC). (0.5 Hz frequency resolution, 0.5 s time window, 0.05 s time step, and Hamming window).

Bryde's whale downsweeping moans were not observed as frequently as either the double-barrel or long monotonic calls. Downsweeps were manually detected on 19 days at Station J1, 16 days at J2, and 10 days at J3. Detections occurred sporadically throughout the year with an increase in early June at Station J2 (Figure 31). A downsweeping moan is shown in Figure 32. These moans decreased from 150 to 40 Hz and lasted for 0.5–2 s.

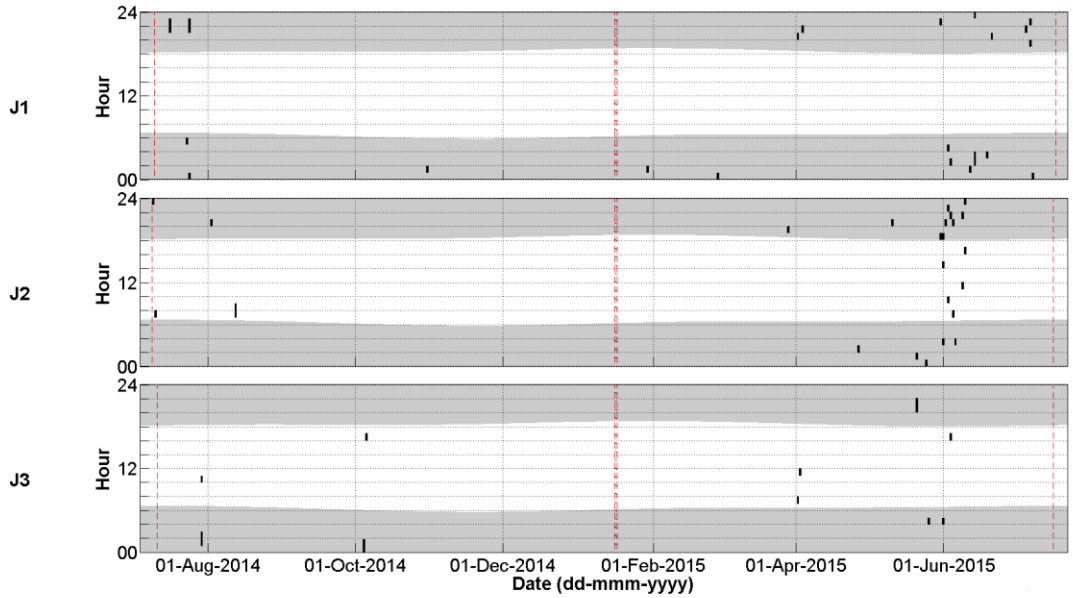

Figure 31. Presence of manually validated downsweeping Bryde's whale calls (normalised on a 0.5 h basis) at Stations J1, J2, and J3 from July 2014 to July 2015 in the Timor Sea The grey areas indicate hours of darkness from sunset to sunrise (Ocean Time Series Group 2009). The red dashed lines indicate the start and end of recording time.

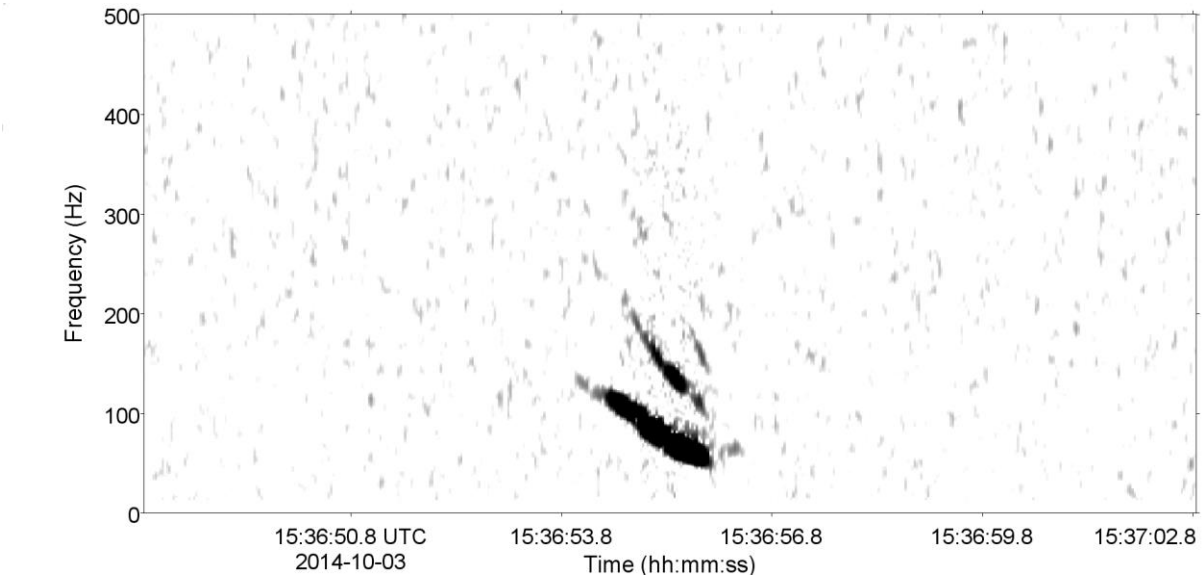

Figure 32. Spectrogram of a downsweeping Bryde's whale call recorded at Station J3 on 3 October 2014 (UTC) (2 Hz frequency resolution, 0.128 s time window, 0.032 s time step, and Hamming window).

3.2.2.2.2. Automated Detections

Detections of the double-barrel/monotonic Omura's calls were higher at Stations J1 (off Evans Shoal) and J2 (at the Barossa field) than Station J3 (Caldita field) for Deployment 1, but higher at Stations J1 and J3 for Deployment 2 (Table 12). The latter is largely due to a hydrophone interference issue at Station J2 (see Section 3.3.1) introducing low frequency noise to the data and preventing the detection of these calls in the associated frequency bands after 10 June. The mean call rate (calls/14 min) was greater during deployment 2 and was consistently higher at the deepest station (J2) than either J1 or J3 during both deployments (Figure 33). Across all stations, detections of Omura's and Bryde's calls were most common from May to July, while after November 1, no Omura's calls were

detected until late December (Figure 34), and no Bryde's whale calls were detected from mid-October until early January (Figure 38). No obvious diurnal pattern was observed.

Table 12. Omura's and Bryde's whale detection summary.

Station	Total detection days	Days with Omura's whale double barrel/monotonic calls	Days with Bryde's whale downsweep calls
Deployment 1, 10–11 Jul 2014 to 15 Jan 2015			
J1	59	55	9
J2	58	57	6
J3	34	27	9
Deployment 2, 16–17 Jan to 15–16 Jul 2015			
J1	154	148	51
J2	100	97	16
J3	119	108	28

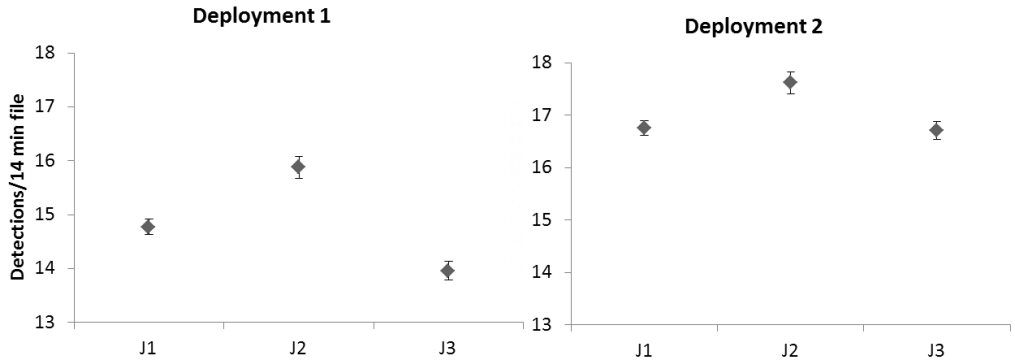

Figure 33. Mean number of Omura's whale double-barrel/monotonic call detections per 14 min 48 ksps sample for samples with at least 1 detection with 95% confidence intervals for Stations J1, J2, and J3 during both deployments.

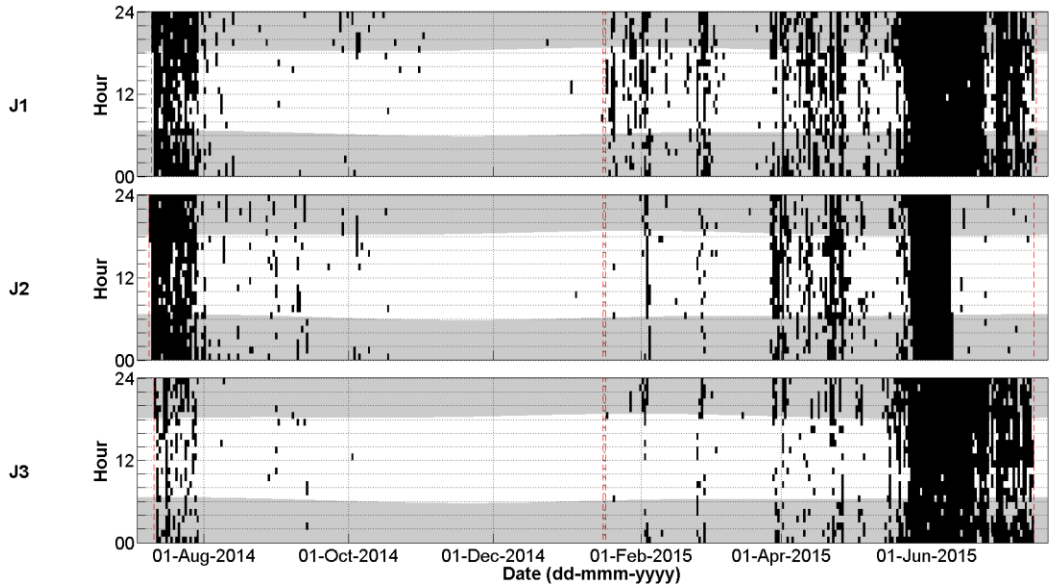

Figure 34. Hourly (expressed as an index) and daily presence of automatically detected Omura's whale double barrel/monotonic calls at Stations J1, J2, and J3. Presence of automatically detected calls normalised on a 1 h basis. The grey areas indicate hours of darkness from sunset to sunrise (Ocean Time Series Group 2009). The red dashed lines indicate the start and end of recording time.

Omura's whale double-barrel/monotonic call SPLs at Stations J1, J2, and J3 overall had similar variation about the mean call SPL/station (Figure 35). From the beginning of the recording period to the end of July 2014 calls were detected continuously at all stations (Figure 35). Call regularity began to decrease in August 2014 with the calls first ending at Station J3 on 2 October, then at Station J2 on 16 October, and lastly at Station J1 on 1 November (Figure 36).

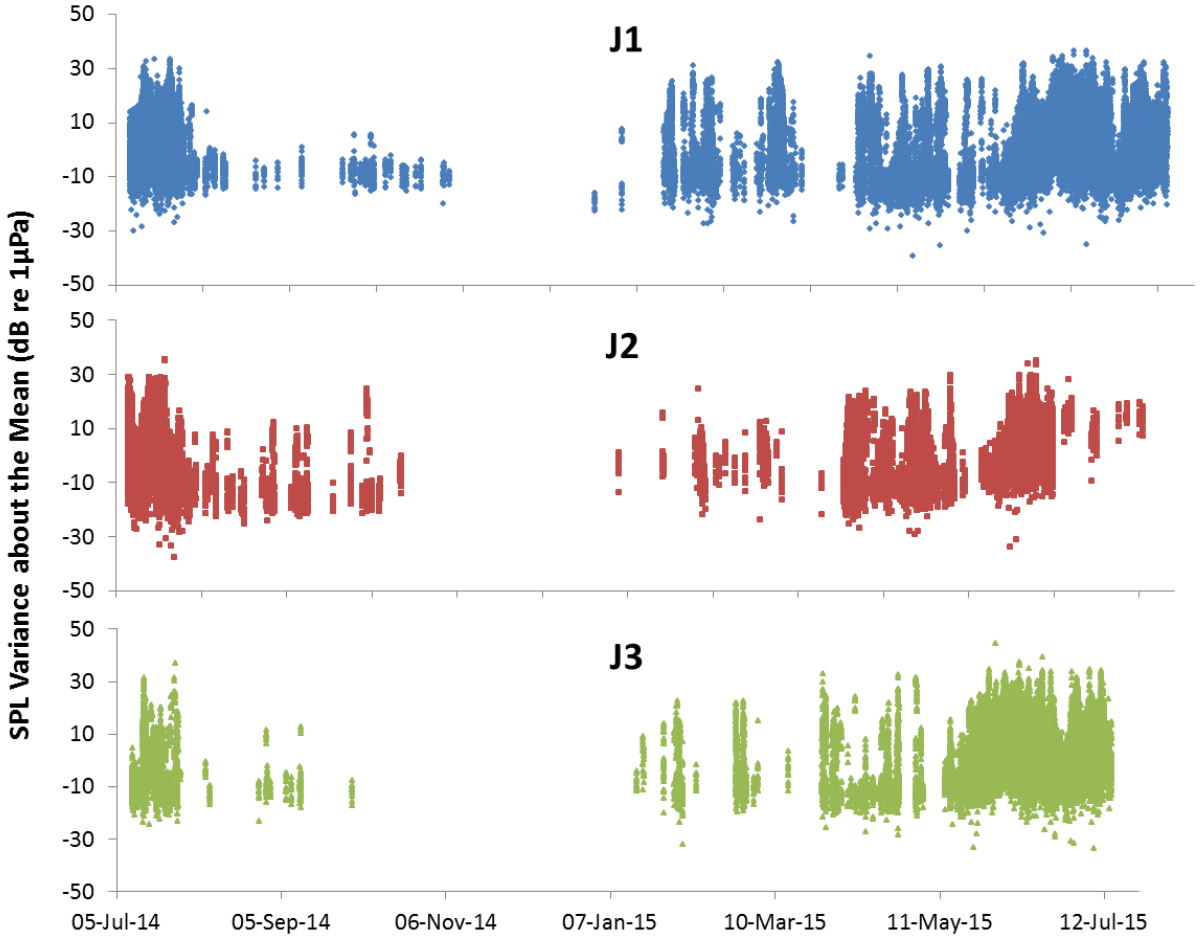

Figure 35. Plot of Omura's whale double-barrel/monotonic call SPL above and below the mean call SPL/station for Stations J1 (top), J2 (middle), and J3 (bottom) from 10 July 2014 to 15 July 2015.

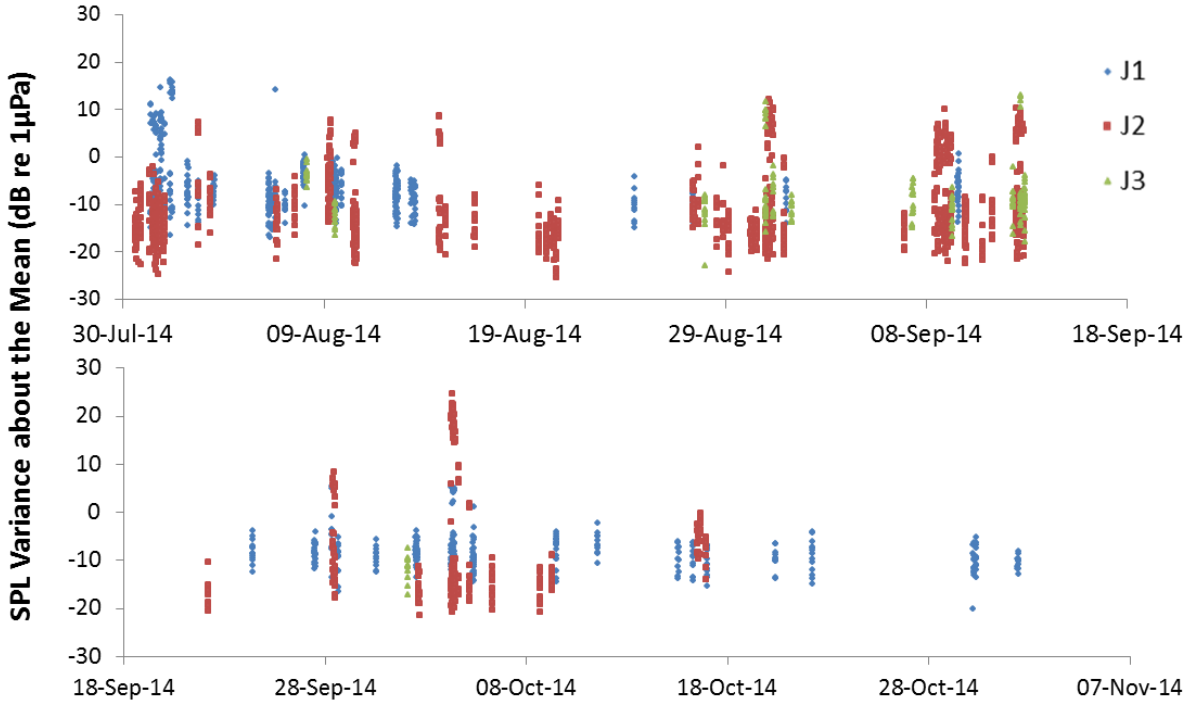

Figure 36. Plot of Omura's whale double-barrel/monotonic call SPL above and below the mean call SPL/station for Stations J1, J2, and J3 from 30 July to 18 September 2014 (top) and 18 Sept to 7 Nov 2014 (bottom).

Omura's whale double-barrel/monotonic calls were not detected again until late 2014 - early 2015 when they first occurred at Station J1 (23 December), followed by Station J2 (4 January) and finally Station J3 (17 January) (Figure 35 and Figure 37). The reoccurrence of double-barrel/monotonic calls came in a number of pulses. The first robust pulse of detections occurred from 17–21 January primarily at Station J1 (Figure 37). The second pulse began three days later when detections occurred at Station J1 from 24–29 January, with detections also at Station J3 on 27 January. The night of 30 January the third pulse was detected at Station J1 followed the next afternoon by detections at Stations J2 and J3, with the detection rate decreasing after 4 February. Detections were sporadic until 22 February when the number of detections increased. This appeared to represent a number of whales moving across the area, with the pulse subsiding on approximately 5 March. Detections were again sparse until 26 March when detections occurred across all stations and remained nearly constant until the end of recording in mid-July.

Figure 37. Plot of Omura's whale double-barrel/monotonic call SPL above and below the mean call SPL/station for Stations J1, J2, and J3 from 16 Jan to 10 Feb 2015 (top), 10 February to 7 March 2015 (middle), and 7 March to 1 April 2015 (bottom).

Bryde's whale downsweeping call detections were similar at all stations and more common during Deployment 2 (Figure 38, Table 12). While the mean call rate (detections/14 min) was slightly lower at Station J2 than either Stations J1 or J3, the difference wasn't significant (Figure 39). Calls occurred during two periods: July-October 2014 and January-July 2015 with no obvious diurnal pattern (Figure 44). In 2014 calls were initially detected solely at Station J2 on 9, 11, 12 June. Detections then occurred only at Station J1 on 16, 23, 24 June. Finally, they were detected only at Station J3 on 20 August, 30 September, and 3, 10 October 2014 (Figure 40). Downsweeps did not occur again until 2015 when they were first detected at Station J3 (6, 29 January, and 4, 22 February). Detections also began to occur at Station J1 on 26 February, and by 19 April were taking place semi-regularly at all three stations until the end of recording in mid-July. It is worth noting that in 2015 detected calls were consistently louder at Station J2 than either Station J1 or J3 (Figure 45).

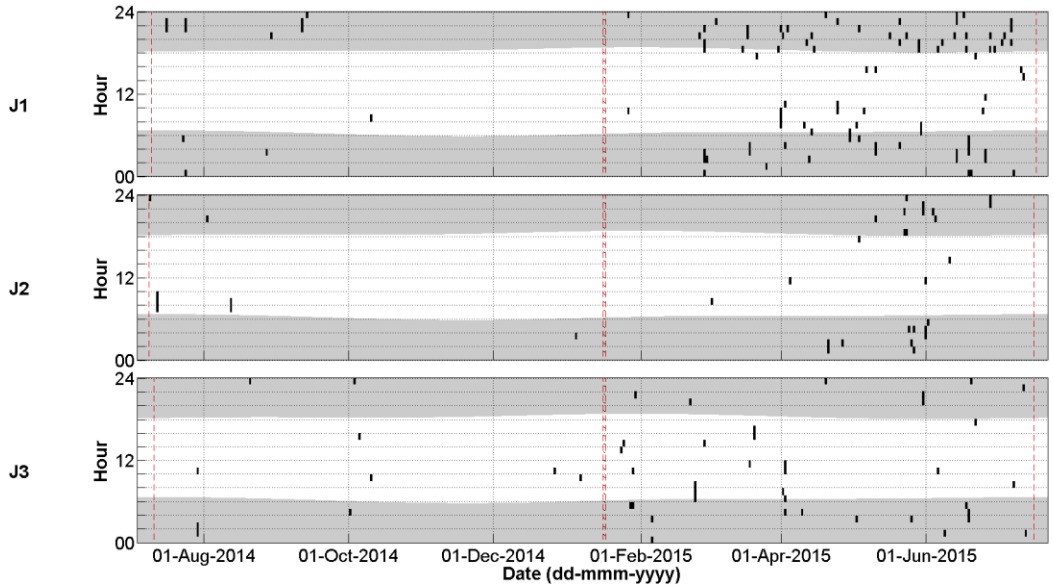

Figure 38. Hourly (expressed as an index) and daily presence of automatically detected Bryde's whale downsweep calls at Stations J1, J2, and J3. Presence of automatically detected calls normalised on a 1 h basis. The grey areas indicate hours of darkness from sunset to sunrise (Ocean Time Series Group 2009). The red dashed lines indicate the start and end of recording time.

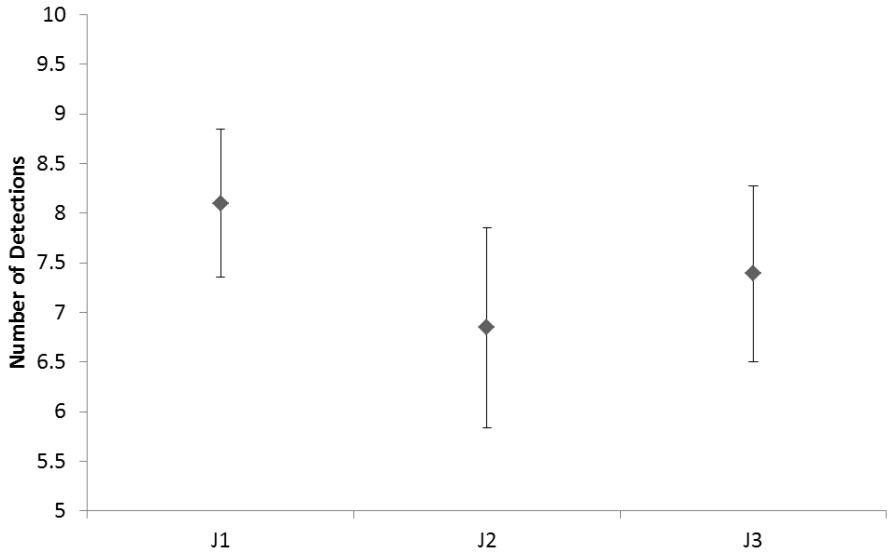

Figure 39 Mean number of Bryde's whale downsweeping call detections per 14 min 48 ksps sample for samples with at least 1 detection with 95% confidence intervals for Stations J1, J2, and J3.

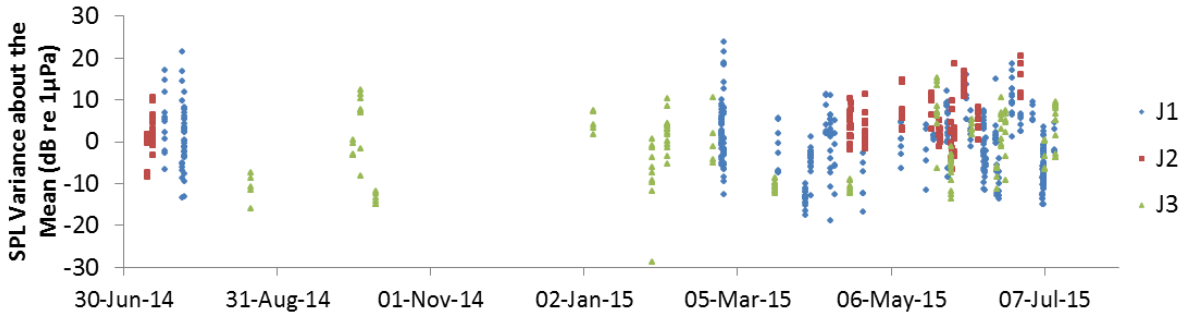

Figure 40. Plot of monotonic call SPL above and below the mean call SPL/station for Stations J1, J2, and J3 from 30 June 2014 to 7 July.

3.2.2.2.3. Regional use approximation

To provide some context about the possible use of the region by Omura's and Bryde's whales, an estimate of the distances from Station J2 using the minimum, median and maximum received call levels determined through analysis of the automated detections was performed.

Along with the received call levels (Table 13), an approximate source level of 155 dB re 1 µPa was used, based on estimates for minke whales (Gedamke et al. 2001), sei whales (McDonald et al. 2005) and Bryde's whales (Širović et al. 2014). The reported call levels for Bryde's whales (Širović et al. 2014) was 155 dB re 1 µPa at 1 m, +/- 14 dB. An estimated whale depth of 30 m was selected for the Omura's and Bryde's whale based upon observations in Cerchio et al. (2015) (mean of 31 m with a standard deviation of 48 m) and the lack of recorded information about the typical dive depth for a Bryde's whale. These inputs were used with a transmission loss curve derived from running JASCO's Marine Operations Noise Model (MONM) over a single transect line at a bearing of 303.96°, taking advantage of the theory of reciprocity. The exact migration path of the whales is unknown, and while a single transect is not accurate, it allows for a comparison of possible distances from Station 2 to the whales. The modelling transect used for the Omura's and Bryde's is the same as used for the pygmy blue for simplicity. A more detailed investigation should select transects for each whale species based upon an analysis of their movements across the region.

The maximum received call levels are within the first range step of the modelling, i.e. between the source at 30 m depth and the receiver at 240 m. Therefore it is assumed that the whales are within this range.

The calculated distances of the whales from Station J2 along the selected transect range, are shown in Table 14.

Table 13. Whale call modelling parameters

Whale call	Estimated Broadband Call SL (dB)	Received Level (dB)			Call depth (m)	Call Frequency (Hz)	Modelled 1/3 Octave band centre Frequency (Hz)
		Minimum	Median	Maximum			
Monotonic call (Omura's)	155	55.6	93.2	128.6	30	26–28	25
Downsweep call (Bryde's)	155	80.4	92.2	109.2	30	150-40	50

Table 14. Whale distance estimation (m)

Whale call	Estimated Broadband Call SL (dB)	Estimated Distance (m)		
		Min. received level	Median received level	Max. received level
Monotonic call (Omura's)	155	$3.6x10^3$	2160	<240 (water depth)
Downsweep call (Bryde's)	155	$5.6x10^3$	1,260	<240 (water depth)

3.2.3. Odontocetes

3.2.3.1. Beaked whales

3.2.3.1.1. Manual Detections

Beaked whale clicks were positively identified during manual validation analysis at Station J2 on 3 April 2015 and at Station J3 on 31 August 2014 as well as 3 May and 17 May 2015. Examples of beaked whale clicks that may represent separate species and/or click-types are shown in Figure 23 and Figure 42. Clicks recorded at Station J2 (Figure 42) were higher in frequency (60–140 kHz) and shorter in duration (0.3 ms) than those recorded at Station J3 (Figure 23), which had a duration of ~ 1 ms and ranged from 21–116 kHz.

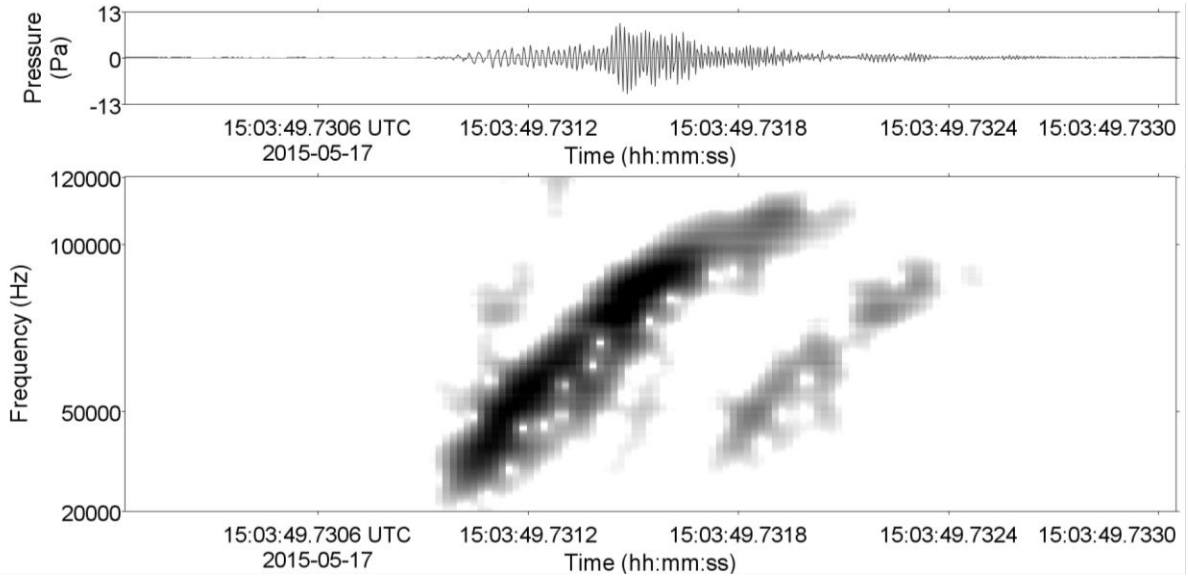

Figure 41. Spectrogram of beaked whale click recorded at Station J3 on 17 May 2015 (UTC) (512 Hz frequency resolution, 0.266 ms time window, 0.02 ms time step, and Hamming window).

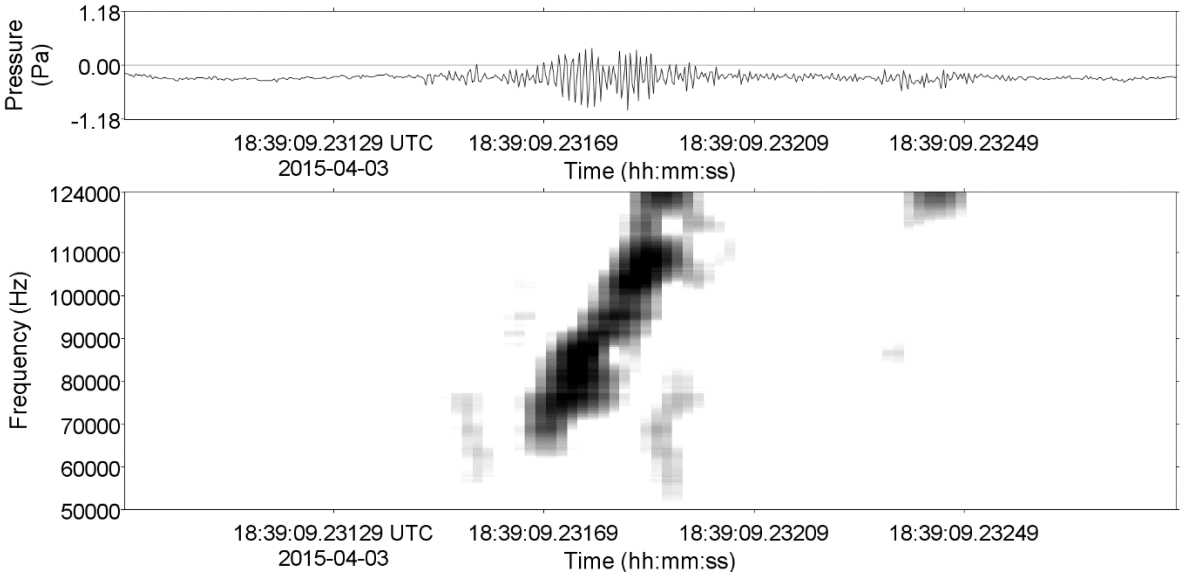

Figure 42. Spectrogram of beaked whale click recorded at Station J2 on 3 April 2015 (UTC) (512 Hz frequency resolution, 0.266 ms time window, 0.02 ms time step, and Hamming window).

3.2.3.1.2. Automated Detections

Beaked whale clicks were automatically detected on three days at Station J3: 31 August 2014, 3 May 2015 and 17 May 2017. These results coincide with the manual analysis results in Section 3.2.3.1, only missing the clicks observed at Station J2 on 3 April 2015. This is reflective of there being few files with beaked whale click detections above the assigned threshold; all files were already reviewed during manual analysis.

3.2.3.2. Unidentified Odontocetes

3.2.3.2.1. Manual Detections

Odontocetes were positively identified during manual validation analysis from July 2014 to July 2015 at all stations (Figure 43). Calls were observed at Station J1 on 123 days (79 with clicks and whistles, 42 with only clicks, and 2 with only whistles), at Station J2 on 145 days (94 with clicks and whistles, 49 with only clicks, and 2 with only whistles), and at Station J3 on 117 days (78 with clicks and whistles, 38 with only clicks, and 1 with only whistles). An example of odontocete clicks and whistles is shown in Figure 44. The centre frequency of clicks ranged from 13–110 kHz. Whistles occurred from 2–20 kHz both in repeated patterns and at random.

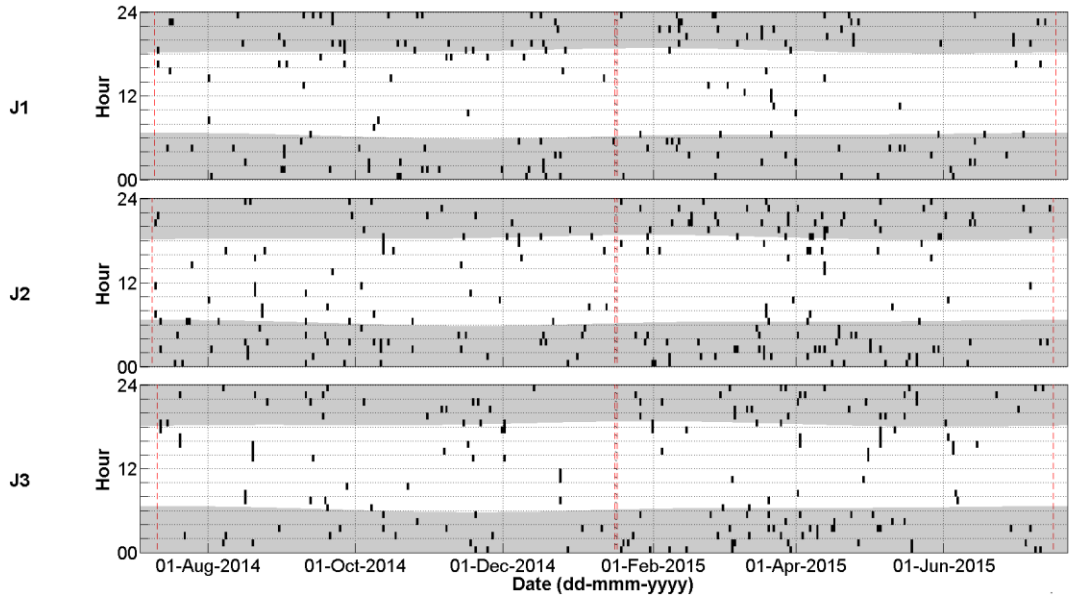

Figure 43. Presence of manually validated odontocete clicks and whistles (normalised on a 1 h basis) at Stations J1, J2, and J3 from July 2014 to July 2015 in the Timor Sea. The grey areas indicate hours of darkness from sunset to sunrise (Ocean Time Series Group 2009). The red dashed lines indicate the start and end of recording time.

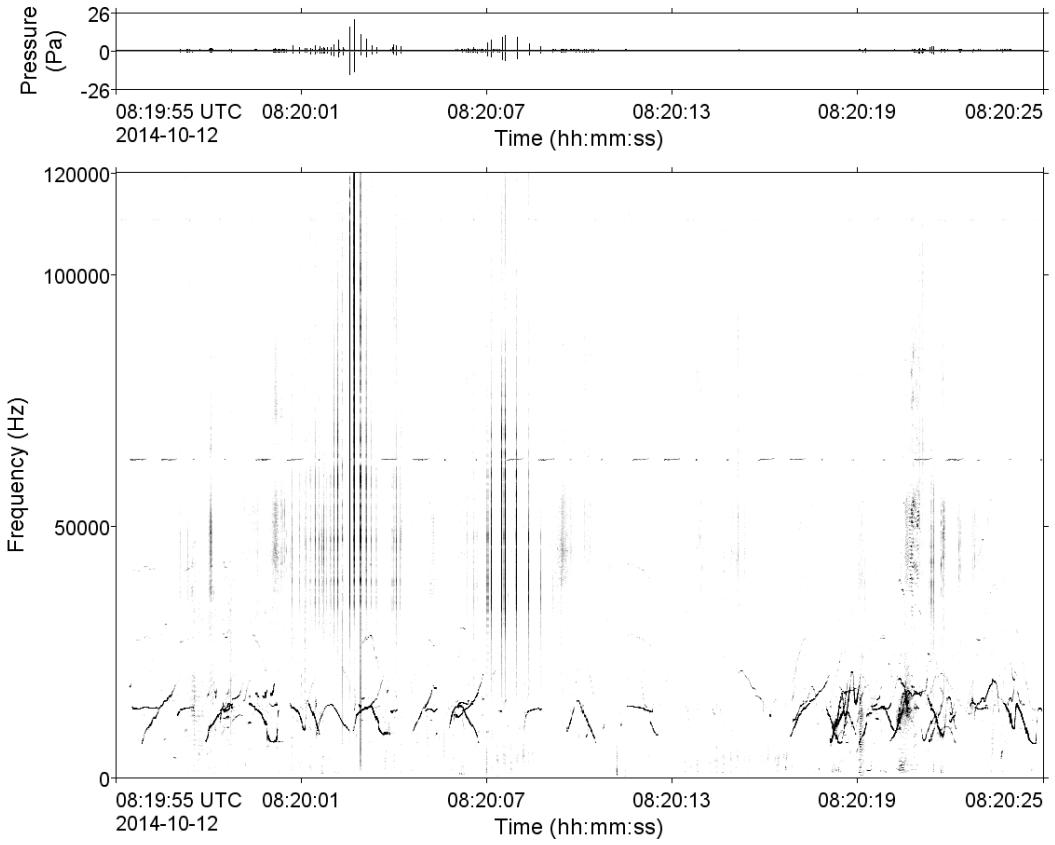

Figure 44. Spectrogram of odontocete clicks and whistles recorded at Station J2 on 12 October 2014 (UTC) (2 Hz frequency resolution, 0.128 s time window, 0.032 s time step, and Hamming window).

3.2.3.2.2. Automated Detections

Odontocetes were detected at Station J1 on 368 out of 371 days: clicks and whistles were detected on 238 days, clicks only were detected on 130 days, and whistles were never detected by themselves. Station J2 had 366 out of 370 days of detections: clicks and whistles were detected on 287 days, clicks only were detected on 77 days, and whistles were detected by themselves on only two days. Detections at Station J3 occurred on 363 out of 368 days: clicks and whistles were detected on 247 days, clicks only were detected on 118 days, and whistles were never detected by themselves. Clicks and whistles were consistently detected throughout the recording period at Stations J2 and J3, predominantly during hours of darkness (Figure 46).

An example of the detectors in operation is shown in Figure 45. The dense nature of detections at Station J1 during Deployment 1 suggests that these results are not real, but rather a product of unknown noise at Station J1 that created a large number of false positives in our click detector (Figure 48). The noise was observed during manual analysis, and is discussed in Section 4.1.2, and attributed to crustaceans such as snapping shrimp, and the noise from the flow through the rocks and the sea fans. The source of the unknown noise seems to decrease during Deployment 2, as by mid deployment the detection rate is similar to the other stations. Based on manually verified click and whistle detections (Figure 43), and automated detections of whistles (Figure 47), odontocetes at Station J1 have been observed in a similar pattern to that of J2 and J3, in that they were present throughout the recording period and especially vocal at night.

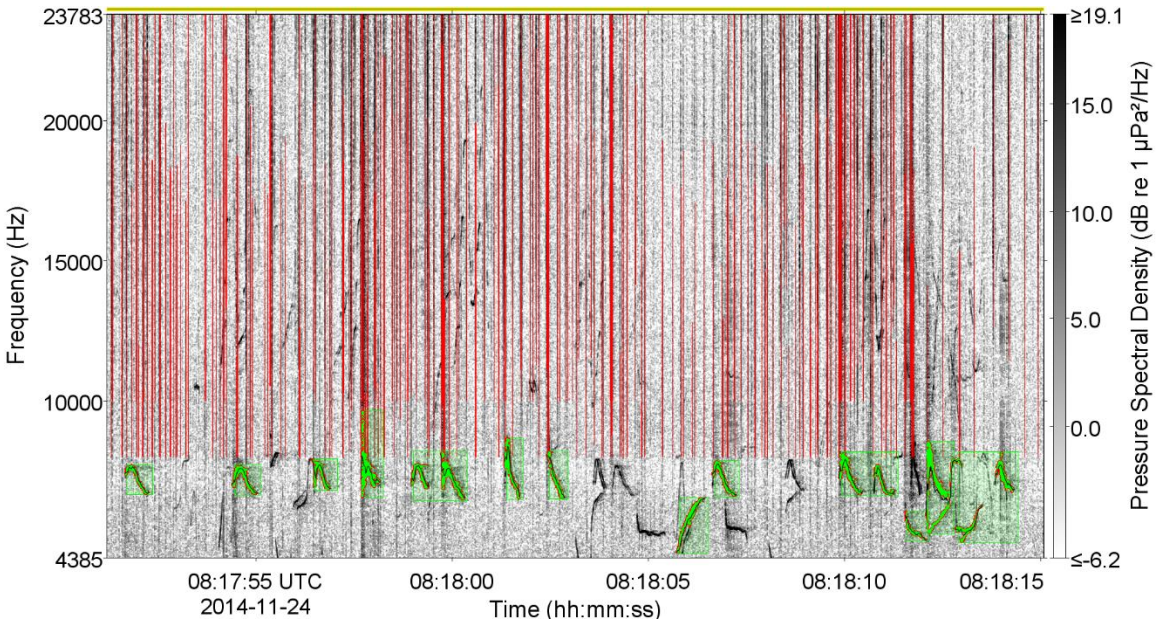

Figure 45. Example click and whistle detections of suspected pilot whales recorded at Station J1 on 24 November 2014 (UTC) (4 Hz frequency resolution, 0.05 s time window, 0.01 s time step, and Hamming window). Click detections are shown as red lines, and whistle detections as green boxes.

Table 15. Odontocete detection summary, both deployments.

Station	Total days	Total days with detections	Days with click and whistle detections	Days with click only detections	Days with whistle only detections
Deployment 1, 10–11 Jul 2014 to 15 Jan 2015					
J1	190	189	117	72	0
J2	191	188	156	31	1
J3	189	185	126	59	0
Deployment 2, 16–17 Jan to 15–16 Jul 2015					
J1	181	179	121	58	0
J2	179	178	131	46	1
J3	179	178	121	57	0

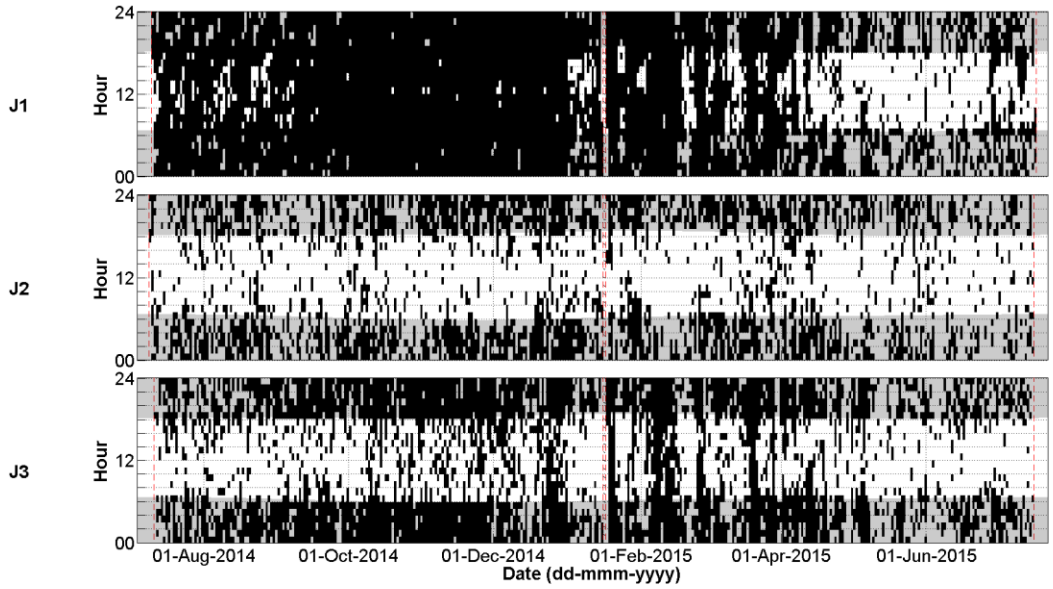

Figure 46. Hourly and daily (expressed as an index) presence of automatically detected odontocete clicks at Stations J1, J2, and J3. Hourly presence of automatically detected odontocete (normalised on a 1 h basis). The grey areas indicate hours of darkness from sunset to sunrise (Ocean Time Series Group 2009). The red dashed lines indicate the start and end of recording time.

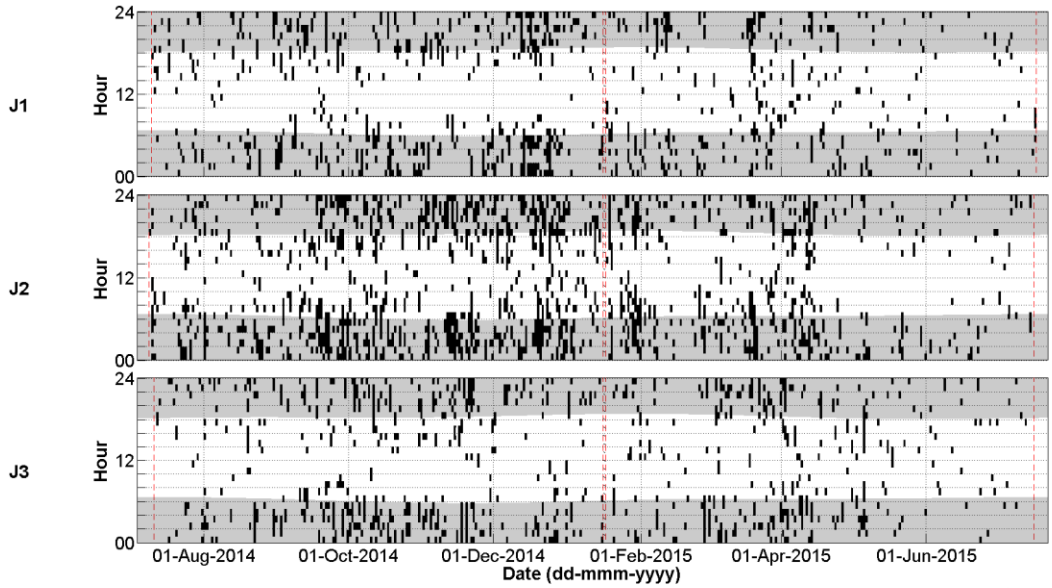

Figure 47. Hourly and daily (expressed as an index) presence of automatically detected odontocete whistles at Stations J1, J2, and J3. Hourly presence of automatically detected odontocete (normalised on a 1 h basis). The grey areas indicate hours of darkness from sunset to sunrise (Ocean Time Series Group 2009). The red dashed lines indicate the start and end of recording time.

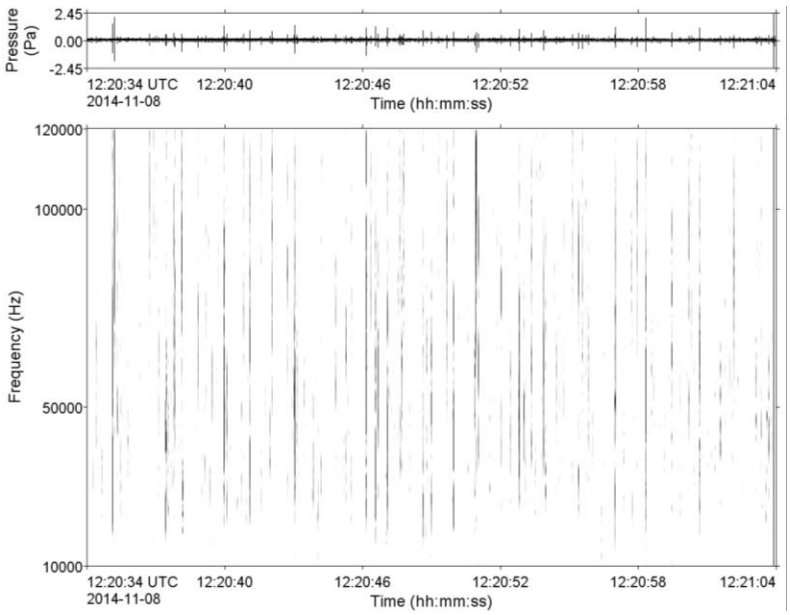

Figure 48. Spectrogram of unknown noise causing false click detections recorded at Station J1 on 8 November 2014 (UTC) (128 Hz frequency resolution, 0.001 s time window, 0.0005 s time step, and Hamming window).

3.2.4. Opportunistic Detections

3.2.4.1. Pilot Whales

Whistles resembling those produced by pilot whales (Sayigh et al. 2013) were observed on 21 September and 24 November 2014 at Station J1 and on 9 October at Station J2. An example of whistles likely produced by pilot whales is shown in Figure 49. These whistles ranged from 10–20 kHz, were 0.4–0.8 s. in duration, and occurred in a repeated pattern.

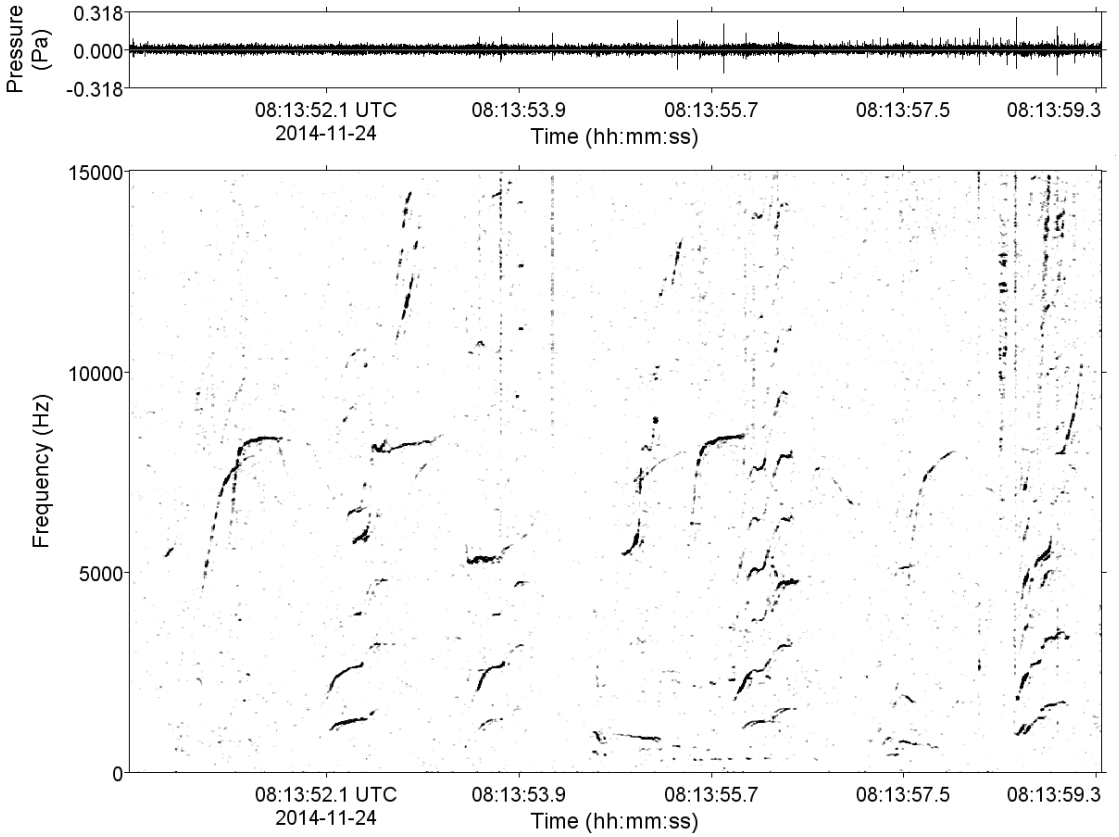

Figure 49. Spectrogram of whistles thought to be produced by pilot whales recorded at Station J1 on 24 November 2014 (UTC) (4 Hz frequency resolution, 0.05 s time window, 0.01 s time step, and Hamming window).

3.2.4.2. Fish

The first fish calls were opportunistically observed on 9 October 2014 at Station J2 as shown in Figure 50.

Fish chorusing can be seen in the weekly spectrograms (Figure 51), through the elevated levels from 200–800 Hz during the dawn chorus, and from 2–4 kHz during the evening chorus. The evening chorus also had a band of energy in the range of 150-200 Hz. These chorusing events can be seen in the example monthly spectrograms from Station J1, despite the presence of elevated levels from weather and the commencement of MODU operations (Figure 52). During Deployment 2, chorusing events were more prevalent at Station J1 than either of the other stations, with Station J3 recording very little fish chorusing activity. Figure 53 shows the monthly spectrograms for April 2015, in which the dawn and dusk choruses are most obvious for Station J1, less so for Station J2, and the dawn chorus is the only chorus present at Station J3, and only noticeable on occasion.

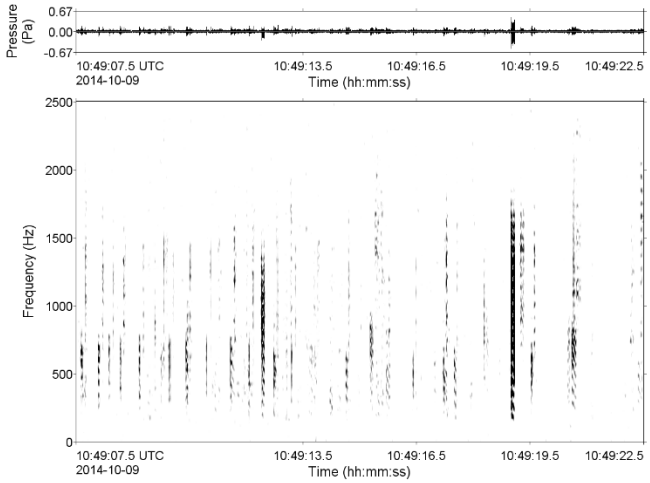

Figure 50. Spectrogram of fish recorded at Station J2 on 9 October 2014 (UTC) (2 Hz frequency resolution, 0.128 s time window, 0.032 s time step, and Hamming window).

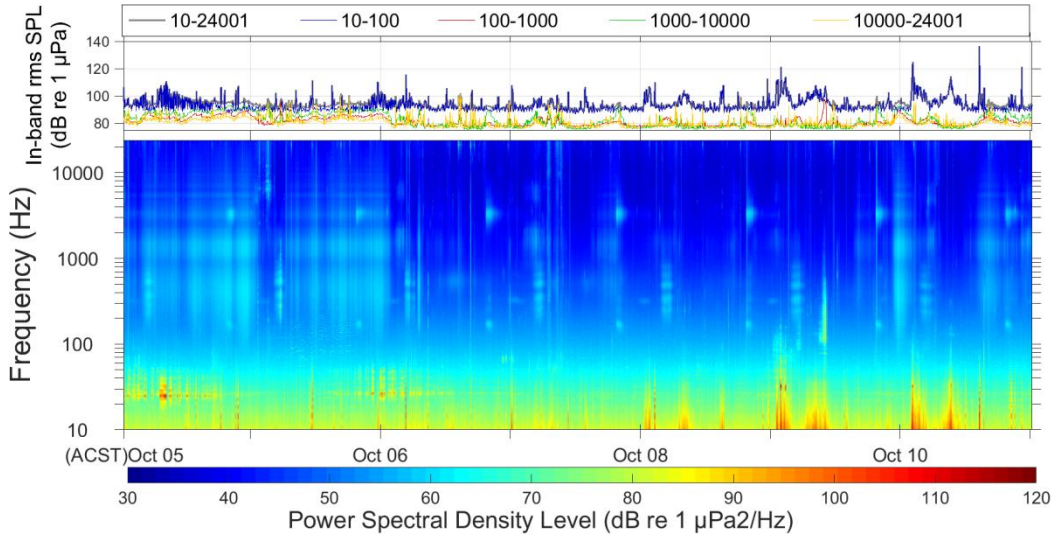

Figure 51 Weekly spectrogram for Station J2 for 4–11 October 2014 showing dawn (200–800 Hz) and evening (2–4 kHz) fish choruses. The evening chorus also has energy at 150-200 Hz.

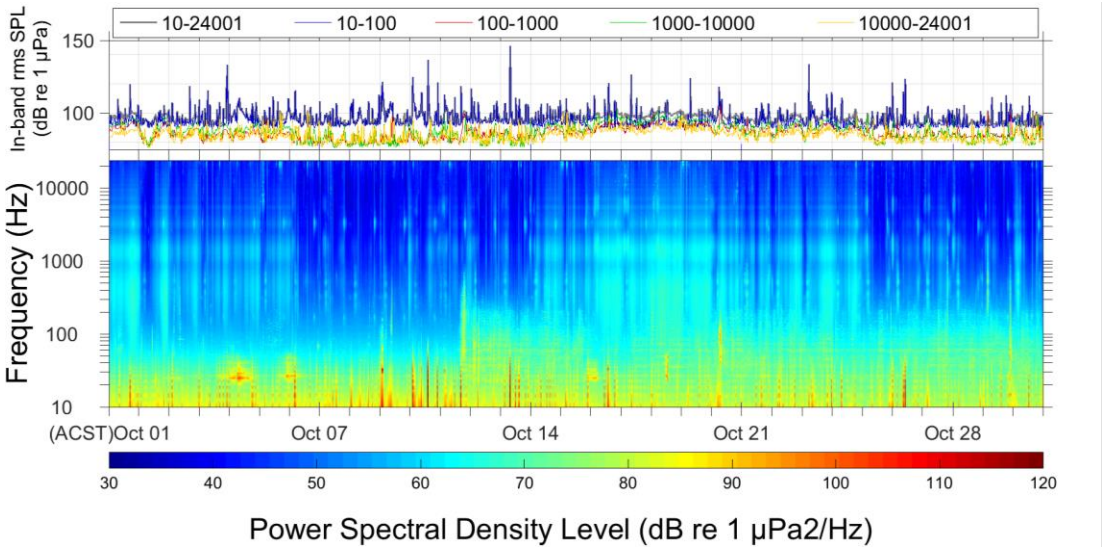

Figure 52. Monthly spectrogram for Station J1 for October 2014 showing dawn and evening fish choruses, and the presence of the MODU from 12 October 2014.

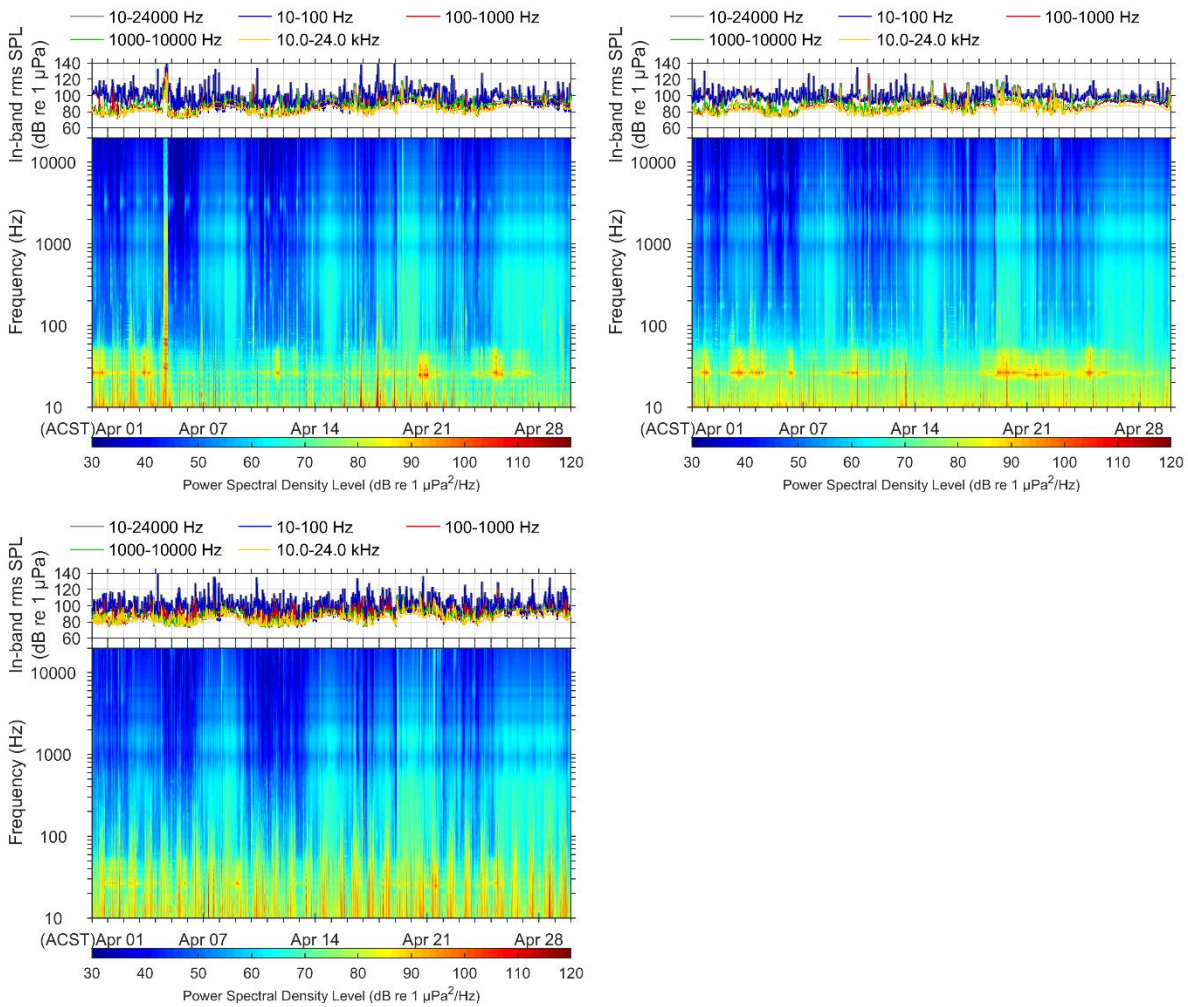

Figure 53. Monthly spectrograms for April 2015 at Station (top left) J1, (top right) J2, and (bottom left) J3.

3.3. Ambient Noise Measurements

The overall ambient sounds are shown as spectrograms and band level plots (Section 3.3.1), sound levels statistics (Section 3.3.2) and power spectral density sound levels (Section 3.3.3). Anthropogenic events are discussed in Section 3.4.

3.3.1. Spectrograms

The spectrogram and band-level plots (Figures 54–59) provide an overview of the sound variability in time and frequency from each station for each deployment presenting an overview of presence and level of contribution from different sources. Short-term events appear as vertical stripes on the spectrograms and spikes on the band level plots. Long-term events affect (increasing or decreasing accordingly) the band level over the event period and appear in the spectrograms as horizontal bands of colour.

During Deployment 1 (Figures 54, 55 and 56) the spectrograms show elevated sound levels at frequencies from 20 Hz–24 kHz from deployment until early September (Stations J2 and J3), or October (Station J1) and again from the start of January until retrieval for all stations. These raised levels are predominantly due to weather events, including the more localised elevation of levels at Station J1 in October. Elevated sound levels from mid-October until retrieval below 200 Hz at Station J1, below 900 Hz at Station J2, and below 300 Hz at J3, were due to the presence of the MODU at Barossa−3 (see Section 3.4.2). It was difficult to differentiate any fish chorusing events at this time

scale due to the influence of weather and the MODU. However, these events are more obvious at the monthly level (e.g. Figure 52), and are discussed further in Section 4.1.3. Mysticete calls are apparent below 80 Hz with a peak near 26–28 Hz at all stations intermittently throughout the entire deployment.

The spectrogram and band plots for Deployment 2 are shown in Figures 57, 58 and 59. The spectrograms for 21-23 January 2015 at all stations show elevated sound levels across the entire frequency range, which is an example of storm activity increasing the received sound levels. The MODU at Barossa-4 exploration well location (Section 3.4.2), close to Station J2, raised levels at frequencies below 900 Hz until 26 March, however was barely detected at the other stations. Similar to Deployment 1, it is difficult to differentiate any fish chorusing events at this time scale due to the influence of weather, however the 2–4 kHz evening fish chorus is apparent at Station J1. Energy from odontocete clicks and whistles above 10 kHz increased sound levels at all stations periodically during the entire deployment. Noise levels at Station J2 were influenced by what appears to be benthic organism or crustaceans on the hydrophone from 10 June 2015 (Figure 60). Mysticete detections stopped after June 10 at J2, but odontocete detections were generally unaffected. The period after 10 June 2015 has been excluded from further analysis of sound level statistics.

Mysticete calls (Omura's or Bryde's whales) are significant contributors to the soundscape below 80 Hz with a peak near 26–28 Hz at all stations throughout the entire deployment.

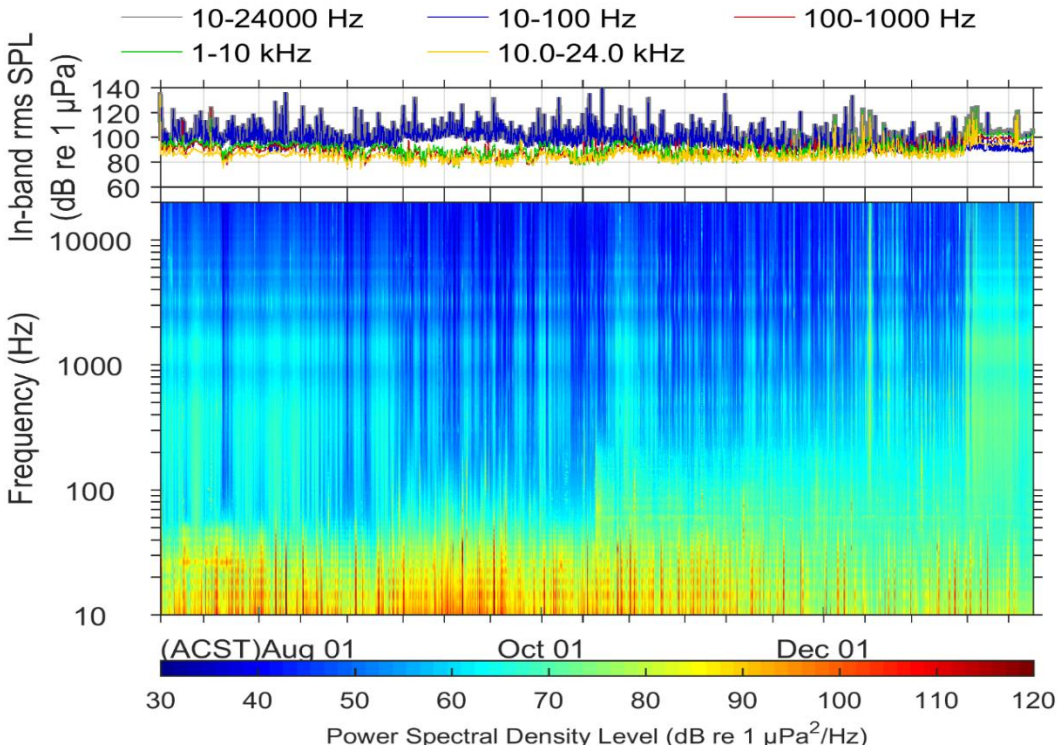

Figure 54. Deployment 1: Sound level summary for Station J1, 10 July 2014 to 15 January 2015. Top: In-band SPLs. Bottom: Spectrogram of power spectral densities. Calls of Omura's or Bryde's whales created a 26–28 Hz tone in this data in July.

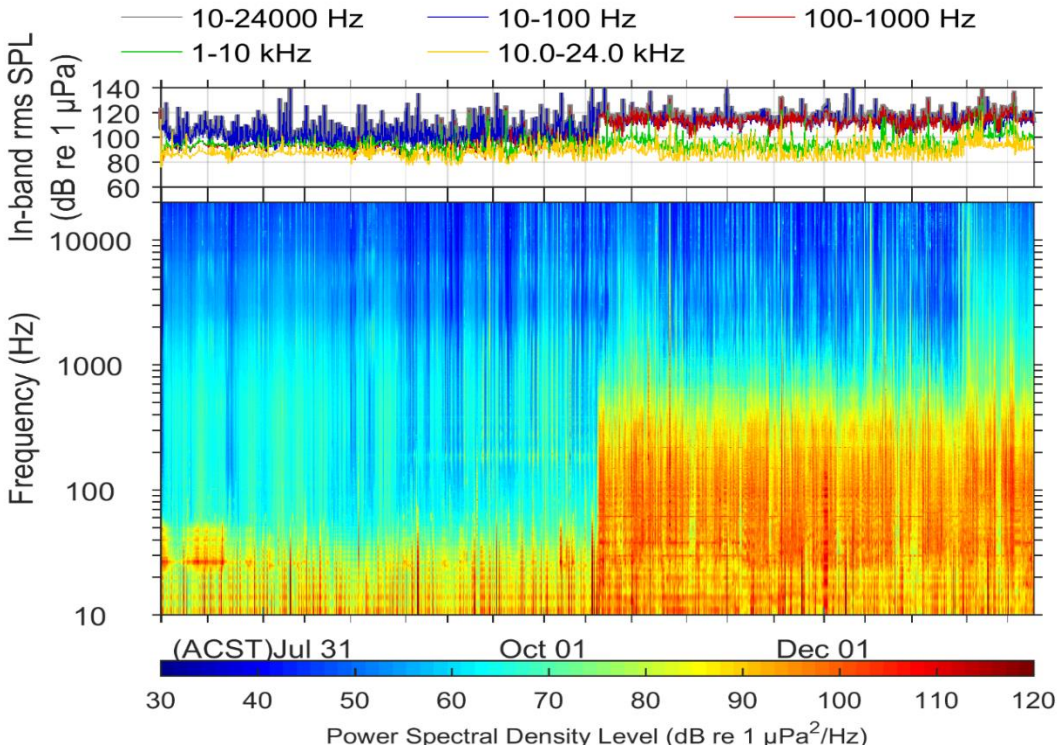

Figure 55. Deployment 1: Sound level summary for Station J2, 10 July 2014 to 15 January 2015. Top: In-band SPLs. Bottom: Spectrogram of power spectral densities. Calls of Omura's or Bryde's whales created a 26–28 Hz tone in this data in July. The arrival of the MODU at Barossa-4 on the 11 October increased sound levels up to 900 Hz.

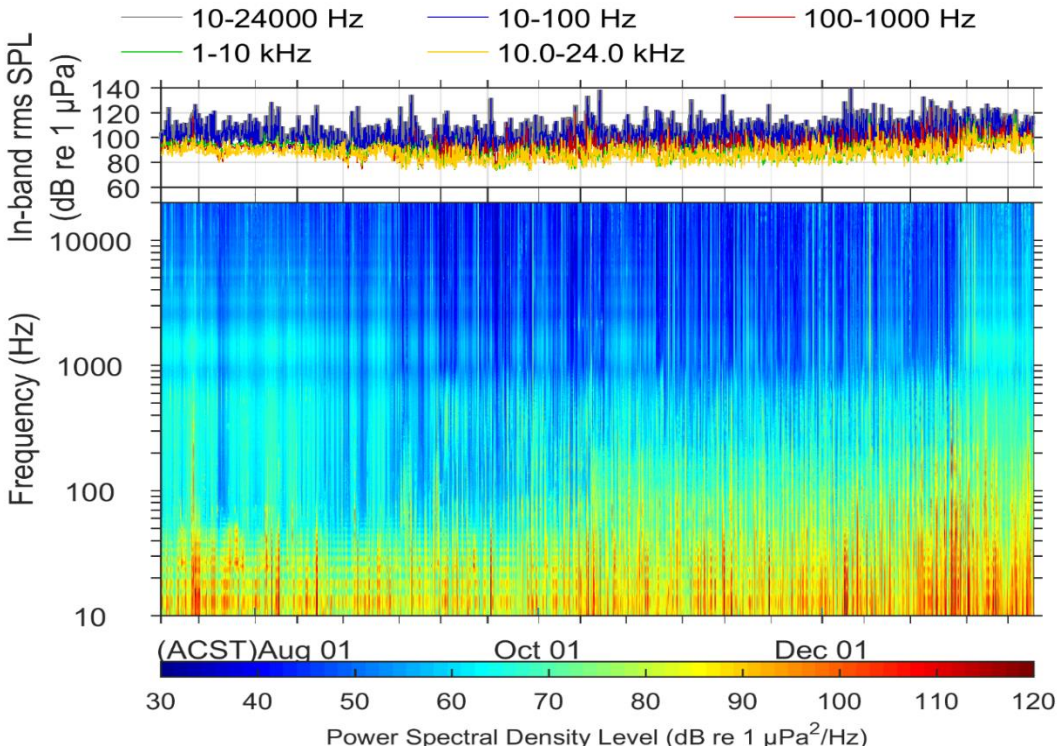

Figure 56. Deployment 1: Sound level summary for Station J3, 10 July 2014 to 15 January 2015. Top: In-band SPLs. Bottom: Spectrogram of power spectral densities.

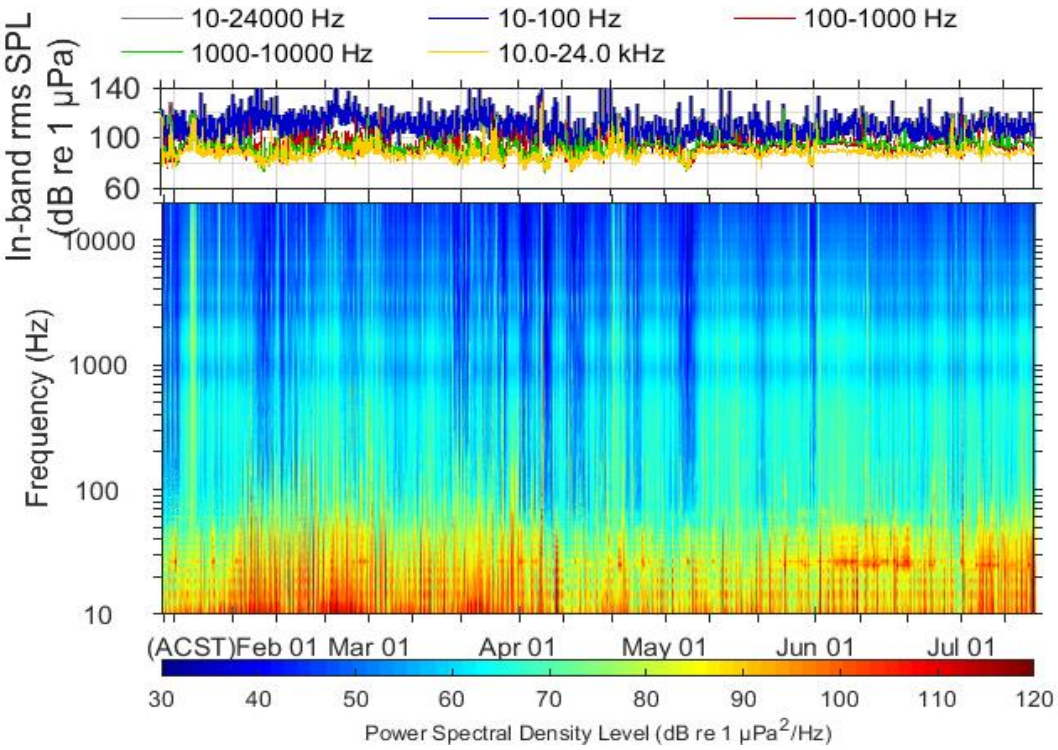

Figure 57. Deployment 2: Sound level summary for Station J1, 16 January to 16 July 2015. Top: In-band SPLs. Bottom: Spectrogram of power spectral densities. Periods of calling from Omura's or Bryde's whales appear at 26–28 Hz throughout the data, but become much more prevalent from May.

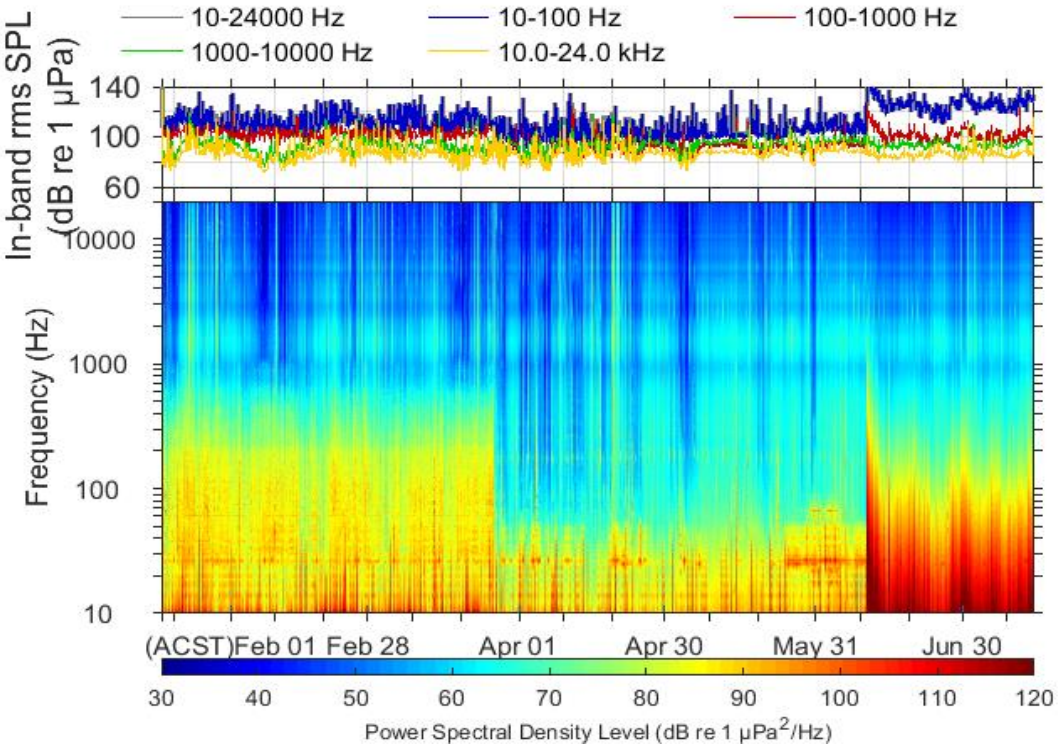

Figure 58. Deployment 2: Sound level summary for Station J2, 17 January to 15 July 2015. Top: In-band SPLs. Bottom: Spectrogram of power spectral densities. Omura's or Brydes whale calls are visible at 26–28 Hz throughout the deployment. The presence of the MODU is clearly seen by the elevated sound levels up to 500-600 Hz until late march. On June 10th an animal, possibly a crustacean took up residence on the hydrophone.

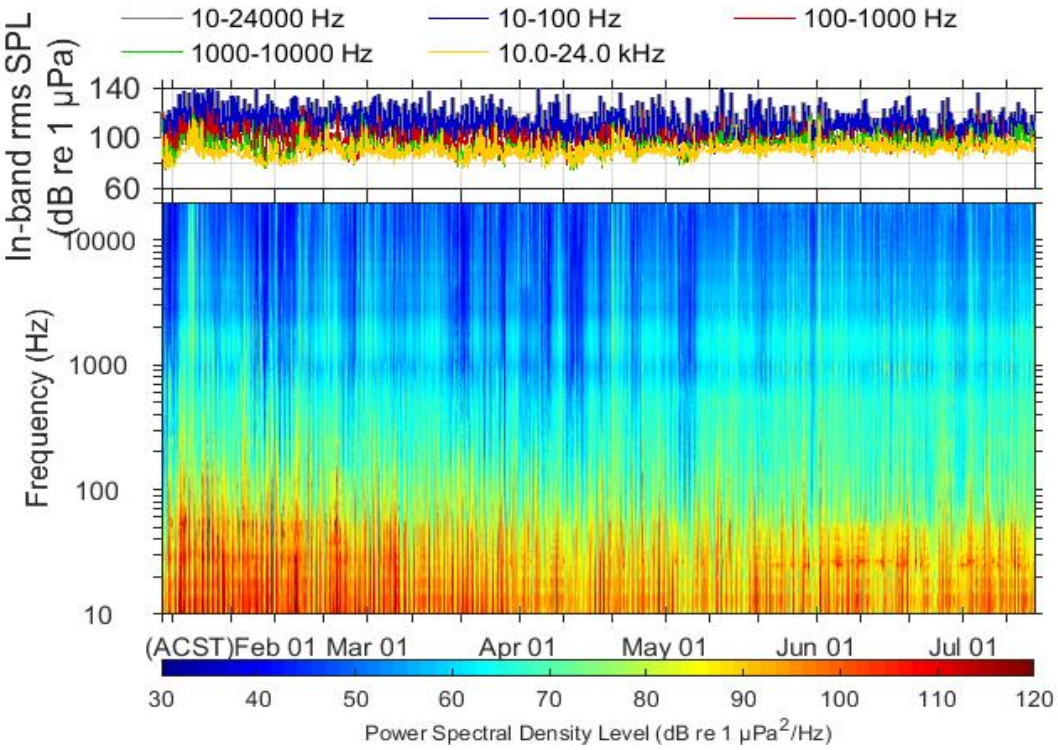

Figure 59. Deployment 2: Sound level summary for Station J3, 17 January to 15 July 2015. Top: In-band SPLs. Bottom: Spectrogram of power spectral densities. The Omura's or Bryde's whale calls at 26–28 Hz are less pronounced on this Station than J1 and J2.

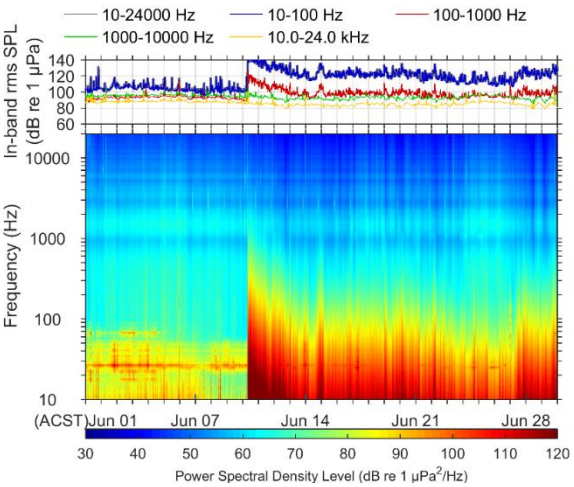

Figure 60. Monthly spectrogram for June 2015 at Station J2 showing Bryde's or Omura's whale calls at 26–28 Hz, as well as the arrival of an animal creating local noise on the hydrophone starting on 10 June.

3.3.2. Statistical analysis

A statistical analysis of the data recorded on the 48 ksps channel was conducted. Figure 61 shows the statistical analysis of sound distributions of the 1-minute SPLs for all stations; the values are shown in Table 16. Exceedance of the 120 dB re 1 µPa level were determined to assist possible impact assessments in the region. The statistics can be contrasted against any modelling studies which compare results against the current interim U.S. National Marine Fisheries Service (NMFS 2014) threshold for behavioural response criteria due to non-pulsed noise 120 dB re 1 µPa.

The Deployment 1 median 1-min SPLs were 95.2, 96.2 and 91.7 dB re 1 µPa at J1, J2 and J3 respectively, while for Deployment 2 they were 97.7, 100.9 and 98.2 dB re 1 µPa. Stations J1 and J3 have the majority of their sound energy in the bands of 100-1000 Hz and 1000-10000 Hz which is associated with wind and wave sound sources as well as the fish choruses. Station J2 has the majority of its sound energy in the band of 10-100 Hz which is generally associated with anthropogenic sound sources like the MODU or seismic surveys. The mysticete calls are also in this band.

Station	Deployment 1 (10 July 2014 to 15 January 2015)	Deployment 2 (16/17 January to 15/16 July 2015)
J1	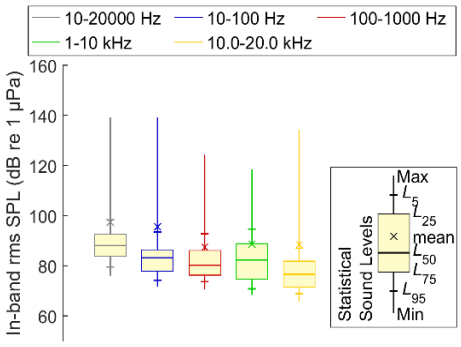	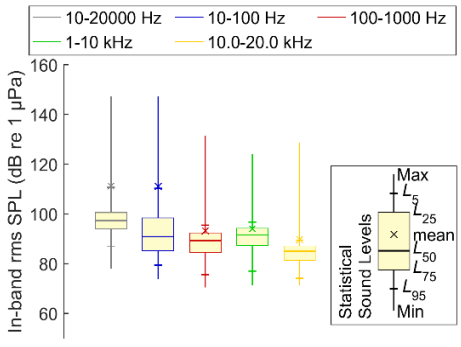
J2	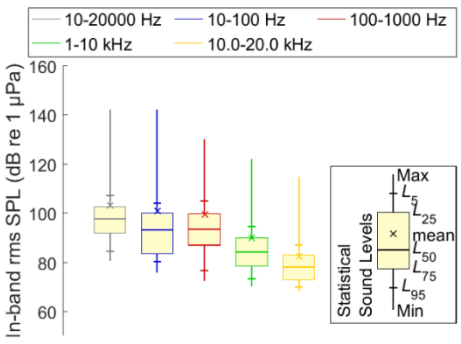	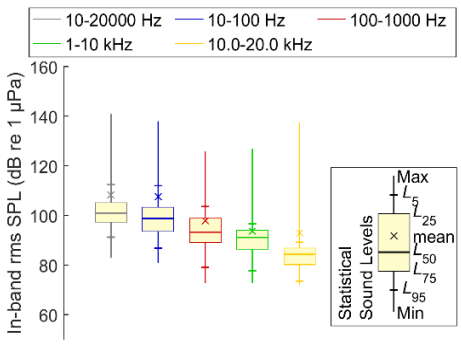
J3	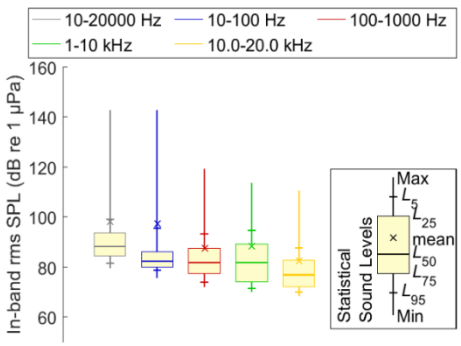	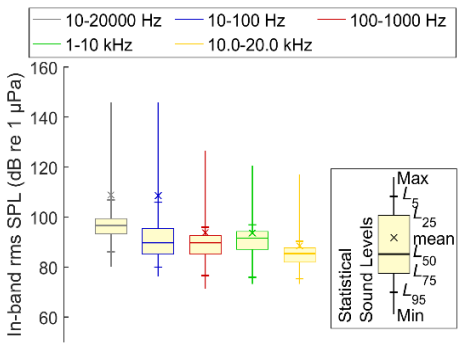

Figure 61. The 1-min SPLs for all stations from both deployments.

Table 16. Statistical analysis of sound levels for Stations J1, J2, and J3. SPL units: dB re 1 µPa, Station J2 for the second deployment is only analysed until 10 June 2015.

Sound level statistic	J1		J2		J3	
	PK	1-min SPL	PK	1-min SPL	PK	1-min SPL
Deployment 1 (10 Jul 2014 to 15 Jan 2015)						
Minimum	103.8	83.1	99.2	83.6	101.4	81.1
L_{95}	113.9	90	108.9	91.5	109.1	83.8
L_{75}	120.1	92.4	113.5	96.9	113.3	87.9
L_{50}	125.4	95.2	124.9	106.2	117.3	91.7
L_{25}	131.9	98.4	131.7	117.3	123.6	96.8
L_{5}	144.2	106.6	136.6	121.8	138.3	102.1
Maximum	170.5	146.3	176.2	156.1	170.8	144.6
Mean	141.5	104.8	138.5	117.1	141	103.6
% of 1-min periods when data exceeds 120 dB re 1 µPa	76.32	0.58	58.3	12.67	37.78	0.11
Deployment 2 (16/17 Jan to 15/16 Jul 2015)						
Minimum	100.5	79.1	98.6	82.6	105.4	81.4
L_{95}	110.2	87.7	109.5	91.3	113.3	88.4
L_{75}	114.5	94.1	115	97.6	117.4	95.2
L_{50}	118.6	97.7	118.7	100.9	121.5	98.2
L_{25}	124.6	100.8	122.2	104.7	128.3	101.2
L_{5}	138.7	111.1	128.3	109.2	142.8	110.4
Maximum	165.4	146.5	166.1	142	167.1	147.9
Mean	136.8	109.9	130.3	105.9	142	109.5
% of 1-min periods when data exceeds 120 dB re 1 µPa	43.94	1.12	41.54	0.17	59.91	0.76

Analysis periods relevant to the dominant soundscape contributors for Deployment 1 were defined to analyse the median 1 minute SPLs in a meaningful way. As outlined above, the weather was the dominant contributor from July until early September at Stations J2 and J3, therefore the first period was defined as 10 July –1 September 2014. The next period, 1 September to 10 October 2014, was selected as it lies between the weather reducing in dominance and the MODU commencing operations. The third period, 10 October 2014 to 1 January 2015, was selected as it aligned with the presence of the MODU under similar weather conditions, and the final period 1–15 January 2015 was selected as it encompasses the presence of the MODU under intensified weather conditions.

The median 1 minute SPLs for the periods determined by weather and MODU presence are shown in Table 17, the entire deployment is shown in Table 16 above.

Deployment 2 did not have clearly defined weather periods like Deployment 1, and while the MODU was present, it was only a noticeable contributor to the soundscape at Station J2 due to its proximity, and distance from the other stations. Therefore, the statistical analysis for Deployment 2 was not broken down into periods as it was for Deployment 1, but rather analysed as a whole (see Table 16).

Table 17. Deployment 1, pattern analysis periods, median 1 minute SPLs sound levels (dB re 1 µPa) for Stations J1, J2, and J3. SPL units: dB re 1 µPa.

Station	10 Jul–1 Sep 2014	1 Sep–10 Oct 2014	10 Oct 2014–1 Jan 2015	1–15 Jan 2015
J1	97.3	93.7	93.6	106.4
J2	97.5	95.6	116.9	118.7
J3	96.6	88.1	89.9	98.1

3.3.3. Percentile Power Spectral Density Results

The percentile power spectral density (PSD) results for Deployment 1 are shown in Figures 62–64 for Stations J1–J3. At Stations J1 and J3, the PSDs decay relatively smoothly from 10 Hz to 24,000 Hz (the 24-bit channel recorded bandwidth), while Station J2 exhibits a strong peak centred at 100 Hz. The median (L_{50}) curve at Station J1 decays 9 dB from 100–1000 Hz, and 10 dB from 1000–10,000 Hz. At Station J2 the median level decays 12 dB from 100–1000 and 11 dB from 1000–10,000 and at Station J3 the median level decays 12 dB from 100–1000 and 10 dB from 1000–10,000.

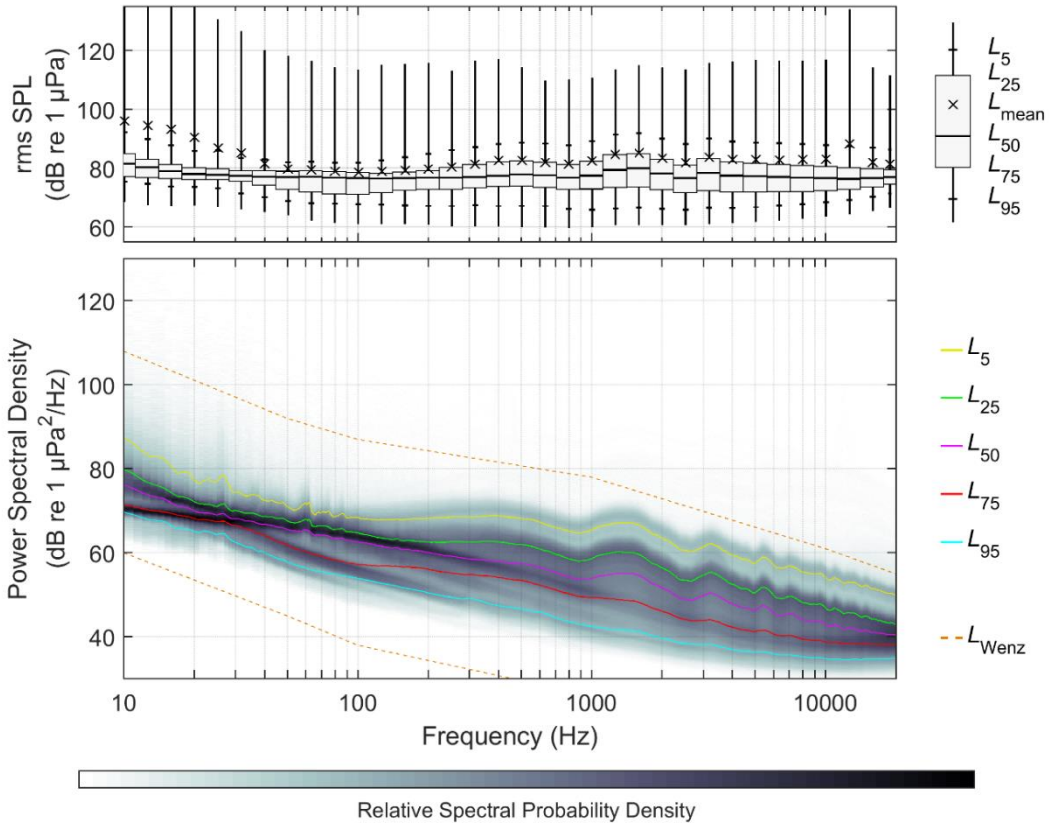

Figure 62. Deployment 1: Percentile power spectral density sound levels at Station J1 for 10 July 2014 to 15 January 2015.

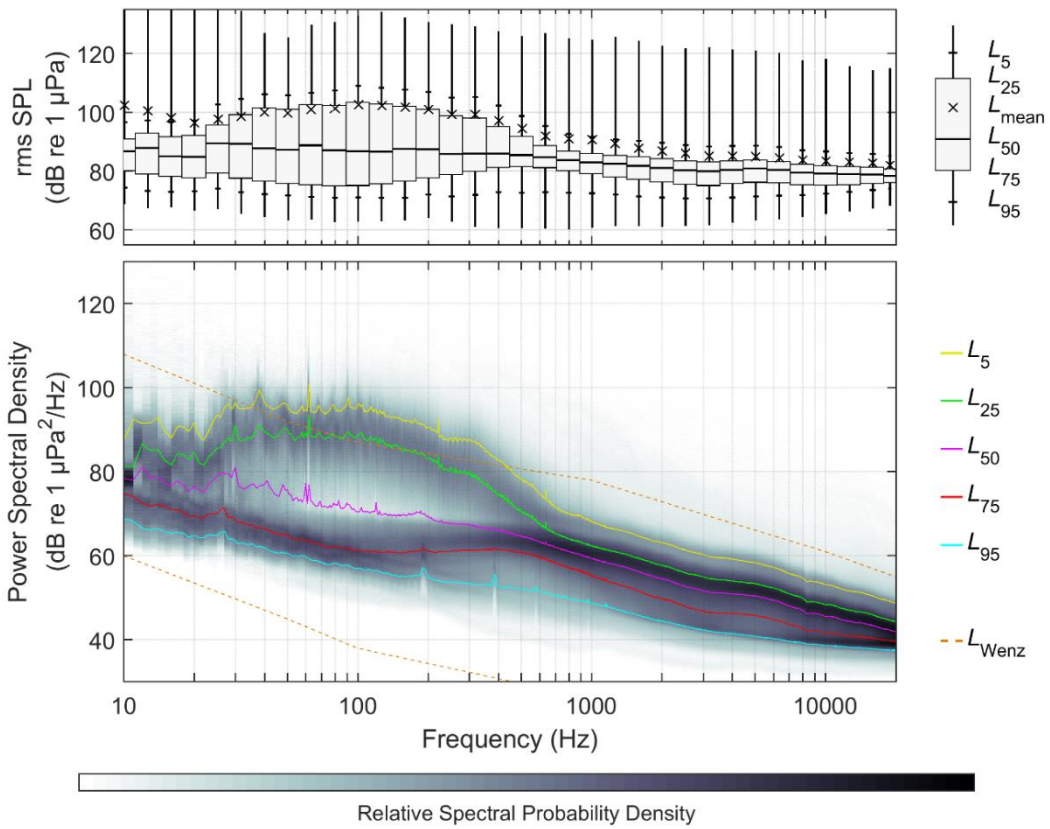

Figure 63. Deployment 1: Percentile power spectral density sound levels at Station J2 for 10 July 2014 to 15 January 2015.

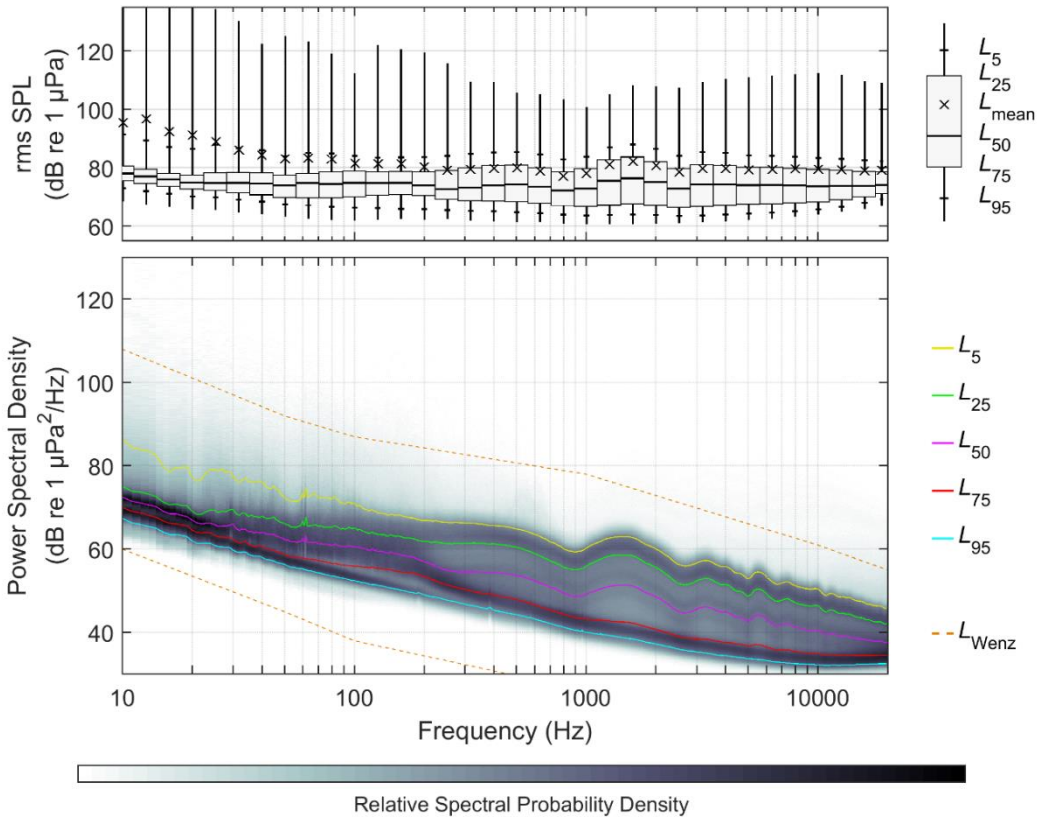

Figure 64. Deployment 1: Percentile power spectral density sound levels at Station J3 for 10 July 2014 to 15 January 2015.

The percentile power spectral density (PSD) results for Deployment 2 are shown in Figures 65–67 for Stations J1–J3. Unlike Deployment 1, none of the PSDs demonstrate a relatively smooth decay over the recorded bandwidth, with more variability present at frequencies below 1 kHz. At frequencies above 1 kHz, the decay pattern is similar at all three stations, and while approximately 5 dB higher than the levels at Stations J1 and J3 from Deployment 1, Station J2 follows the same trend. Peaks are present at all percentiles (except L_5, Station J2) at around 26–28 Hz. The median (L_{50}) curve at Station J1 decays 4 dB from 100–1000 Hz, and 10 dB from 1000–10,000 Hz. At Station J2 the median level decays 16 dB from 100–1000 and 10 dB from 1000–10,000 and at Station J3 the median level decays 9 dB from 100–1000 and 7 dB from 1000–10,000.

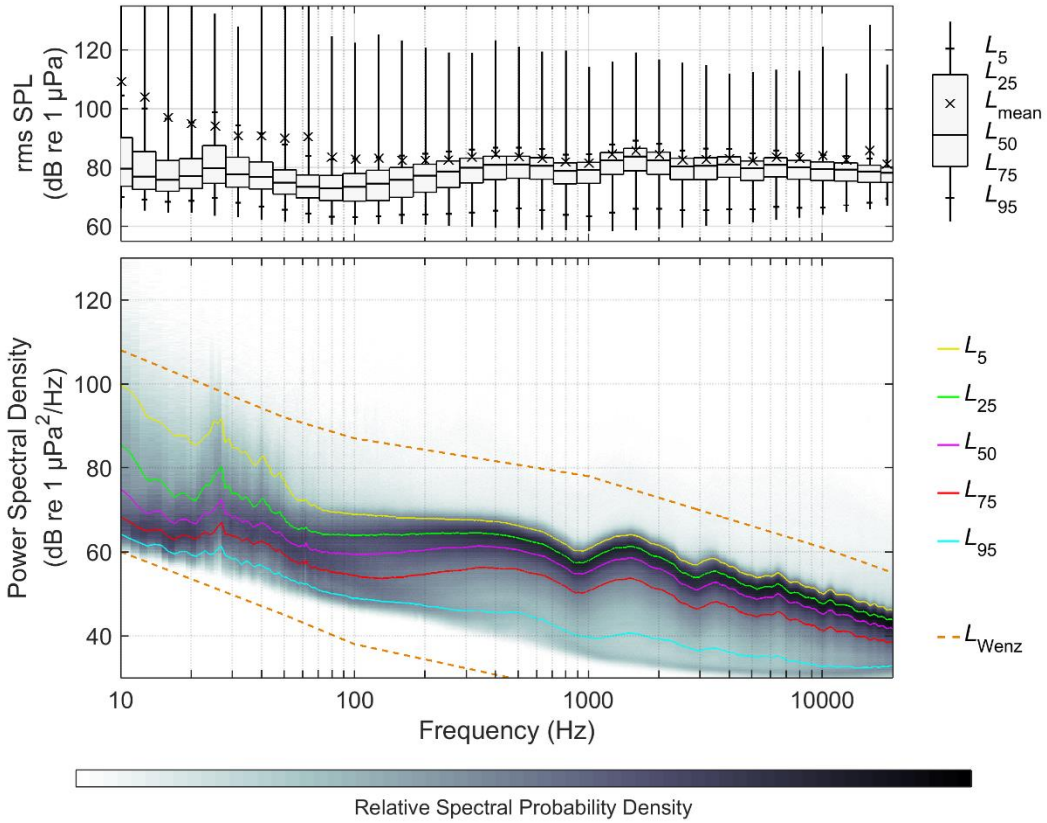

Figure 65. Deployment 2: Percentile power spectral density sound levels at Station J1 for 16 January to 16 July 2015.

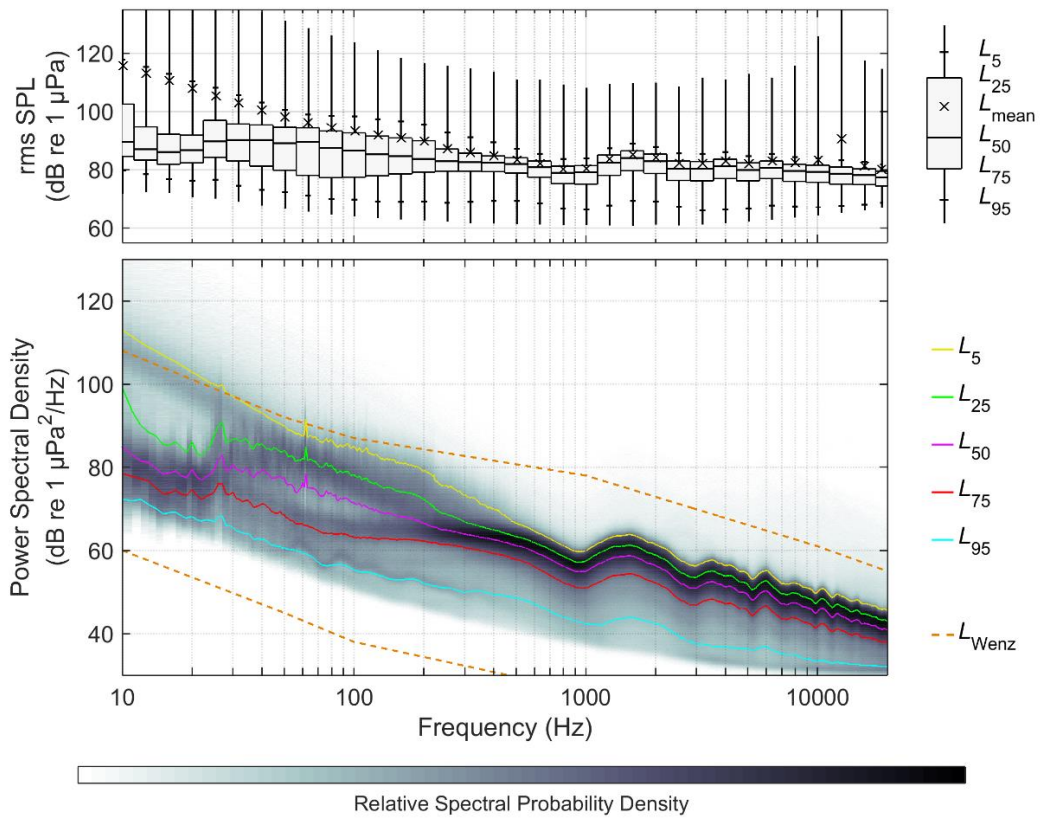

Figure 66. Deployment 2: Percentile power spectral density sound levels at Station J2 for 17 January to 15 July 2015.

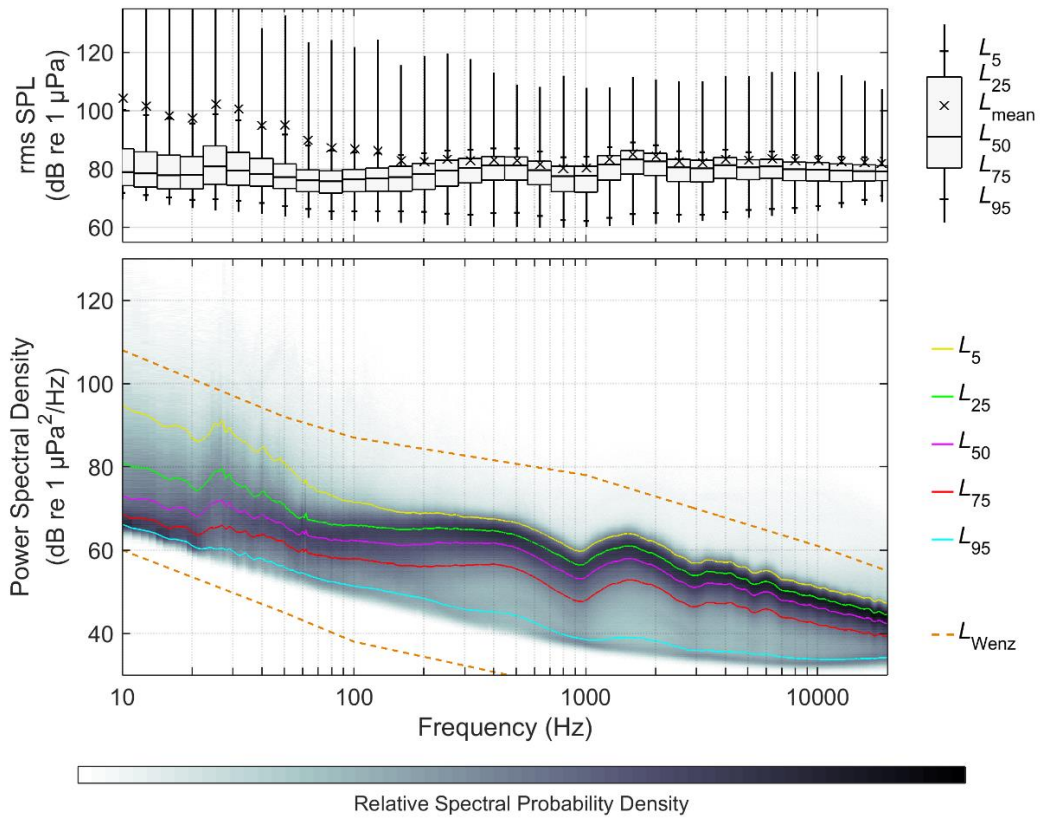

Figure 67. Deployment 2: Percentile power spectral density sound levels at Station J3 for 17 January to 15 July 2015.

The daily SEL values were extrapolated from the measured values and adjusted to account for the duty cycle of 840 s every 1800 s (Table 18). The median daily SEL for both stations was virtually identical during Deployment 1 at Stations J1 and J3 at 145.5 and 145.1 dB re 1 µPa²·s, respectively, and whilst 7 dB higher, only 1 dB different (151.9 as compared to 152.8 dB re 1 µPa²·s respectively) for Deployment 2. The median daily SEL at Station J2 was approximately 16 dB higher than the other stations during Deployment 1, but only approximately 1.5 dB higher during Deployment 2. A similar trend was observed for the mean daily SEL at all stations over both deployments. Across all stations for both deployments, the minimum daily SELs were within 9 dB of each other, whilst the maximums have a separation of 12.7 dB between the highest (Station J2, Deployment 1) and the smallest (Station J1, Deployment 1).

Table 18. Statistical analysis of sound levels for Stations J1, J2, and J3 SEL units: dB re 1 µPa²·s, Station J2 for the second deployment is only analysed until 10 June 2015.

Sound level statistic	Daily SEL		
	J1	J2	J3
Deployment 1 (10 Jul 2014 to 15 Jan 2015)			
Minimum	139.7	141.1	135.1
L_{95}	141.5	143.8	138.6
L_{75}	143.3	147.7	142.1
L_{50}	145.7	161.9	145.1
L_{25}	148.9	167.8	148.4
L_{5}	155.9	171.5	154.9
Maximum	166.8	178.5	168.1
Mean	150.6	166.1	150.1
Deployment 2 (16/17 Jan to 15/16 Jul 2015)			
Minimum	141.5	144	143.1
L_{95}	145.2	145.9	145.8
L_{75}	149	148.6	149.7
L_{50}	151.9	153.8	152.8
L_{25}	155	157.3	155.6
L_{5}	167.6	164.1	162.4
Maximum	175.1	165.8	173.2
Mean	160.6	157.4	158.2

3.4. Anthropogenic Sound

3.4.1. Vessel Detections

The daily SELs at each station, showing the overall daily SEL and the SEL attributed to detectable shipping are shown in Figure 68. During Deployment 1, the large number of vessel detections at Station J2 was due to either the MODU being detected as a vessel during periods of its activity, or the presence of its support vessels. During Deployment 2 there was more vessel activity, with the MODU presence at Station J2 again being a major contributor. There was a timing correlation between the

drilling program detected at Stations J1 and J2 over Deployment 2, with many detections occurring at similar times. The seismic survey (Section 1.2.2) from July 2015 occurred at a similar time to a number of vessel detections. The seismic survey was detected at Station J1 and J3. The average number of vessels detected per day over Deployment 1 during the pattern analysis periods is listed in Table 19, while those for both deployments are listed in Table 20.

Station	Deployment 1 (10 July 2014 to 15 January 2015)	Deployment 2 (16/17 January to 15/16 July 2015)
J1	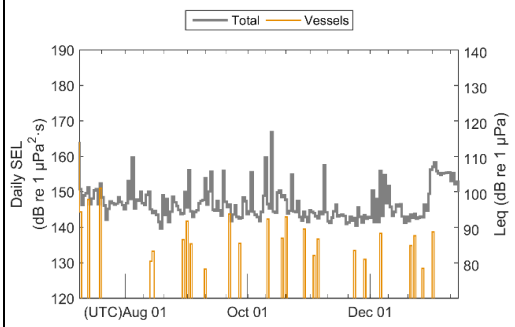	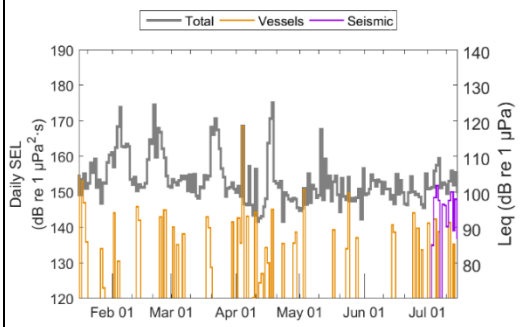
J2	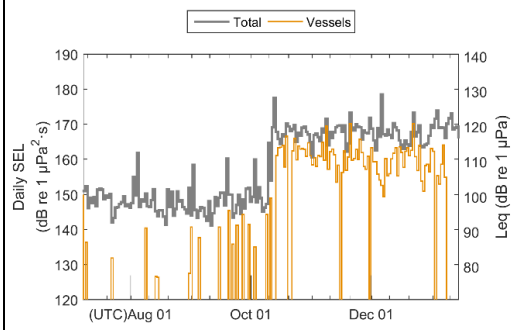	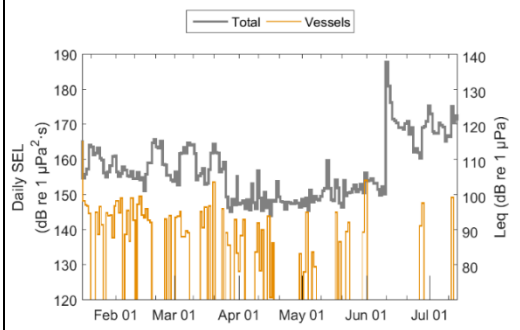
J3	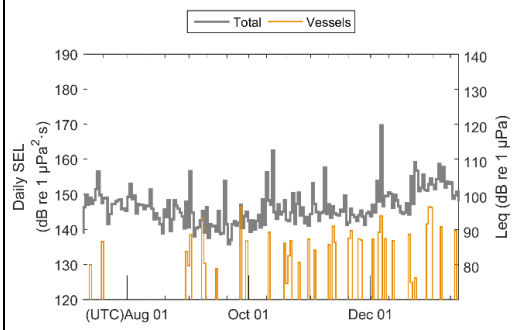	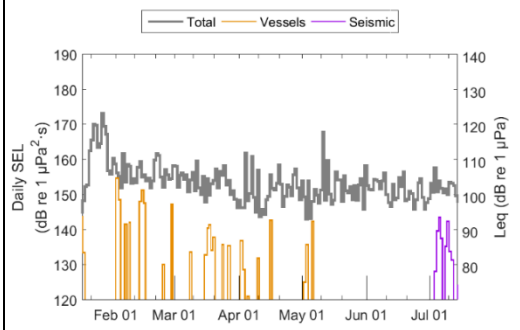

Figure 68. Daily SELs at all stations, showing the overall daily SEL and the SEL attributed to detectable shipping and seismic activity (see Section 3.4.4). Note that a crustacean was present on Station J2 during Deployment 2 after 10 June 2015, however the daily SEL data is still shown to keep the figures axes consistent across stations.

Table 19. Deployment 1: Mean daily vessel detections at each station for four time periods, aligned with pattern analysis periods and normalised for effort.

Station	10 Jul–1 Sep 2014	1 Sep–10 Oct 2014	10 Oct–01 Jan 2015	01 Jan–15 Jan 2015
J1	0.1	0.1	0.2	0.1
J2	0.1	0.3	2.8	0.8
J3	0.2	0.3	0.3	0.1

Table 20. Mean daily vessel detections at each station for both deployments, normalised for effort.

Station	Deployment 1	Deployment 2
J1	0.1	0.4
J2	1.4	0.7
J3	0.3	0.3

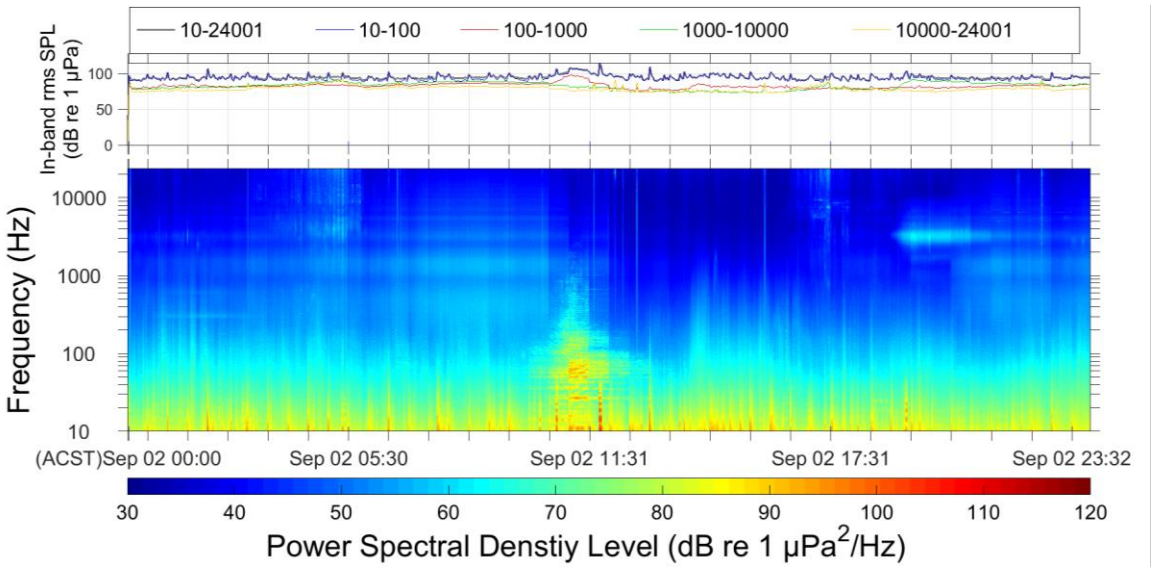

Figure 69. A passing vessel at long range from Station J1 at ~11:15 on 2 September 2014. The dusk fish chorus is also clearly visible at ~1800 hrs between 2-4 kHz.

3.4.2. MODU Operations

3.4.2.1. Deployment 1

MODU operations were a dominant contributor to the soundscape after it arrived on 12 October 2014. Figure 52 shows the influence of the MODU on a monthly timescale, while Figure 70 provides a daily spectrogram demonstrating the contribution. The majority of the contribution is below 200 Hz. This spectrogram also shows the pre-dawn fish chorus from 200–900 Hz and an individual vessel movement occurring around 20:30.

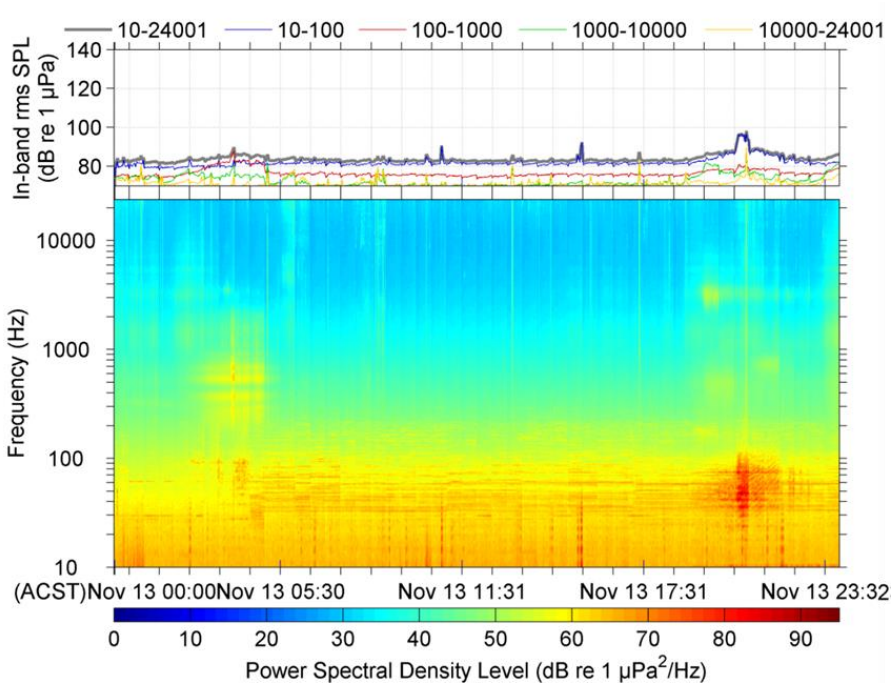

Figure 70. Example daily spectrogram of MODU operations, Station J2, 13 November 2014.

3.4.2.2. Deployment 2

For the first three months of Deployment 2, the MODU was again a dominant contributor to the soundscape at Station J2. The majority of the contribution was below 200 Hz, although it was still very influential up to approximately 600 Hz (Figure 71). During March, there was little fish chorusing activity at Station J2.

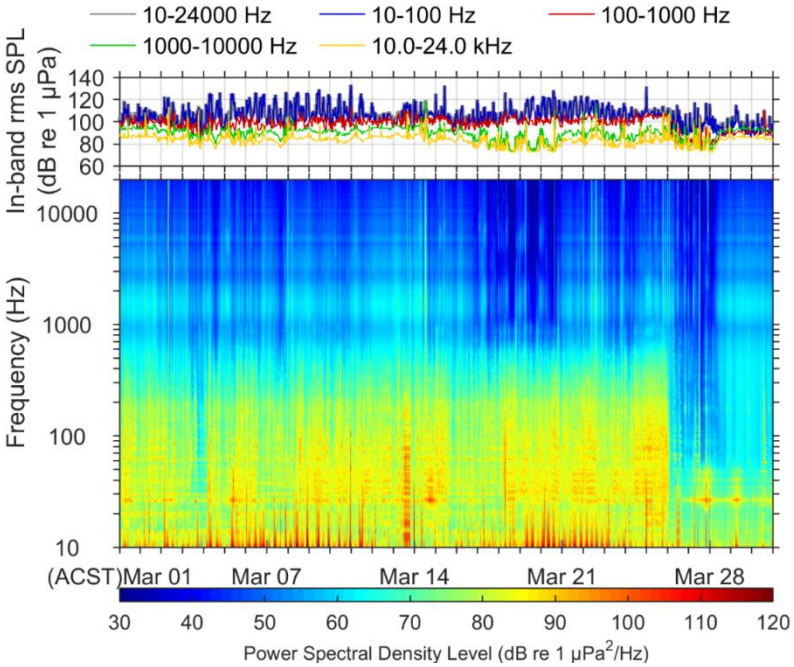

Figure 71. Example monthly spectrogram of MODU operations, Station J2, March 2015.

3.4.3. Airplane Overflight

Other anthropogenic sound sources were occasionally identified in the dataset. For example, a propeller airplane was detected at Station J2 on 7 September 2014 (Figure 72). The type of aircraft was determined by manual identification. Opportunistic detections such as these are not reported with the automatic anthropogenic analysis.

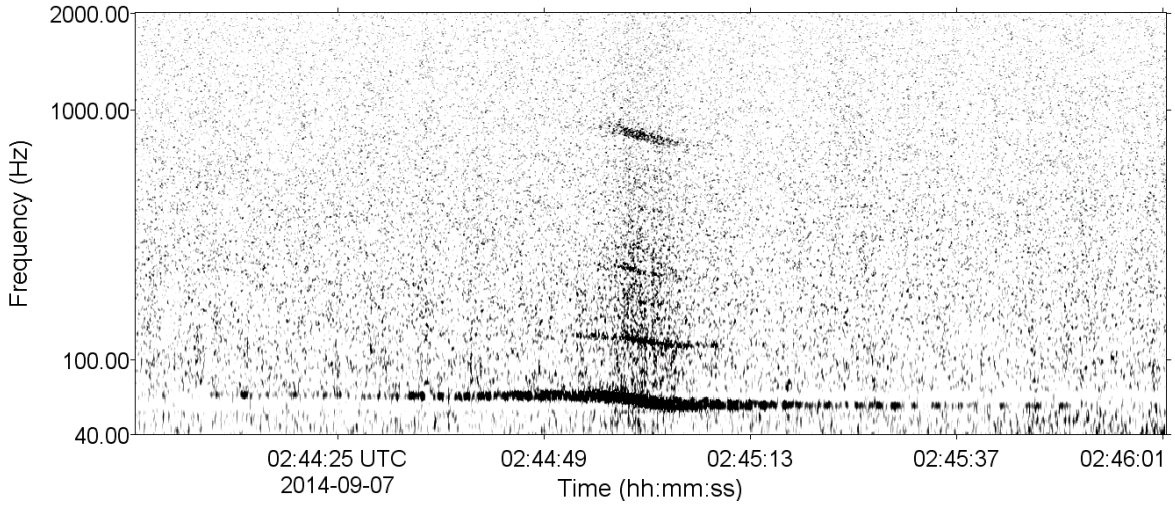

Figure 72. Doppler shift pattern of an airplane overflight at Station J2 on 07 September 2014.

3.4.4. Seismic Survey

A seismic survey, thought to be the CGG 2D BandaSeisV survey (Section 1.2.2), was detected at Stations J1 and J3 by the automated seismic detector, with the per pulse statistics shown in Table 21. At Station J1, the first shots were detected from 06:55 on 04 July 2015, and the last from 23:20 on 15 July 2015, while at Station J2, the first shots were detected from 09:49 on 04 July 2015, and the last from 23:20 on 14 July 2015. The average shot spacing at both stations was 10.5 seconds. The spectrogram for the period 1–17 July (Figure 73) shows the intermittent nature of the survey events, which can be seen as the periods below 100 Hz with levels greater than 90 dB. A fine timescale comparison of all three stations (Figure 74, left) confirms the lack of automated detections at Station J2. It also provides an example of the difference in the pulse time and frequency structure between the two stations (Figure 74, right), with the SPL of the first two seconds of a pulse at Station J1 being 119 dB, compared to 107 dB re 1 µPa at Station J3. While Figure 74 shows the time axis as synchronised, the stations have not been synchronised to the point of being able to do localisation, although the shot logs from the seismic survey would allow this to occur. July was also a period of extensive mysticete calling, which had similar amplitudes to the seismic source at J1 (Figure 75). The minor contribution of the seismic survey to the ambient statistics calculated over the entire second deployment is shown in Figures 76 and 77.

Table 21. Seismic survey per pulse statistics. SPL units: dB re 1 µPa, SEL units: dB re 1 µPa²·s.

Pulse statistics	Per Pulse Average SPL		Per Pulse Average SEL	
	Station J1	Station J3	Station J1	Station J3
Minimum	96.7	95.6	102.4	101.5
Maximum	125.0	118.6	126.0	119.3
Average	108.0	103.6	113.2	108.6
Median	107.1	102.6	112.5	108.1

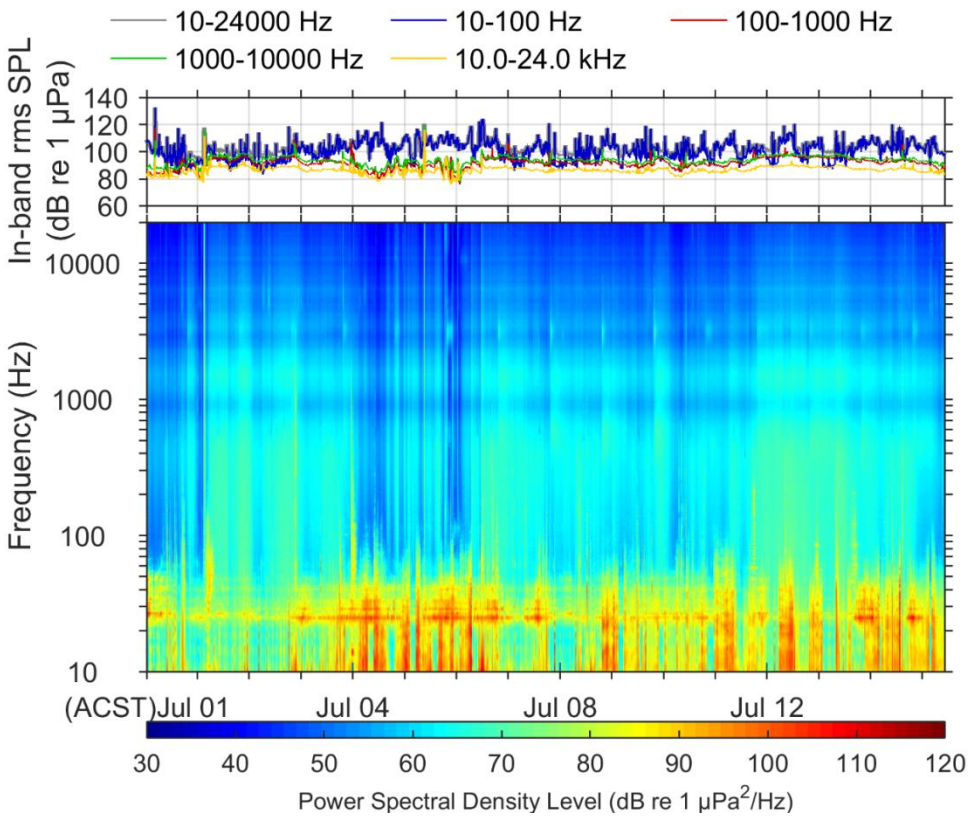

Figure 73. Spectrogram of Station J1, July 2015, showing seismic survey activity below 100 Hz. The 26–28 Hz tone from mysticete calls is visible even during the seismic activity.

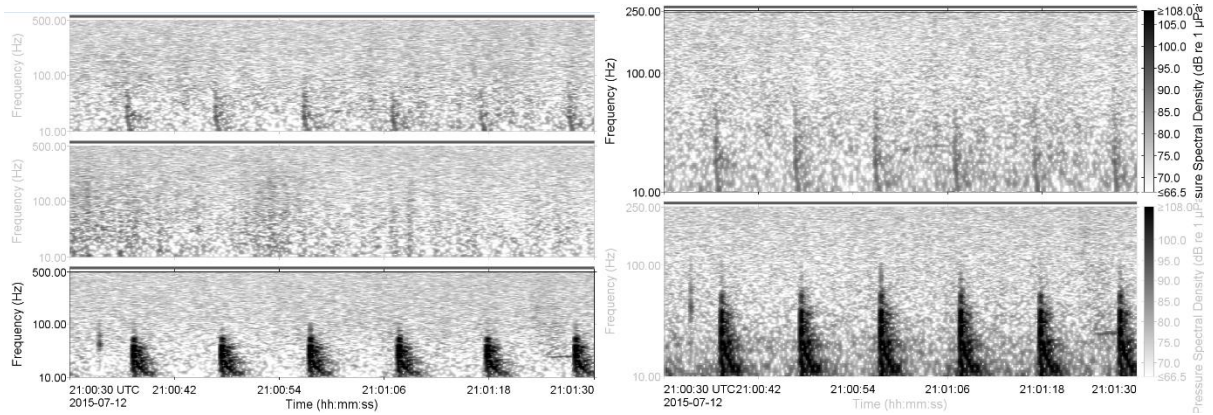

Figure 74. Left: Spectrogram of 12 July from 21:30 for Stations J1-J3 (bottom to top), and right: spectrogram of Stations J1 (bottom) and J3 (top) for the same period, showing PSD levels, (1 Hz frequency resolution, 1s time window, 0.1 s time step, and Hamming window).

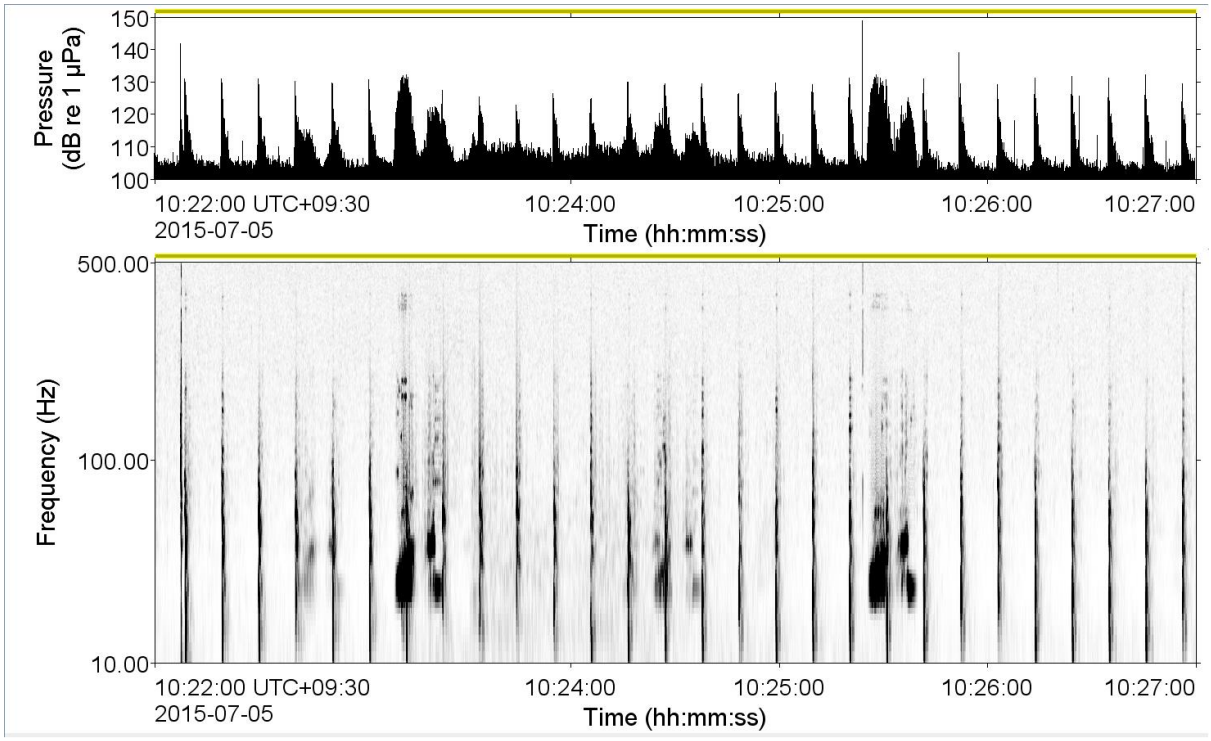

Figure 75. Five minutes of data from J1 on 5 July 2015 showing mysticete calls equal amplitude to the seismic pulses.

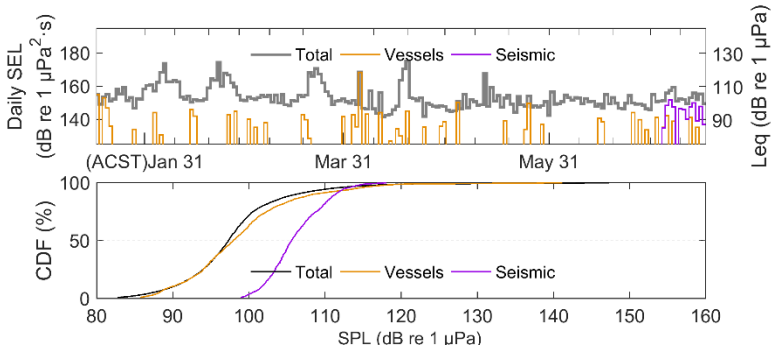

Figure 76. Station J1, Deployment 2, accumulated SEL and SPL cumulative distribution function

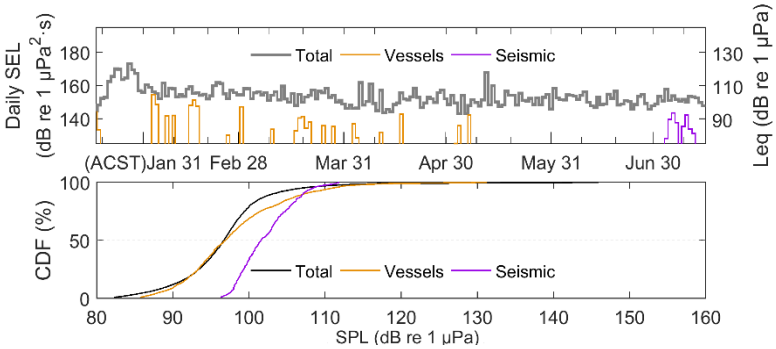

Figure 77. Station J3, Deployment 2, accumulated SEL and SPL cumulative distribution function

3.4.5. ROV Operation

A Remotely Operated Vehicle (ROV) was used to deploy a tertiary acoustic release at Station J1 on 4 April 2015 due to a malfunction of the releases on the mooring. The presence of the *MV Warrego* and the ROV on station was a dominant contributor to the soundscape from 10 Hz–24 kHz for the period it took to complete the operation (Figures 78 and 79).

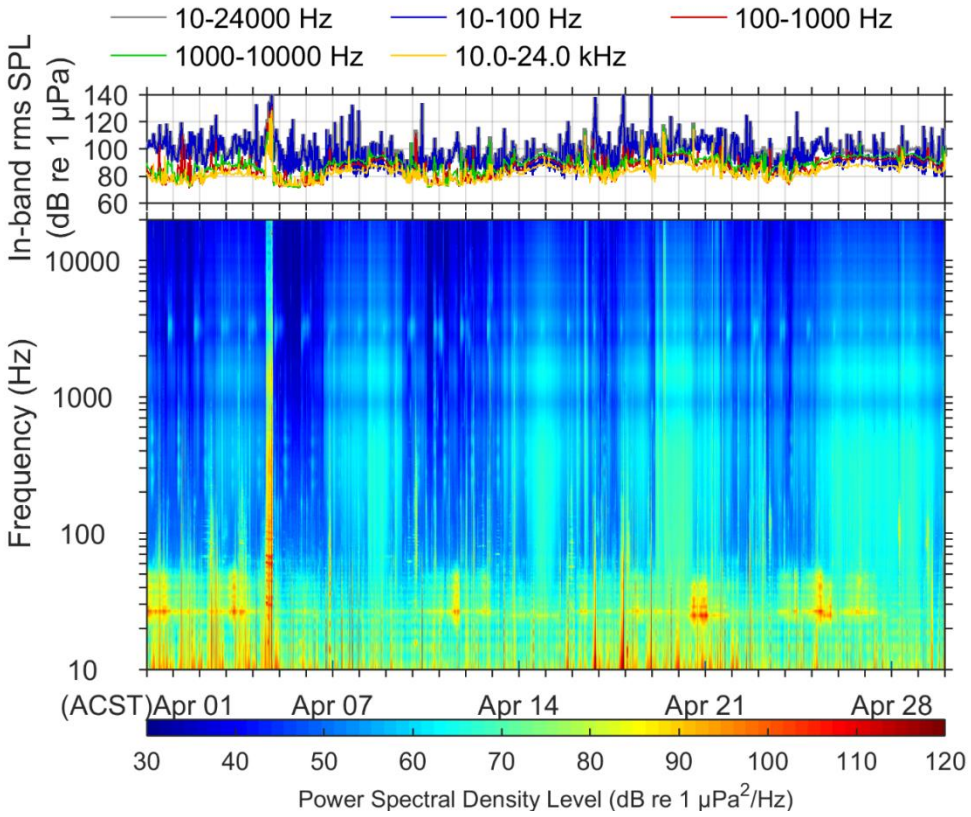

Figure 78. Monthly spectrogram for Station J1, April 2015. The ROV operations are the vertical red line on 5 April. The daily dawn chorus from 200-900 Hz and the evening chorus from 2-4 kHz can also be seen, as well as periods of mysticete calling at 26–28 Hz.

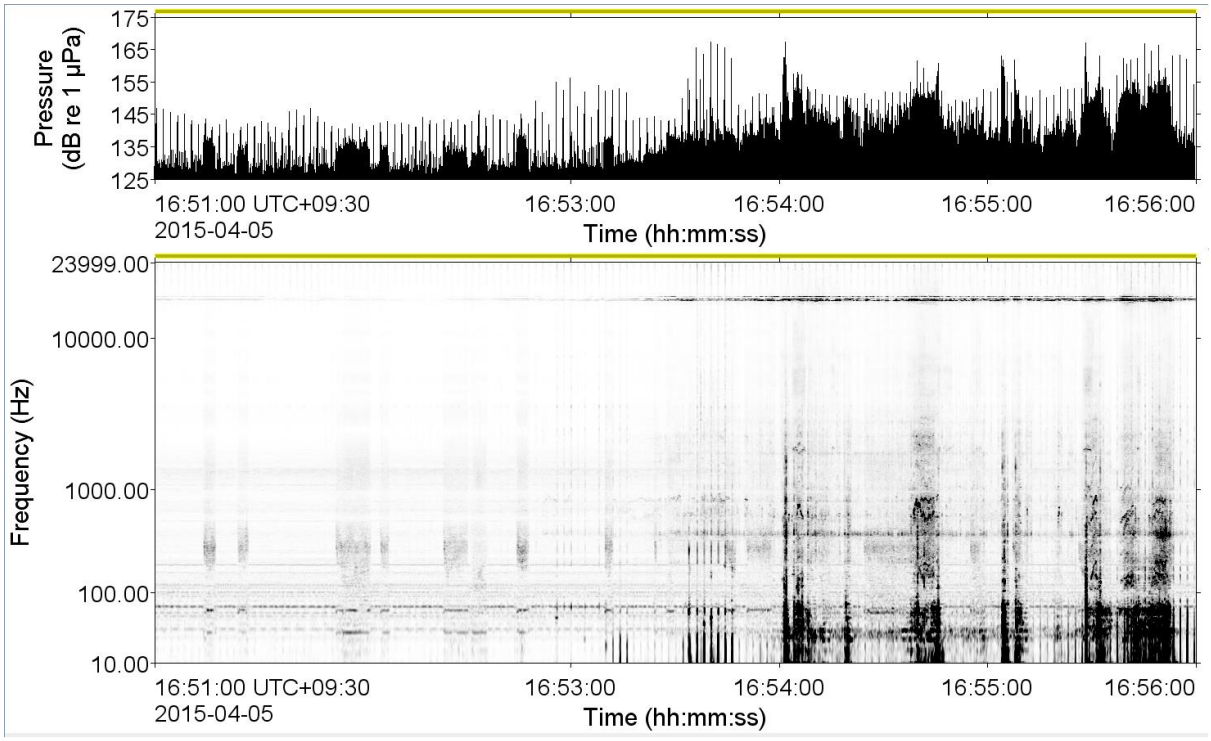

Figure 79. 5 minutes of data from 5 April 2015 during the ROV operations. The first two minute contain thruster manoeuvring as the ROV approached the J1 mooring. The last two minutes contains hydraulic sounds from the ROV manipulator arms. The spikes in the time series display are from acoustic locator beacons or from the M/V Warrego's echosounder.

3.5. Rhythmic Pattern Analysis

3.5.1. Deployment 1

The first deployment data were analysed over the entire period (Figure 80) and broken into three six-week periods (10 July to 1 September, 1 September to 10 October, and 10 October to 1 January) based upon different weather events and the presence of the MODU (Table 22). Patterns emerged from trends in the data over these periods in terms of biological contributors and the relative contributions of weather and the MODU-associated operations.

Analysis of the daily rhythms at Station J1 (Figure 81) shows that the low frequency decade (10-100 Hz) had approximately the same amplitude for all periods and all times of day at ~85 dB re 1 µPa. The 100-1000 Hz and 1000-10000 Hz decade bands were significantly above the 10-100 Hz band during the first period, but below the 10-100 Hz band during the other two periods. The two higher decades are often associated with wind and wave activity which was higher during the first period. The first and second periods appear to have increased wind and wave noise later in the day suggesting a deil heating increasing the winds in the afternoon.

The rhythms also confirmed the presence of the fish chorusing events, however only the evening chorus in the 1000–10000 Hz band is apparent during all periods, and the dawn chorus in the 100–1000 Hz is only apparent in the period 10 October–January 1. This aligns with the observations in Section 4.1.3. The weather events were less of a contributor in this period, thus the fish chorusing became detectable from the background in the total sound levels.

Analysis of the daily rhythms at Station J2 (Figure 82) show that the overall sound levels are generally consistent over a 24 h period, with only a slight difference between day and night. The 'bump' in the 100–1000 Hz band 1 September to 10 October at approximately 20:00 is also due to unknown causes. Weather raised the low frequency 10–100 Hz band sounds by 5–7 dB in the first period compared with the second period, whereas the MODU when present in the period 10 October–1 January raised the 10-100 Hz band sound levels by 20 dB compared to the 1 September–10 October

period. A similar effect was observed in the 100–1000 Hz band, with weather raising the median SPL by 10 dB, while the MODU raised it by 10–15 dB. The presence of the MODU did not contribute to the 1000–10000 Hz band. In other periods weather increased the median SPL by approximately 10 dB during the first period compared to the second. Fish choruses were in the spectrograms (Section 3.2.4.2) although they are not apparent in the daily rhythms.

Analysis of the rhythms at Station J3 (Figure 83) shows a greater increase in the overall sound levels during the day relative to the night-time levels. The fish choruses are not apparent in the analysis for this station. The period with the highest influence from the weather, 10 July to 1 September, also had the highest overall levels. The 10–100 Hz band is the primary band in which the diurnal change is present, with an average 5 dB change occurring close to sunrise and sunset.

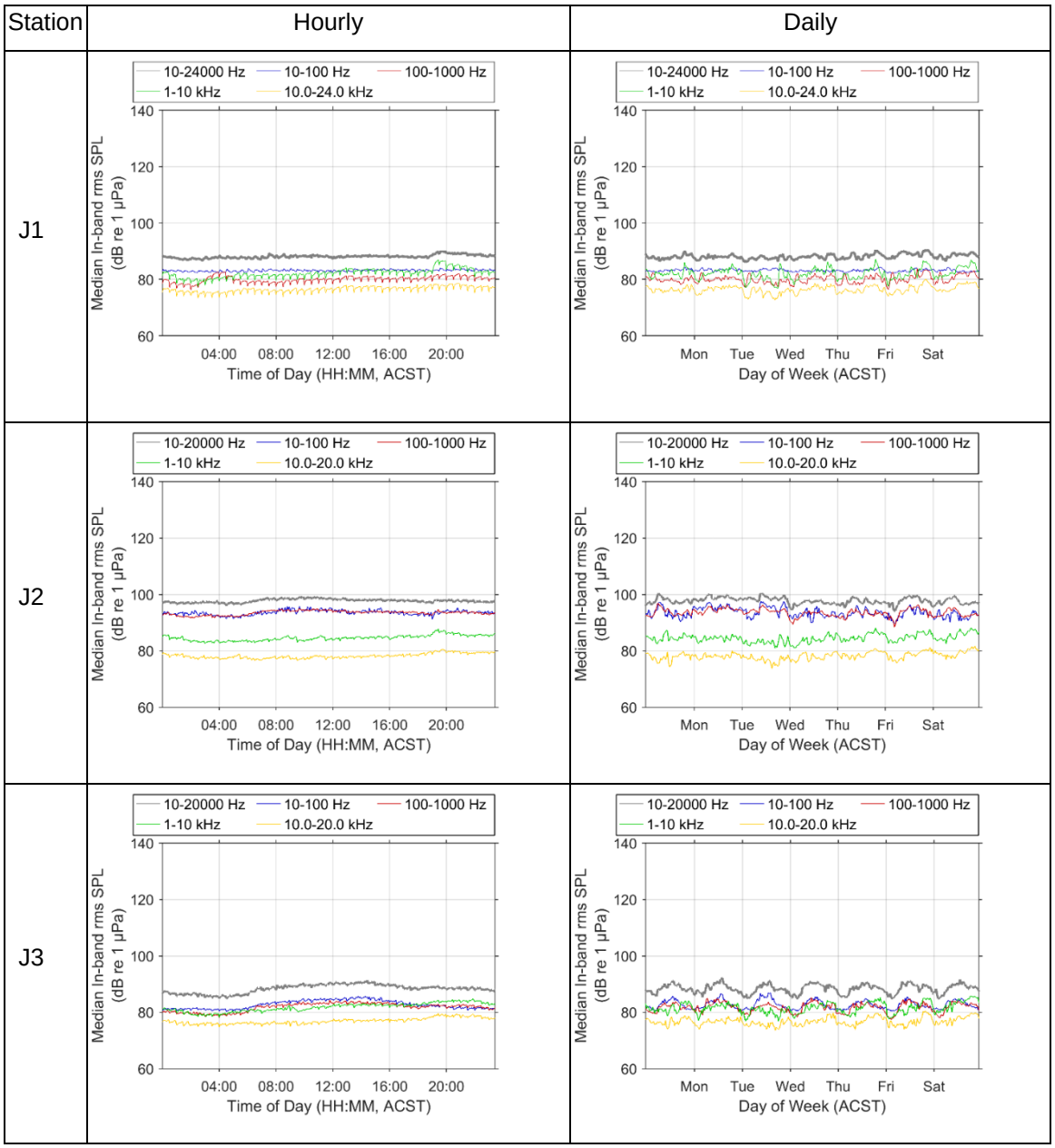

Figure 80. Deployment 1: Pattern analysis for the entire deployment for all stations, hourly (left) and daily (right)

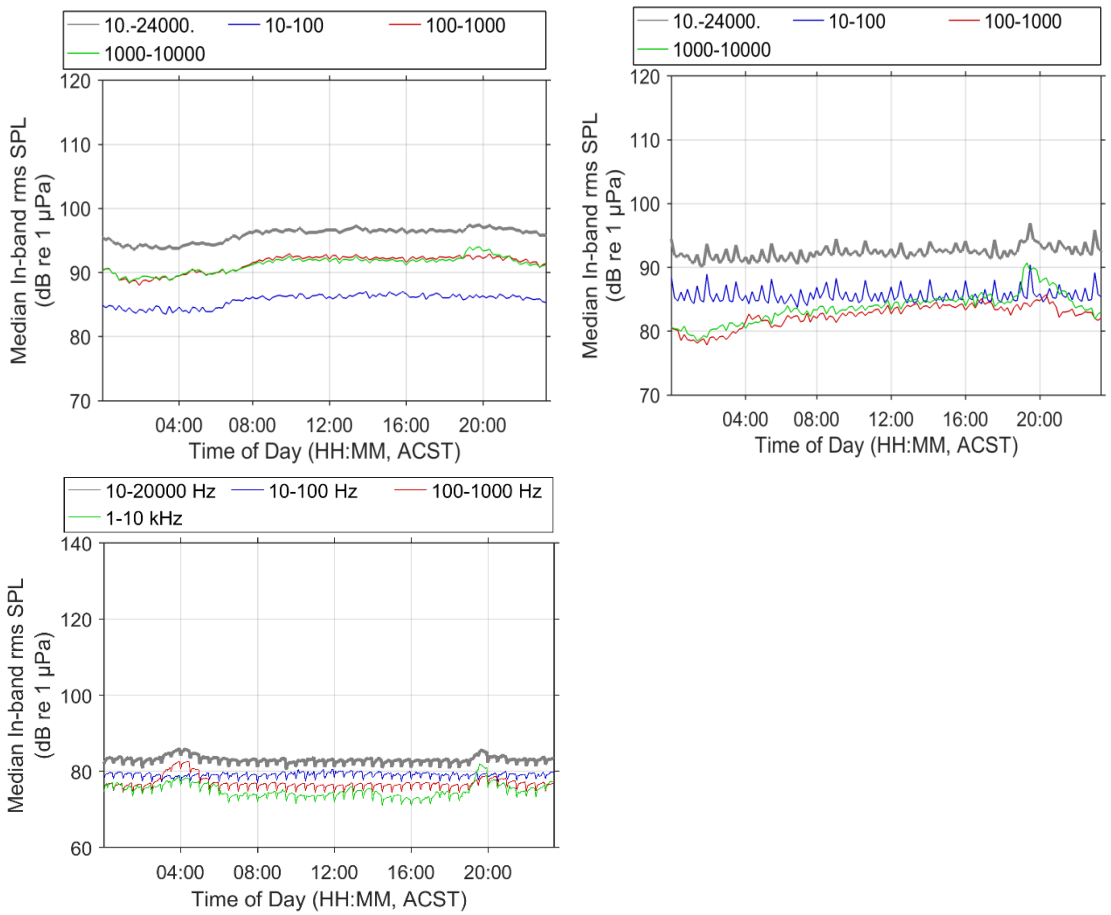

Figure 81. Deployment 1: Pattern analysis for Station J1, (top left) 10 July to 1 September 2014, (top right) 1 September to 10 October 2014, and (bottom left) 10 October 2014 to 1 January 2015.

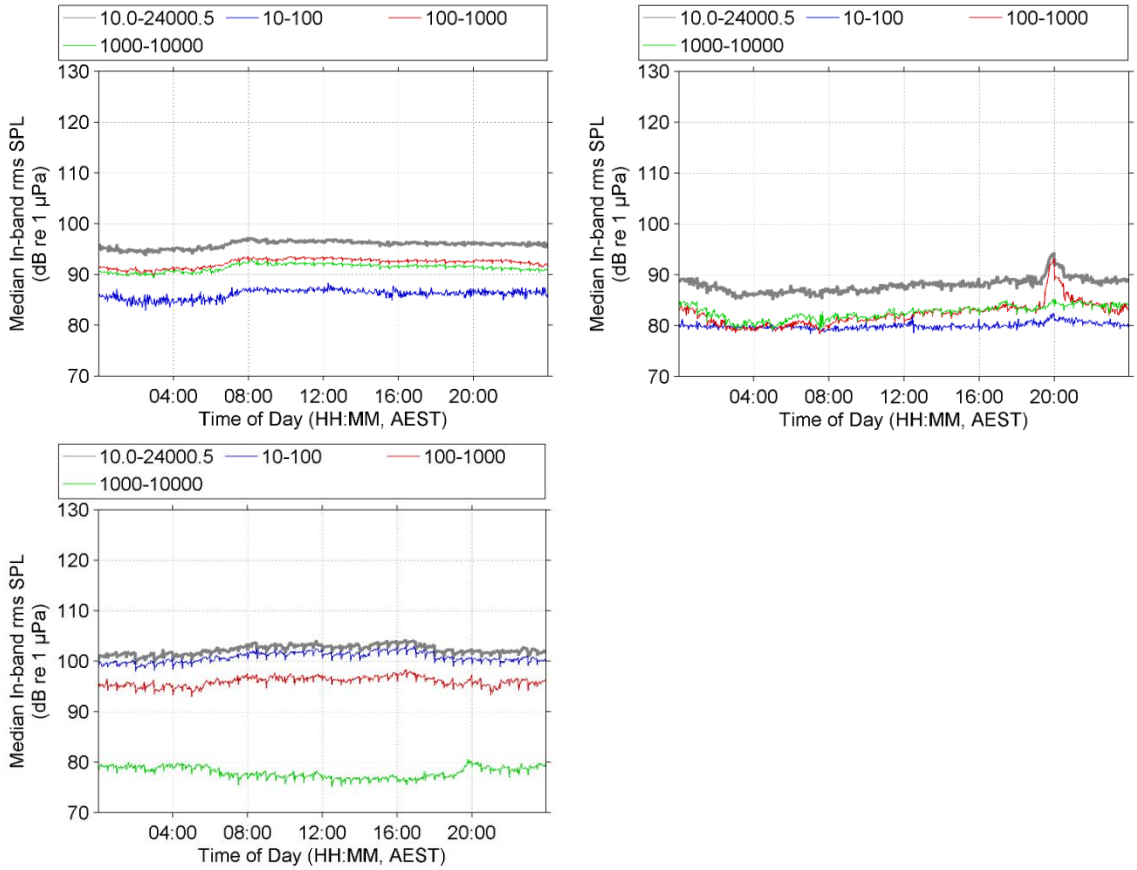

Figure 82. Deployment 1: Pattern analysis for Station J2 (top left), 10 July to 1 September 2014, (top right) 1 September to 10 October 2014, and (bottom left) 10 October 2014 to 1 January 2015.

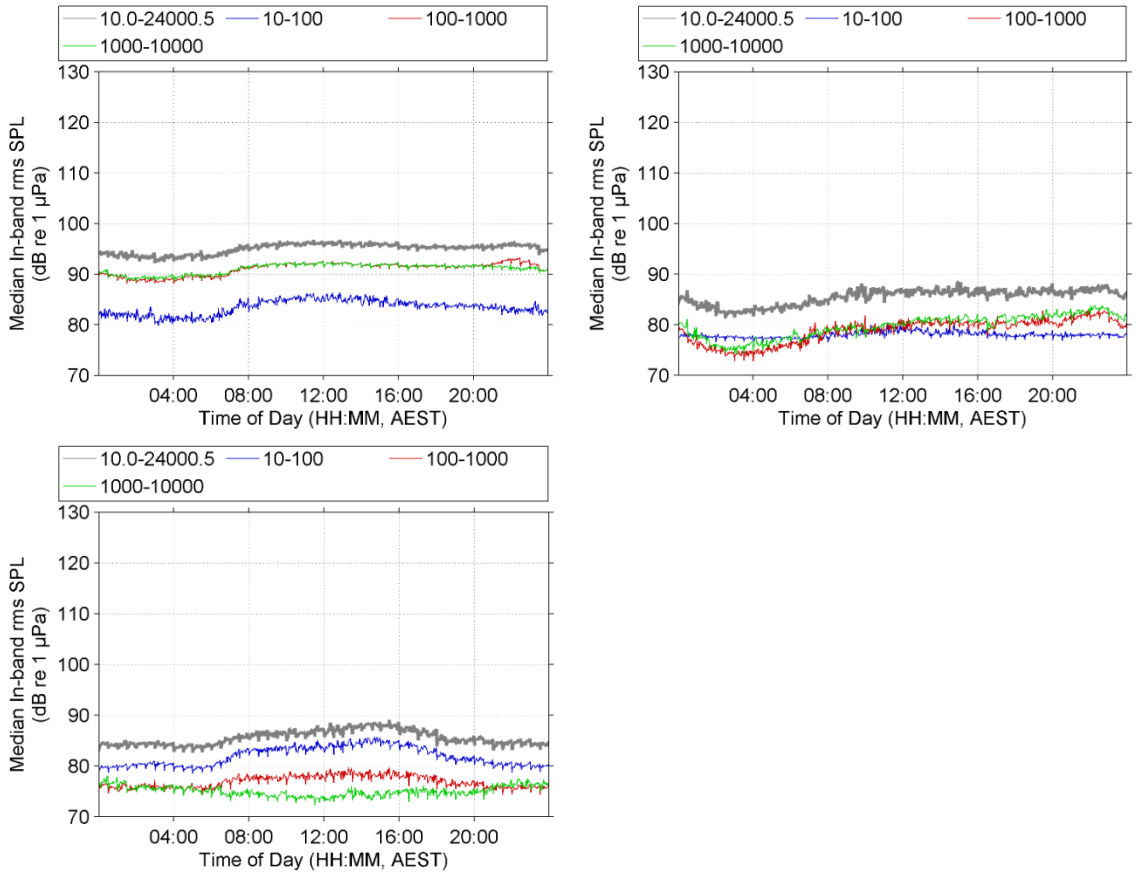

Figure 83. Deployment 1: Pattern analysis for Station J3, (top left) 10 July to 1 September 2014, (top right) 1 September to 10 October 2014, and (bottom left) 10 October 2014 to 1 January 2015.

3.5.2. Deployment 2

The second deployment data were analysed for patterns across the entire period (Figure 84). Similar to the first deployment, patterns emerged from trends in the data over these periods in terms of biological contributors and the relative contributions of weather and the MODU associated operations. The analysis was done on both a daily and weekly basis. Potentially due to the plots being analysed over the entire deployment, some of the minor patterns noted during the Deployment 1 analysis were not found, and it was not possible to determine weather contributions per period using the pattern analysis for this deployment.

Analysis of the rhythms at Station J1 did not show the fish chorusing as clearly as Deployment 1 and that the band levels were reasonably consistent through the entire deployment. The only pattern present was the slight increase in sound levels during the day relative to night-time levels. There was a slight rise in levels in the evening, centred at 20:00, which is possibly due to fish chorusing.

Station J2 sound levels were generally consistent over a 24 h period, with only a slight difference between day and night. The ‘bump’ present in the 100–1000 Hz band during 1 September–10 October at approximately 20:00 from Deployment 1 was also observed in this deployment, however was also present in the 1–10 kHz band; the cause is unknown, however likely due to biological contributors. The 10–100 Hz band is approximately 10 dB higher at this station, which is due to the presence of the MODU early in the deployment. Again, although they were apparent in the data and visible in the spectrograms, fish chorusing events are not apparent in the cyclic period analysis.

The patterns at Station J3 shows a greater increase in the overall sound levels during the day relative to the night time levels than the other stations, which is similar to Deployment 1. The fish choruses are not apparent in the cyclic period analysis for this station. The 10–100 Hz band is the again the primary band in which the diurnal change is present, with an average 5 dB change, similar in magnitude to Deployment 1, occurring close to sunrise and sunset.

Station	Hourly	Daily
J1	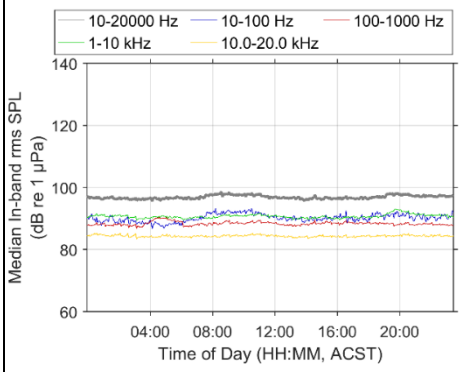	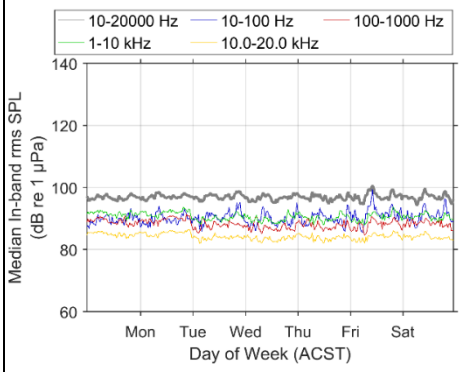
J2	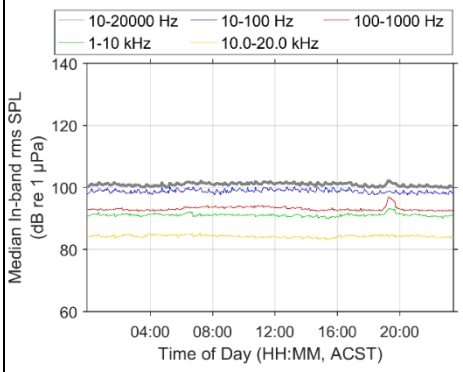	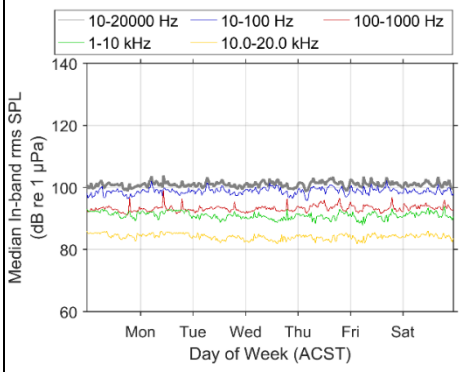
J3	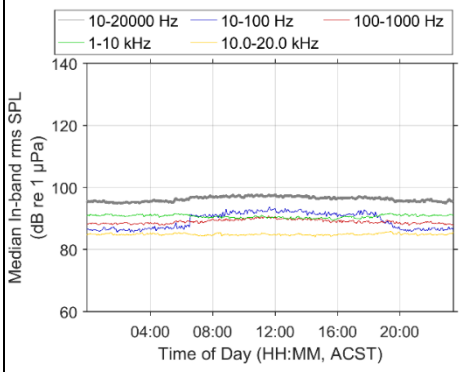	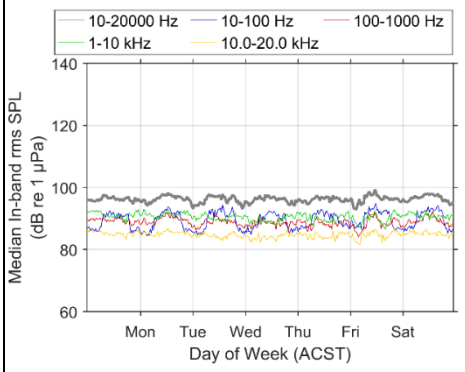

Figure 84. Deployment 2: Pattern analysis for the entire deployment for all stations, hourly (left) and daily (right)

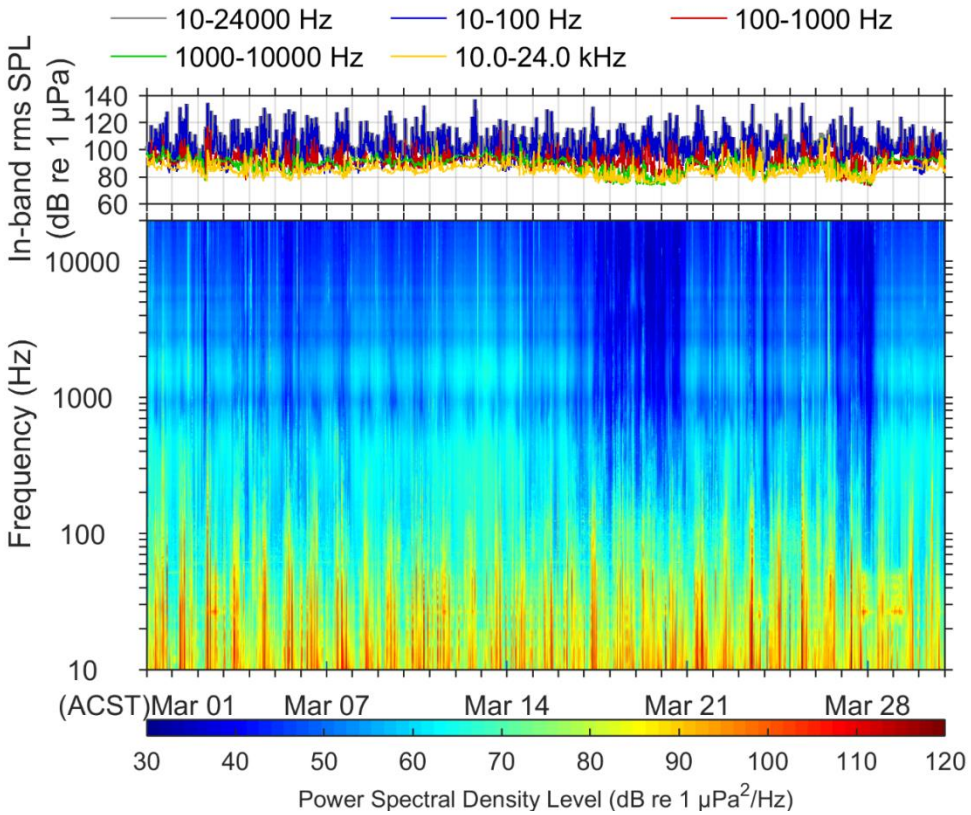

Figure 85. Station J3, difference between day/night

4. Discussion

4.1. Marine Fauna

4.1.1. Mysticetes

Mysticetes—Bryde's, minke, humpback, and pygmy blue whales—may occur in the Timor Sea and surrounding waters according to DoE (2015). In addition it is believed that the Omura's whale is also present.

The acoustic absence of minke and humpback whales in these data can be attributed to one or more of the following:

- They were not present in this part of the Timor Sea
- They were present, but not calling
- They were present and calling, but were masked by noises such as vessels
- The detectors did not adequately detect these species
- The manual analysis was too limited in scope to capture these species

Minke, and humpback whales migrate to Antarctic waters in the austral summer to feed (Chapman 1974, Kasamatsu et al. 1995, Branch et al. 2007), so they are not likely be present from October through January. However, minke whales might be present from July to September, although they were not detected. Minke whales produce stereotyped calls (Gedamke et al. 2001, Risch et al. 2014) that should make them reliable targets for automatic detectors. In addition, calling rates in this generally acoustically cryptic species increase in winter during the breeding season as in other rorqual whales. Therefore, one could reasonably expect to detect their calls, if present. The absence of detections is thus best explained by the absence of this species in the area.

Humpback whales, another acoustically active species particularly during migration (Dunlop et al. 2007, Smith et al. 2008), were not detected in the data and it is likely that they are absent from the area. Data from Jenner et al. (2001) indicates that between June and mid-November humpback whales use the Kimberley area as a calving ground. This species has been observed seasonally to complete their northern migration in the Camden Sound area of the West Kimberley (Jenner et al. 2001) after feeding in Antarctic waters during summer (Bannister and Hedley 2001). If they were to be present at all it would be most likely to be in the June–August period, but as they were absent from the data during this time, they are unlikely to be present during any time of year.

4.1.1.1. Pygmy Blue Whale

Pygmy blue whales were present in the data, which was unexpected because they typically migrate further west along the edge of the continental shelf (Double et al. 2014, McPherson et al. 2014). Because they are acoustically active when they migrate (McCauley et al. 2001, Gavrilov et al. 2011), it is likely they were only present during the limited detection period and otherwise truly absent from the area, and not missing for one of the above listed reasons.

The calls detected matched those from reports and literature (McCauley et al. 2001, Gavrilov et al. 2011, McPherson et al. 2014), with all three call types recorded. Calls regularly occurred in a consecutive manner from Station J1 to J2, with intermediary detections at Station J3, indicating movement through the region in a south-west to north-east direction in May and June which correlates with the timing and heading of movements by one tagged animal in this area (Double et al. 2014). Calls ranged from faint to loud, as would be expected of animals moving through an area. These movements occurred over limited periods of time suggesting either few individuals traverse the area or they travel in tight groups. The detections presented here are over 400 km further east than the northeast-bound migration corridor of pygmy blue whales described in Double et al. (2014). No detections were logged from the south-bound migration, suggesting a different migration path. Pygmy blue whale call rates were highest at Station J2 (Barossa field), which may reflect its greater depth and proximity to the trench.

The data analysis provides some insight into the usage of the region by the pygmy blue whales. For example, received pygmy blue whale calls at Station J2 (Barossa field) ranged in sound level from ~62-110 dB re 1 µPa with a median SPL of ~94 dB re 1 µPa. The whales, assumed to be calling from a depth of 30 m, were anywhere from approximately 5–80 km from Station J2 with a median distance of over 23 km (call source level of 179 dB re 1 µPa) or over 31 km from Station J2 (call source level of 183 dB re 1 µPa). Further analysis of data from all stations would provide more detailed information about this usage, and could also be used to confirm the published call source levels, along with determine the source levels of the other types of calls. However, the data analysis completed to inform this report is considered adequate to inform a baseline understanding of the species broad use of the area.

4.1.1.2. Omura's/Bryde's Whale

Variation in the spatial and temporal occurrence of double-barrel/monotonic and downsweeping calls indicates that the two call-types are likely not produced by the same species. Based on the year of recordings, double-barrel/monotonic calls occur in the region in all months of the year with the exception of the period between 1 November and 23 December. During periods of increased detection, the calls raised the percentile power spectral density levels near the peak frequency of their call (~26–28 Hz) by ~ 1-5 dB. In the summer whales producing double-barrel/monotonic calls seemed to enter the area in a south-west to north-east direction (calls occurred consecutively at J1 followed by J3 and finally J2). The calls occurred regularly through the autumn and winter, with the call rate greatest at the deepest station (J2). In the spring, double-barrel/monotonic calls became sparser and whales seemed to leave the area in a north-east to south-west direction (calls ended at J2 before J1 with J3 calls being more sporadic).

Downsweeping calls similarly occurred in the region from summer (January) to the following spring (October), but the manner in which they were detected across stations and where they were predominantly detected contrasts to that of the monotonic calls. In the summer through autumn whales producing downsweeping calls moved into the area in a south to north direction (occurring first at J3 followed by J1 then J2), not occurring in the deep most northerly station (J2) until mid-April. Through the late autumn and winter months, downsweeps were detected at all stations, though the calling rate was slightly higher at the shallower stations of J1 and J3. In the spring, rather than leaving the area closer to J1 as the whales producing double-barrel/monotonic calls did, the whales producing downsweeps were last heard at the shallowest most southerly J3 station. The contrasting trends observed in double-barrel/monotonic and downsweeping calls provide evidence that these call types are likely produced by two different mysticete species, Omura's and Bryde's whales.

The double-barrel/monotonic calls presented here have previously been ascribed to Bryde's whales by McCauley and Kent (2009) and JASCO during a previous acoustic monitoring program in the Browse Basin (McPherson et al. 2014) and the western Timor Sea (McPherson et al. 2012). McDonald (2006) describes a ~5 s, 22 Hz tonal call and paired 26 Hz calls with ~ 120 s spacing and tentatively (not conclusively) assigns it to Bryde's whale. However, there are no peer-reviewed publications from northern Australia attributing such calls to Bryde's whales. Therefore, there is still a considerable amount of uncertainty surrounding the taxonomy of the Bryde's whale clade. Small rorqual whales caught off Western Australia and maturing at a small size (11–12 m) were identified as "Bryde's whales" (Bannister 1964). They may have been a local form, possibly related to small forms of Bryde's whales found elsewhere, but they may also have been the Omura's whale (*B. omurai*). Oleson et al. (2003) described nine Bryde's call-types, none of which reached the duration observed in the double-barrel/monotonic calls observed here. Since the previously mentioned studies took place, new information on the range and calls of Omura's whales, a distant relative of the Bryde's, has come to light, providing a more likely candidate for the production of the double-barrel/monotonic calls.

Cerchio et al. (2015) studied the calls of the Omura's whale in Madagascar, and described them as occurring between 15–50 Hz, lasting for 8–9 s, and in a repeated sequence every 2–3 minutes. The authors suggest that these song-like calls may be mating displays and are potentially indicative of breeding habitat. These long calls are very similar to the monotonic calls detected during this study (Section 3.2.2.2, Figure 30), differing only in peak frequency, which may be the result of geographic variations in call attributes as noted between populations of several other rorqual species. The Madagascar population of Omura's has also been described as producing double-barrel calls similar to what has been observed here (Cerchio, personal communication).

Omura's whales were only described as a new species in 2003 (Wada et al. 2003) and remain poorly understood in terms of their spatio-temporal distribution as well as physical appearance and vocal behaviour, making misidentification during visual surveys common. Omura's whales are believed to be present in the Timor Sea, through the habitat and water temperature range described in Cerchio et al. (2015), the aforementioned paper, the distribution map on the IUCN Red List (Reilly et al. 2008b), sightings reported at Marinemammalscience.org, and carcasses washed ashore in Western Australia. While in the region they have been described opportunistically by tour groups as feeding over deep shoals and reefs with newborn calves present (Marinemammalscience.org). The available information strongly suggests that the double-barrel/monotonic calls observed here were produced by the little known Omura's whale.

The downsweeping calls described in Section 3.2.2.2.1 (Figure 32), have been observed in the western Timor Sea previously (McPherson et al. 2012). Omura's whales have not been reported to produce downsweeps, although the species' repertoire description is in its infancy. In contrast, downsweeps are known to be produced by Bryde's whales in several areas (Oleson et al. 2003, Širović et al. 2014). The presence of Bryde's whales would be expected based on findings by a number of studies that noted the species' occurrence in the area and the surrounding waters (Rudolph et al. 1997, Heaney et al. 1998, McDonald 2006, Reilly et al. 2008a, Dethmers et al. 2009). It is important to recognise that much of the previous literature describing Bryde's whales in the region took place before the Omura's whale was described, and after the fact it would be difficult to visually discern between the two species at a distance or in any reduced visibility. Therefore, it is possible that a portion of previously described Bryde's whale sightings were actually Omura's. Regardless, based on the available information, it is reasonable to conclude that the downsweeping calls described here were produced by Bryde's whales.

Unlike many mysticetes, Bryde's and Omura's whales are not known for long-distance, low-high latitude migrations, but some Bryde's populations have been observed to move toward the equator in the winter and away from it in the summer (Best 1977, Valdivia et al. 1981, Wiseman et al. 2011), similar to what has been observed here. The high Omura's calling rate at the deepest station suggests that, like the blue whales, they find some benefit in the deeper waters. The opposite trend was observed in Bryde's which showed slight preference for shallower areas. Similarly, Alves et al. (2010) found Bryde's to stay near shore and make predominantly shallow dives. However, the trend observed here was minimal and therefore may be unreliable due to a small sample size; alternatively, it may be evidence of variation between the species in feeding preferences. The findings in this report shed new light on the spatio-temporal distribution of the poorly understood Bryde's and Omura's whales in the Timor Sea.

4.1.2. Odontocetes

The clicks and whistles recorded across the three stations varied immensely in characteristics, suggesting the occurrence of a number of odontocete species. Such has been observed by Rudolph et al. (1997) and Dethmers et al. (2009) who found short-finned pilot whales, sperm whales, false killer whales, pygmy killer whales, melon-headed whales, Risso's dolphins, Fraser's dolphins, spotted dolphins, rough-toothed dolphins, and spinner dolphins to be present in the area. While it would be ideal to discriminate between species, success has been limited using automated detectors and the detailed manual analysis required to identify individual species (Steiner 1981, Rendell et al. 1999, Oswald et al. 2003, Baron et al. 2008) is beyond the scope of this report. From the data analysis undertaken, whistles similar to those of short-finned pilot whales were found on a number of occasions indicating the likely presence of the species in the more northern stations (Sayigh et al. 2013).

Due to the overlap in call types of many odontocetes, the presence of any of the aforementioned species with the exception of sperm whales cannot be conclusively ruled out. Sperm whale clicks are unique in nature and easily detected, therefore they were likely absent. Such is supported by (Dethmers et al. 2009) who only observed one sperm whale in a nearby area while small odontocetes were reported in the hundreds.

Vocalisations of beaked whales, species unknown, were positively identified during manual analysis, and a detector was created specifically for them. The data were re-processed using this detector, and they were found to be present on 3 days at Station J3 and one day at Station J2 (Section 3.2.3.1) over the entire monitoring program. One of the calls detected is similar to those defined as 'beaked whale

G' (BWG) (Baumann-Pickering et al. 2013), and as such does not match any of those currently attributed to a specific species. Baumann-Pickering et al. (2013) state that to date there has not been any indication that a single species might produce multiple types of frequency-modulated pulses, and while they agree that this cannot be ruled out, current evidence suggests that frequency-modulated pulse types are species-specific. Acoustic recordings in the presence of identified beaked whales do not exist for five known species, including the ginkgo-toothed beaked whale (*Mesoplodon ginkgodens*) which distribution range overlaps the Barossa area (Reilly et al. 2008c) and has little information known about it. The detected calls therefore could either belong to a species for which no vocalisation information exists, a yet undescribed species, or a known species may produce multiple signal types. The only beaked whale thought to be in the region, based on the DoE Protected Matters search (2015), is Cuvier's, the known vocalisations of which are quite different to those recorded.

The predominance of odontocete clicks and whistles during hours of darkness likely corresponds to foraging on prey species that follow the diel vertical migrations of zooplankton. Similar patterns have been observed in a number of whale species (Víkingsson 1997, Au et al. 2000, Wiggins et al. 2005, Baumgartner and Fratantoni 2008, Sayigh et al. 2013), and JASCO in other studies conducted northern Australian waters (McPherson et al. 2012, McPherson et al. 2014).

The high number of false click detections at Station J1 during Deployment 1 can be attributed to compounding physical and biological factors. An ROV found this station to be in a high-current, rocky-bottom area with gorgonian sea fans, sponges and soft corals (Figure 86). Such a habitat would be ideal for crustaceans such as snapping shrimp, which, combined with the noise from the water flow through the rocks and the sea fans, likely resulted in the noise causing false click detections.

Figure 86. Sea floor at Station J1, with mooring line.

4.1.3. Fish

Dawn and dusk fish chorusing activity was present throughout the entire deployment at all three stations. It varied in intensity across the deployment period, however was reasonably consistent in timing. Fish chorusing is not currently able to be analysed through automated detections, and the scope of work did not include a requirement for manual analysis of chorusing event levels.

The dawn chorus is quieter during winter, appearing to increase in level throughout the deployment, with the loudest chorusing events in December. In contrast, the dusk chorus was louder during winter (July) and appears to decrease in level throughout the deployment, with the quietest chorusing events occurring in December. During Deployment 2, chorusing events were more prevalent at Station J1 than either of the other stations, with Station J3 recording very little fish chorusing activity. The higher level of fish chorusing activity closer to Evans Shoal across the entire program suggests that this area has a higher fish abundance. Little is known about the vocalisations of specific fish species in the Barossa field region, although it is expected that nocturnal planktivorous fishes, believed to be of the families Holocentridae, Priacanthidae and Apogonidae are dominant contributors, particularly for chorusing events (McCauley 2012).

Individual calls were detected at all three stations, although the relative densities were not analysed, as a detector for the types of fish calls recorded had not been implemented. A number of the individual calls observed were similar to those made by lutjanids, which are best characterised by *Rhomboplites aurorubens* (Luna 2014). There is a lack of knowledge about vocalisations of the most

common fish species present in the region. However it is possible that a large number of the observed vocalisations are attributable to members of the *Lutjaninae* family.

4.2. Anthropogenic contributors

Statistical analysis of sound levels for all stations over the monitoring program included examining the minimum, maximum and quartile percentiles for both PK and 1-min SPL, along with the percentage of exceedance of the 120 dB level (Table 16), the mean, median, minimum, maximum and daily SELs (Table 18), and the median 1 minute SPLs for the previously discussed pattern analysis periods for Deployment 1 (Table 17).

Generally, there was a low level of anthropogenic contribution across Deployment 1, with the exception of the presence of the MODU *Nan Hai VI* and associated support vessels. Table 22 summarises Tables 17–20 for the three stations for Deployment 1 to assist with comparison. The presence of vessels cannot be used to predict sound levels, as weather is also a contributor to the soundscape. When the mean daily vessel detection levels between the stations diverge, as occurs for the two periods after 10 October 2014, the median 1-min SPLs also diverge, being 25.15 and 16.45 dB higher for Station J2 than the combined average of both other stations, which are within 3.7 and 8.3 dB of each other respectively. The contribution of the MODU and associated support vessels to the soundscape is more noticeable than in other regions of Australia, for instance the North-West Shelf, due to the low volumes of shipping traffic. The highest mean daily detections over all stations and deployments is 1.4 at Station J2 during Deployment 2, likely associated with the MODU.

Although the MODU and associated support vessels were present for the first three months of Deployment 2, again close to Station J2, their impact over the entire deployment on the median daily SELs is minimal, causing a 1.45 dB relative increase as opposed to a 16.5 dB increase. Even though there is only one-month difference in the duration of presence, the additional distance between the MODU and the monitoring stations (23, 7.5 and 13 km extra respectively) has reduced the received levels.

At the two stations farthest from the MODU and the primary vessel activity in the region (i.e., Stations J1 and J3), anthropogenic activity typically does not determine either the median 1 min SPL sound levels or the average daily SEL, with natural and biological sources being dominant. Therefore, the MODU and rig tenders, while a dominant feature of the soundscape at close range, are less influential than the natural and biological sources typical of the region, and can be said to have a localised impact. When the MODU is 15.5 km away from Station J2 during Deployment 2, the mean daily SEL is less at Station J2 then at both other stations, indicating that at this range it doesn't define the soundscape when its contribution is considered over a six-month time period.

The seismic survey detected from 4–14 July 2015 was only a minor contributor to the soundscape, due to the low levels of the received pulses – the maximum per-pulse SEL was 126.0 dB re 1 µPa²·s, and the intermittent nature of the detections. The survey occurred to the north of the Barossa field, however received levels were consistently higher at Station J1 than Station J3 (the median per-pulse average SEL was 4.4 dB higher), and no pulses were detected at Station J2.

Table 22. Deployment 1, mean daily vessel detections, median 1 min SPLs sound levels and average daily SEL, Stations J1, J2, and J3. SPL units: dB re 1 µPa, SEL units: dB re 1 µPa²·s

Stn	10 Jul–1 Sep 2014			1 Sep–10 Oct 2014			10 Oct 2014–1 Jan 2015			1 Jan–15 Jul 2015		
	Mean daily vessel detect-ions	1-min SPL L_{50}	Mean SEL	Mean daily vessel detect-ions	1-min SPL L_{50}	Mean SEL	Mean daily vessel detect-ions	1-min SPL L_{50}	Mean SEL	Mean daily vessel detect-ions	1-min SPL L_{50}	Mean SEL
J1	0.1	97.3	146.9	0.1	93.7	146.3	0.2	93.6	145.3	0.1	106.4	154.6
J2	0.1	97.5	150	0.3	95.6	151.1	2.8	116.9	168.7	0.8	118.7	170.2
J3	0.2	96.6	147.8	0.3	88.1	144.8	0.3	89.9	151.9	0.1	98.1	151.7

Table 23. Mean daily vessel detections, median 1 min SPLs sound levels and average daily SEL, Stations J1, J2, and J3, both deployments SPL units: dB re 1 µPa, SEL units: dB re 1 µPa²·s

Stn	Deployment 1			Deployment 2		
	Mean daily vessel detect-ions	1-min SPL L_{50}	Mean SEL	Mean daily vessel detect-ions	1-min SPL L_{50}	Mean SEL
J1	0.1	95.2	150.6	0.4	97.7	160.6
J2	1.4	98.3	152.6	0.7	100.9	157.4
J3	0.3	89.8	147.7	0.3	98.2	158.2

5. Conclusion

The goals of this study were to characterise the contributions to the marine soundscape from natural sources, including sounds generated by tides and events, biological sources (including fish, whales (mysticetes and odontocetes) and crustaceans), and anthropogenic sources, including vessel traffic and the MODU's drilling operations.

Marine mammals were detected acoustically in the Barossa area during the entire deployment period. Pygmy blue, Omura's and Bryde's whales were detected, with detections commonly occurring during the months of May – August, while no detections occurred between 1 November and 23 December. The pygmy blue whale detections are over 400 km farther east than the currently estimated north-bound migration corridor of pygmy blue whales, and their detection is a significant regional scientific contribution.

Omura's whales were detected consistently from April to September inclusive, with a peak in June and July. Based on the year of recordings, the whales seemed to enter the region in a south-west to north-east direction, then maintain a higher presence within the Barossa field area (than compared to the Evans Shoal or Caldita field areas) for the autumn and winter months. They appeared to leave the region in a north-east to south-west direction, reversing their entry path, leaving the area by the start of November.

Pygmy blue whales were detected during their northward migration once in August 2014, over a few consecutive days in late May-early June 2015, on the 16 and 30 June, and 1 July 2015. No detections were logged from the south-bound migration, suggesting a different migration path. The highest calling rates of the three monitoring station occurred at the Barossa field.

Bryde's whales, distinguished from the Omura's whales through variations in the spatial and temporal occurrence of vocalisations, were present in the region from January to October. They appear to move into the area in a south to north direction during summer and autumn, then utilise the region with a preference for the shallower sections (Evans shoal and Caldita field areas) over the Barossa field region. They then leave the area in a north – south direction, with the last detections in early October.

Detections of odontocetes were abundant, equally distributed across the deployment period at Stations J2 and J3 and primarily occurred at night. The distribution of click detections at Station J1 during Deployment 1 and part of Deployment 2 was influenced by a large number of false positives due to the presence of crustaceans such as snapping shrimp. Based on manually verified click and whistle detections compared to automated detections of whistles, odontocetes at Station J1 were observed at a similar frequency to that at J2 and J3: i.e., present throughout the recording period and primarily at night. The presence of potentially unknown beaked whales is a significant scientific finding, however their rare presence, four days over the monitoring program, suggests they are not resident in the region. Unknown beaked whale species were detected on four days over the entire program at Stations J2 (Barossa field) and J3 (Caldita field).

Fish chorused at dawn and dusk over the entire deployment period at all three stations. Their chorusing varied in intensity over the deployment period, but was consistent in diel pattern.

The ambient sound levels indicate a region with low anthropogenic sound presence. A mean SPL of 95.7 dB re 1 µPa (s=2.6) was calculated from data collected at Stations J1 and J3 (at greater distance from the MODU operations), while a mean SPL of 103.55 dB re 1 µPa (s=2.65) was calculated from data collected at Station J2 closer to the operations. Weather was a significant contributor to the total received sound levels at all stations. Anthropogenic sound sources were only occasionally detected in the data, with the exception of sounds associated with the MODU. The ambient sound data identified minor diel variations in sound levels due to fish chorusing events. Diel variations in ambient sound data were primarily affected by weather events, which at times produced a noticeable diel variation in sound levels, with levels increasing during the day, and decreasing at night.

Based on the data collected, it is concluded that the typical soundscape in the Barossa area is dominated by (geophonic) naturally occurring sources such as wind and waves, with some contributions from biological sources (primarily fish and Omura's whales). There was a low presence of sound-producing anthropogenic activity, with the majority of it related to the exploration drilling program in the Barossa field. Given the short timeline of the activity, this increase in sound levels was also short term. The area appeared to be used consistently by Omura's and Bryde's whales from mid-

autumn through mid-spring, and odontocetes throughout the year. The area is along the edge of the broader migration pathway for pygmy blue whales in winter, as they move through it as part of their broader northward migration. Fish chorusing activity changes with the seasons, and is most pronounced closer to Evans Shoal (Station J1), thereby suggesting that this area has a higher fish abundance.

Acknowledgements

The authors would like the acknowledge the assistance of the JASCO editors Katherine Williams and Karen Hiltz, the project manager and party chief Chris Teasdale from Jacobs, and the Gun Marine vessel crew. Reviews from Jacobs and ConocoPhillips were appreciated.

Glossary

µPa
micropascal, SI unit for f pressure and stress equal to 10^{-6} pascals

1/3-octave-band
Non-overlapping passbands that are one-third of an octave wide (where an octave is a doubling of frequency). Three adjacent 1/3-octave-bands make up one octave. One-third-octave-bands become wider with increasing frequency. See also octave.

90%-energy time window
The time interval over which the cumulative energy rises from 5% to 95% of the total pulse energy. This interval contains 90% of the total pulse energy. Symbol: T_{90}.

90% sound pressure level (SPL(T_{90}))
The root-mean-square sound pressure levels calculated over the 90%-energy time window of a pulse. Used only for pulsed sounds.

ambient noise
All-encompassing sound at a given place, usually a composite of sound from many sources near and far (ANSI S1.1-1994 R2004), e.g., shipping vessels, seismic activity, precipitation, sea ice movement, wave action, and biological activity.

background noise
Total of all sources of interference in a system used for the production, detection, measurement, or recording of a signal, independent of the presence of the signal (ANSI S1.1-1994 R2004). Ambient noise detected, measured, or recorded with a signal is part of the background noise.

cetacean
Any animal in the order Cetacea. These are aquatic, mostly marine mammals and include whales, dolphins, and porpoises.

continuous sound
A sound whose sound pressure level remains above ambient sound during the observation period (ANSI/ASA S1.13-2005 R2010). A sound that gradually varies in intensity with time, for example, sound from a marine vessel.

decibel (dB)
One-tenth of a bel. Unit of level when the base of the logarithm is the tenth root of ten, and the quantities concerned are proportional to power (ANSI S1.1-1994 R2004).

duty cycle
The time when sound is periodically recorded by an acoustic recording system.

F score
Metric used to measure the performance of an automated detector/classifier. The F score is computed as the harmonic mean of precision and recall.

false negatives (FN)
A signal of interest missed (i.e., not detected) by an automated detector/classifier.

false positives (FP)
A noise classified as a signal of interest by an automated detector/classifier (i.e., a false alarm).

FFT
Fast Fourier Transform.

FM
Frequency Modulated.

frequency
The rate of oscillation of a periodic function measured in cycles-per-unit-time. The reciprocal of the period. Unit: hertz (Hz). Symbol: *f*. 1 Hz is equal to 1 cycle per second.

ksps
kilosamples per second

hertz (Hz)
A unit of frequency defined as one cycle per second.

hydrophone
An underwater sound pressure transducer. A passive electronic device for recording or listening to underwater sound.

median
The 50th percentile of a statistical distribution.

mysticete
Mysticeti, a suborder of cetaceans, use their baleen plates, rather than teeth, to filter food from water. They are not known to echolocate, but use sound for communication. Members of this group include rorquals (Balaenopteridae), right whales (Balaenidae), and the gray whale (*Eschrichtius robustus*).

octave
The interval between a sound and another sound with double or half the frequency. For example, one octave above 200 Hz is 400 Hz, and one octave below 200 Hz is 100 Hz.

odontocete
The presence of teeth, rather than baleen, characterizes these whales. Members of the Odontoceti are a suborder of cetaceans, a group comprised of whales, dolphins, and porpoises. The toothed whales' skulls are mostly asymmetric, an adaptation for their echolocation. This group includes sperm whales, killer whales, belugas, narwhals, dolphins, and porpoises.

peak sound pressure level (PK)
The maximum instantaneous sound pressure level, in a stated frequency band, within a stated period. Also called zero-to-peak sound pressure level. Unit: decibel (dB).

peak-to-peak sound pressure level (peak-to-peak)
The difference between the maximum and minimum instantaneous sound pressure levels. Unit: decibel (dB).

percentile level, exceedance
The sound level exceeded *n* % of the time during a measurement.

point source
A source that radiates sound as if from a single point (ANSI S1.1-1994 R2004).

power spectrum density
The acoustic signal power per unit frequency as measured at a single frequency. Unit: $\mu Pa^2/Hz$, or $\mu Pa^2 \cdot s$.

power spectrum density level
The decibel level ($10\log_{10}$) of the power spectrum density, usually presented in 1 Hz bins. Unit: dB re 1 $\mu Pa^2/Hz$.

precision (P)
Metric used to measure the performance of a detector. The precision measures the exactness of an automated detector/classifier and is calculated based on the numbers of true positives (TP) and false positives (FP). Precision is usually used in conjunction with Recall (R).

pressure, acoustic
The deviation from the ambient hydrostatic pressure caused by a sound wave. Also called overpressure. Unit: pascal (Pa). Symbol: *p*.

recall (R)
Metric used to measure the performance of a detector. The recall measures the completeness of a detector and is calculated based on the number of true positives (TP), and false negatives (FN). Recall is usually used in conjunction with Precision (P).

received level
The sound level measured at a receiver.

rms
root-mean-square.

rms sound pressure level (SPL)
The root-mean-square average of the instantaneous sound pressure as measured over some specified time interval. For continuous sound, the time interval is one second. See also sound pressure level (SPL) and 90% SPL.

sound
A time-varying pressure disturbance generated by mechanical vibration waves travelling through a fluid medium such as air or water.

sound exposure
Time integral of squared, instantaneous frequency-weighted sound pressure over a stated time interval or event. Unit: pascal-squared second ($Pa^2 \cdot s$) (ANSI S1.1-1994 R2004).

sound exposure level (SEL)
A measure related to the sound energy in one or more pulses. Unit: dB re 1 $\mu Pa^2 \cdot s$.

sound intensity
Sound energy flowing through a unit area perpendicular to the direction of propagation per unit time.

sound pressure level (SPL)
The decibel ratio of the time-mean-square sound pressure, in a stated frequency band, to the square of the reference sound pressure (ANSI S1.1-1994 R2004).

For sound in water, the reference sound pressure is one micropascal (p_0 = 1 µPa) and the unit for SPL is dB re 1 µPa:

$$\text{SPL} = 10\log_{10}\left(p^2 / p_0^2\right) = 20\log_{10}\left(p / p_0\right)$$

Unless otherwise stated, SPL refers to the root-mean-square sound pressure level (SPL).

sound speed profile
The speed of sound in the water column as a function of depth below the water surface.

source level (SL)
The sound pressure level measured 1 meter from a theoretical point source that radiates the same total sound power as the actual source. Unit: dB re 1 µPa @ 1 m.

spectrogram
A visual representation of acoustic amplitude versus time and frequency.

spectrum
An acoustic signal represented in terms of its power (or energy) distribution versus frequency.

true positives (TP)
A signal of interest correctly classified as such by an automated detector/classifier.

Literature Cited

[DoE] Department of the Environment. 2015. *EPBC Act Protected Matters Search Tool* (webpage). http://www.environment.gov.au/erin/ert/epbc/index.html (Accessed 16 May 2015).

[NRC] National Research Council. 2003. *Ocean Noise and Marine Mammals*. National Research Council (U.S.), Ocean Studies Board, Committee on Potential Impacts of Ambient Noise in the Ocean on Marine Mammals. The National Academies Press, Washington, DC. 192 pp. http://www.nap.edu/openbook.php?record_id=10564.

ANSI S1.1-1994. R2004. *American National Standard Acoustical Terminology*. American National Standards Institute, New York.

ANSI/ASA S1.13-2005. R2010. *American National Standard Measurement of Sound Pressure Levels in Air*. American National Standards Institute and Acoustical Society of America, New York.

Arveson, P.T. and D.J. Vendittis. 2000. Radiated noise characteristics of a modern cargo ship. *Journal of the Acoustical Society of America* 107(1): 118-129.

Au, W.W.L. 1993. *The Sonar of Dolphins*. Springer-Verlag, New York.

Au, W.W.L., J. Mobley, W.C. Burgess, M.O. Lammers, and P.E. Nachtigall. 2000. Seasonal and diurnal trends of chorusing humpback whales wintering in waters off Western Maui. *Marine Mammal Science* 16(3): 530-544.

Bannister, J.L. 1964. Australian whaling 1963 catch results and research. *Marine Laboratory, Cronulla, Australia.*

Bannister, J.L. and S.L. Hedley. 2001. Southern hemisphere Group IV humpback whales: Their status from recent aerial survey. *Memoirs of the Queensland Museum* 47(2). http://www.countingwhales.co.uk/PDF/Bannister%20Hedley.pdf.

Baron, S.C., A. Martinez, L.P. Garrison, and E.O. Keith. 2008. Differences in acoustic signals from Delphinids in the western North Atlantic and northern Gulf of Mexico. *Marine Mammal Science* 24(1): 42-56.

Baumann-Pickering, S., M.A. McDonald, A.E. Simonis, A. Solsona Berga, K.P. Merkens, E.M. Oleson, M.A. Roch, S.M. Wiggins, S. Rankin, et al. 2013. Species-specific beaked whale echolocation signals. *J Acoust Soc Am* 134(3): 2293-301. NLM.

Baumgartner, M.F. and D.M. Fratantoni. 2008. Diel periodicity in both sei whale vocalization rates and the vertical migration of their copepod prey observed from ocean gliders. *Limnology and Oceanography* 53(5): 2197-2209.

Best, P. 1977. Two allopatric forms of Bryde's whale off South Africa. *Report of the International Whaling Commission (Special Issue)* 1: 1-9.

Branch, T., K. Stafford, D. Palacios, C. Allison, J. Bannister, C. Burton, E. Cabrera, C. Carlson, B. Galletti Vernazzani, et al. 2007. Past and present distribution, densities and movements of blue whales *Balaenoptera musculus* in the Southern Hemisphere and northern Indian Ocean. *Mammal Review* 37(2): 116-175.

Cerchio, S., B. Andrianantenaina, A. Lindsay, M. Rekdahl, N. Andrianarivelo, and T. Rasoloarijao. 2015. Omura's whales (Balaenoptera omurai) off northwest Madagascar: ecology, behaviour and conservation needs. *Royal Society Open Science* 2(10). http://rsos.royalsocietypublishing.org/royopensci/2/10/150301.full.pdf.

Chapman, D.G. 1974. Status of Antarctic Rorqual Stocks. *In* Schevill, W. (ed.). *The Whale Problem*. Harvard University Press, Cambridge. 218-238 pp.

Dethmers, K.E.M., R. Chatto, M. Meekan, A. Amaral, C. de Cunha, N. de Carvalho, and K. Edyvane. 2009. *Marine megafauna surveys in Timor Leste: Identifying opportunities for potential ecotourism – Final Report*. Ministry of Agriculture & Fisheries, Government of Timor Leste.

Double, M.C., V. Andrews-Goff, K.C.S. Jenner, M.-N. Jenner, S.M. Laverick, T.A. Branch, and N.J. Gales. 2014. Migratory Movements of Pygmy Blue Whales (<italic>Balaenoptera musculus brevicauda</italic>) between Australia and Indonesia as Revealed by Satellite Telemetry. *PLoS ONE* 9(4): e93578. http://dx.doi.org/10.1371%2Fjournal.pone.0093578.

Dunlop, R.A., M.J. Noad, D.H. Cato, and D. Stokes. 2007. The social vocalization repertoire of east Australian migrating humpback whales (*Megaptera novaeangliae*). *Journal of the Acoustical Society of America* 122(5): 2893-2905.

Gavrilov, A.N., R.D. McCauley, C. Salgado-Kent, J. Tripovich, and C. Burton. 2011. Vocal characteristics of pygmy blue whales and their change over time. *J Acoust Soc Am* 130(6): 3651-3660. http://scitation.aip.org/content/asa/journal/jasa/130/6/10.1121/1.3651817.

Gedamke, J., D.P. Costa, and A. Dunstan. 2001. Localization and visual verification of a complex minke whale vocalization. *Journal of the Acoustical Society of America* 109(6): 3038-3047.

Heaney, L.R., D.S. Balete, L. Dolar, A.C. Alcala, A. Dans, P.C. Gonzales, N. Ingle, M. Lepiten, W. Oliver, et al. 1998. A synopsis of the mammalian fauna of the Philippine Islands. *Fieldiana Zoology* 88: 1–61.

Ichihara, T. 1966. The pygmy blue whale, Balaenoptera musculus brevicauda, a new subspecies from the Antarctic. *Whales, dolphins and porpoises*: 79-113.

Jenner, K.C.S., M.N. Jenner, and K.A. McCabe. 2001. Geographical and temporal movements of humpback whales in Western Australian waters. *Australian Petroleum Production Exploration Association (APPEA) Journal* (749-765).

Kasamatsu, F., S. Nishiwaki, and H. Ishikawa. 1995. Breeding areas and southbound migrations of southern minke whales *Balaenoptera acutorostrata*. *Marine Ecology Progress Series* 119(1): 1-10. http://www.int-res.com/articles/meps/119/m119p001.pdf.

Luna, S.M. 2014. Rhomboplites aurorubens. http://www.fishbase.org/summary/213 (Accessed 4 May 2015).

McCauley, R. and C.S. Kent. 2009. *Wheatstone Project Appendix 02 – Sea Noise logger Deployment Wheatstone and Onslow, April to July 2009, Preliminary Analysis*. Report Number Report R2010-09. Centre for Marine Science and Technology, Curtin University.

McCauley, R. 2012. *Fish choruses from the Kimberley, seasonal and lunar links as determined by long term sea noise monitoring Acoustics 2012*, 21-23 November 2012, Fremantle, Australia, p. 6.

McCauley, R.D., C. Jenner, J.L. Bannister, C.L.K. Burton, D.H. Cato, and A. Duncan. 2001. *Blue Whale Calling In The Rottnest Trench - 2000, Western Australia*. Document Number R2001-6. Centre for Marine Science and Technology, Perth. http://cmst.curtin.edu.au/local/docs/pubs/2001-06.pdf.

McDonald, M.A., J.A. Hildebrand, S.M. Wiggins, D. Thiele, D. Glasgow, and S.E. Moore. 2005. Sei whale sounds recorded in the Antarctic. *Journal of the Acoustical Society of America* 118(6): 3941-3945.

McDonald, M.A. 2006. An acoustic survey of baleen whales off Great Barrier Island, New Zealand. *New Zealand Journal of Marine and Freshwater Research* 40(4): 519–529.

McDonald, M.A., S.L. Mesnick, and J.A. Hildebrand. 2006. Biogeographic characterization of blue whale song worldwide: using song to identify populations. *Journal of Cetacean Research and Management* 8(1): 55-65.

McPherson, C., B. Martin, and C. Erbe. 2012. *Ambient Noise Monitoring in the Timor Sea: December 2010–December 2011*. JASCO Document 00329, Version 1.0. Technical report by JASCO Applied Sciences for Environmental Resources Management.

McPherson, C., H. Frouin-Mouy, J. MacDonnell, and B. Martin. 2014. *Poseidon Field–Baseline Underwater Acoustic Monitoring: October 2012–February 2014*. Document Number 00737. Technical report by JASCO Applied Sciences for Sinclair Knight Merz.

Ocean Time Series Group. 2009. MATLAB Numerical Scientific and Technical Computing. *In*, Scripps Institution of Oceanography, University of California San Diego. http://mooring.ucsd.edu/software.

Oleson, E.M., J. Barlow, J. Gordon, S. Rankin, and J.A. Hildebrand. 2003. Low frequency calls of Bryde's whales.

Oswald, J.N., J. Barlow, and T.F. Norris. 2003. Acoustic identification of nine delphinid species in the eastern tropical Pacific Ocean. *Marine Mammal Science* 19(1): 20-37. http://swfsc.noaa.gov/uploadedFiles/Divisions/PRD/Programs/Coastal_Marine_Mammal/Oswald.pdf.

Reilly, S.B., J.L. Bannister, P.B. Best, M. Brown, R.L. Brownell Jr., D.S. Butterworth, P.J. Clapham, J. Cooke, G.P. Donovan, et al. 2008a. *The IUCN Red List of Threatened Species* (webpage), Version 2014.3. www.iucnredlist.org (Accessed April 1, 2015).

Reilly, S.B., J.L. Bannister, P.B. Best, M. Brown, B. Jr.R.L., D.S. Butterworth, P.J. Clapham, J. Cooke, G.P. Donovan, et al. 2008b. Balaenoptera omurai. The IUCN Red List of Threatened Species 2008. http://www.iucnredlist.org/details/136623/0 (Accessed 15 October 2015).

Reilly, S.B., J.L. Bannister, P.B. Best, M. Brown, B. Jr.R.L., D.S. Butterworth, P.J. Clapham, J. Cooke, G.P. Donovan, et al. 2008c. Mesoplodon ginkgodens. The IUCN Red List of Threatened Species 2008. http://dx.doi.org/10.2305/IUCN.UK.2008.RLTS.T13246A3427970.en (Accessed 15 October 2015).

Rendell, L.E., J.N. Matthews, A. Gill, J.C.D. Gordon, and D.W. MacDonald. 1999. Quantitative analysis of tonal calls from five odontocete species, examining interspecific and intraspecific variation. *Journal of Zoology* 249: 403-410.

Rice, D. 1998. *Marine mammals of the world: systematics and distribution, special publication number 4, the Society for Marine Mammalogy*. Allen Press, USA. ix+ 231pp.

Risch, D., N.J. Gales, J. Gedamke, L. Kindermann, D.P. Nowacek, A.J. Read, U. Siebert, I.C. Van Opzeeland, S.M. Van Parijs, et al. 2014. Mysterious bio-duck sound attributed to the Antarctic minke whale (Balaenoptera bonaerensis). *Biology letters* 10(4): 20140175.

Rudolph, P., C. Smeenk, and S. Leatherwood. 1997. *Preliminary checklist of Cetacea in the Indonesian archipelago and adjacent waters*. Nationaal Natuurhistorisch Museum.

Sayigh, L., N. Quick, G. Hastie, and P. Tyack. 2013. Repeated call types in short-finned pilot whales, *Globicephala macrorhynchus*. *Marine Mammal Science* 29(2): 312-324.

Širović, A., H.R. Bassett, S.C. Johnson, S.M. Wiggins, and J.A. Hildebrand. 2014. Bryde's whale calls recorded in the Gulf of Mexico. *Marine Mammal Science* 30(1): 399-409.

Smith, J.N., A.W. Goldizen, R.A. Dunlop, and M.J. Noad. 2008. Songs of male humpback whales, *Megaptera novaeangliae*, are involved in intersexual interactions. *Animal Behaviour* 76: 467-477.

Steiner, W.W. 1981. Species-specific differences in pure tonal whistle vocalizations of five western North Atlantic dolphin species. *Behavioral Ecology and Sociobiology* 9(4): 241-246.

Struzinski, W.A. and E.D. Lowe. 1984. A performance comparison of four noise background normalization schemes proposed for signal detection systems. *Journal of the Acoustical Society of America* 76(6): 1738-1742. http://scitation.aip.org/content/asa/journal/jasa/76/6/10.1121/1.391621.

Thode, A.M., G.L. D'Spain, and W.A. Kuperman. 2000. Matched-field processing, geoacoustic inversion, and source signature recovery of blue whale vocalizations. *Journal of the Acoustical Society of America* 107(3): 1286-1300.

Valdivia, J., F. Franco, and P. Ramirez. 1981. The exploitation of Bryde's whales in the Peruvian sea. *Report of the International Whaling Commission* 31: 441-448.

Víkingsson, G.A. 1997. Feeding of fin whales (*Balaenoptera physalus*) off Iceland–diurnal and seasonal variation and possible rates. *J. Northw. Atl. Fish. Sci* 22: 77-89.

Wada, S., M. Oishi, and T.K. Yamada. 2003. A newly discovered species of living baleen whale. *Nature* 426(6964): 278-281. http://dx.doi.org/10.1038/nature02103.

Wenz, G.M. 1962. Acoustic ambient noise in the ocean: Spectra and sources. *Journal of the Acoustical Society of America* 34(12): 1936-1956.

Wiggins, S.M., E.M. Oleson, M.A. McDonald, and J.A. Hildebrand. 2005. Blue whale (Balaenoptera musculus) diel call patterns offshore of Southern California. *Aquatic Mammals* 31(2): 161.

Wiseman, N., S. Parsons, K.A. Stockin, and C.S. Baker. 2011. Seasonal occurrence and distribution of Bryde's whales in the Hauraki Gulf, New Zealand. *Marine Mammal Science* 27(4): E253-E267.